

QUANTIFYING THE EFFICIENCY AND QUALITY OF
AIR VOID DISTRIBUTIONS IN CONCRETE

By

HOPE HALL BECKER

Bachelor of Science in Architectural Engineering
Oklahoma State University
Stillwater, OK
2015

Master of Science in Civil Engineering
Oklahoma State University
Stillwater, OK
2018

Submitted to the Faculty of the
Graduate College of the
Oklahoma State University
in partial fulfillment of
the requirements for
the Degree of
DOCTOR OF PHILOSOPHY
May, 2022

QUANTIFYING THE EFFICIENCY AND QUALITY OF
AIR VOID DISTRIBUTIONS IN CONCRETE

Dissertation Approved:

Dr. M. Tyler Ley

Dissertation Adviser

Dr. Bruce Russell

Dr. Deb Mishra

Dr. Mileva Radonjic

ACKNOWLEDGEMENTS

Throughout my time at Oklahoma State University, I have encountered several academic professors that have influenced my drive to study higher education. One of those influential professors is Dr. Tyler Ley. Dr. Ley has been my academic advisor and mentor throughout my masters and doctoral degrees, and I want to thank him for challenging me to achieve goals within my academic career, my professional career, and my personal development as a leader of his team. Thank you to my committee members, Dr. Bruce Russell, Dr. Deb Mishra, and Dr. Mileva Radonjic who generously agreed to serve on my doctoral committee and support the growth of this study. The professional knowledge and encouragement that they shared was truly helpful. I would also like to extend my gratitude to all my colleagues and to all the graduate and undergraduate students that helped me during my doctoral research. Lastly, thank you to my parents, Joe D. & Vickie, for supporting me in every aspect of this journey, my sister, Grace, for always encouraging me, and my husband, Justin, for always pushing me to be a better person.

Forever Grateful

Name: HOPE ELIZABETH HALL BECKER

Date of Degree: MAY, 2022

Title of Study: QUANTIFYING THE EFFICIENCY AND QUALITY OF AIR VOID
DISTRIBUTION IN CONCRETE

Major Field: CIVIL ENGINEERING

Abstract: This work establishes new ways to measure and examine the air bubble distribution within concrete. This is important to provide freeze thaw durability and resistance to oxychloride formation. These bubbles decrease the fluid pressure on freezing and crystal formation. The quality of the air void distribution is important to maintain from mixing the concrete until it is hardened to ensure durability. If these bubbles are significantly modified or destroyed during construction or are lost over time, then they cannot provide the needed protection. This work studies concrete mixtures immediately after mixing, during placement, after hardening, throughout freezing and thawing cycles, and soaked in chloride solution through temperature changes. The SAM (AASHTO TP 118), Hardened Air Void Analysis (ASTM C), Freeze Thaw Durability Factor (ASTM C666), and Micro computed tomography (Micro-CT) are all utilized to verify and establish the quality of the air void system within concrete mixtures [1-3].

TABLE OF CONTENTS

Chapter	Page
I. INTRODUCTION.....	1
1.1 Introduction	1
1.2 Research Objectives	2
II. FIELD AND LABORATORY VALIDATION OF THE SEQUENTIAL AIR METHOD	4
2.1 Introduction	4
2.2 Experimental Methods.....	5
2.2.1 Laboratory Materials	5
2.2.2 Field Materials.....	8
2.2.3 Laboratory Concrete Mixing and Testing Methods	8
2.2.4 Sequential Air Method	9
2.2.4.1 SAM Number Calculations	10
2.2.4.2 Air Content	11
2.2.4.3 Measurement Variability	11
2.2.5 Sample Preparation for Hardened Air Void Analysis.....	11
2.3 Results and Discussion	12
2.3.1 Comparing the Spacing Factor and Air Volume.....	12
2.3.2 Comparing the SAM Number and Spacing Factor	14
2.4 Practical Implications	21
2.5 Conclusion.....	22
2.6 Acknowledgements	23
III. DETERMINING THE AIR VOID EFFICIENCY OF FRESH CONCRETE MIXTURES WITH THE SEQUENTIAL AIR METHOD	24
3.1 Introduction	24
3.2 Experimental Methods.....	27

Chapter	Page
3.2.1 Laboratory Materials	27
3.2.2 Laboratory Concrete Mixture Procedure and Testing.....	30
3.2.3 Sequential Air Method (SAM) and SAM Number	30
3.2.4 Hardened Air Sample Preparation.....	31
3.3 Estimating Air Void Efficiency with a Quantile Analysis	32
3.4 Results and Discussion	33
3.4.1 SAM Number and Spacing Factor Relationship	33
3.4.2 SAM Number and Air Content Relationship	34
3.4.3 Application of the Efficiency Chart	35
3.4.4 The Impact of Water Reducers on Air Void Efficiency.....	36
3.4.5 The Impact of Cement Type on Air Void Efficiency.....	38
3.5 Practical Implications	40
3.6 Conclusion.....	41
3.7 Acknowledgements	42
IV. EVALUATION OF THE CONCRETE MIXTURE EFFICIENCY WITHIN CONSTRUCTION PRACTICES.....	43
4.1 Introduction	43
4.2 Experimental Methods.....	45
4.2.1 Concrete Materials and Mixture Designs.....	45
4.2.2 Laboratory Concrete Mixing.....	46
4.2.3 Drop Height and Concrete Sampling Procedure	46
4.2.4 Concrete Testing	48
4.2.4.1 Sequential Air Method (SAM)	48
4.2.4.2 Hardened Air Void Analysis Sample Preparation.....	48
4.2.4.3 Freeze-Thaw Durability.....	49
4.2.5 Pumping and Dropping Concrete Mixtures	49
4.2.5.1 Pumping and Dropping Method	49
4.2.5.2 Pumping Mechanisms that Impact Air Void Distribution.....	50
4.3 Results	50
4.3.1 Efficient and Inefficient Concrete Mixture Designs	50

Chapter	Page
4.3.2	Efficiency Chart 51
4.3.3	Compressive Strength Change 52
4.3.4	Air Content Change..... 54
4.3.5	SAM Number Change..... 56
4.3.6	Spacing Factor Change..... 58
4.3.7	Durability Factor Change 59
4.4	Discussion..... 61
4.5	Pump and Drop Comparison 62
4.5.1	Air Content Change..... 62
4.5.2	Sequential Air Method Change 63
4.5.3	Spacing Factor Change..... 64
4.5.4	Durability Factor Change 65
4.5.5	Differences in Drop Height Impact on Pumped and Non-Pumped Concrete 66
4.6	Practical Significance 66
4.7	Conclusions 67
V.	QUANTIFYING CALCIUM OXYCHLORIDE FORMATION USING MICRO- COMPUTED TOMOGRAPHY 69
5.1	Introduction 69
5.2	Experimental Methods..... 71
5.2.1	Concrete Materials and Mixture Designs..... 71
5.2.2	Concrete Mixing..... 72
5.2.3	Concrete and Mortar Sampling and Testing 73
5.2.3.1	Sampling of Concrete and Mortar 73
5.2.3.2	Sequential Air Method (SAM) 73
5.2.3.3	Hardened Air Void Analysis Sample Preparation..... 73
5.2.4	Mortar Testing..... 74
5.2.4.1	Coring and Saturation of Samples 74
5.2.4.2	Temperature Cycling of Samples 75
5.2.5	Micro Computed Tomography (Micro-CT)..... 76

Chapter	Page
5.2.5.1 Image Processing and Analysis	78
5.2.5.2 Alignment of Micro-CT Datasets	78
5.2.5.3 Segmentation	79
5.3 Results	80
5.3.1 Mortar Sample Mass and Length Changes	80
5.3.2 Micro-CT Imaging Analysis	81
5.3.3 Micro-CT Imaging Compared to Segmentation of Voids.....	81
5.3.4 3.1.2 Quantifying Damage within Samples	82
5.3.5 Micro-CT Imaging of Individual Voids	85
5.4 Practical Significance	89
5.5 Conclusions	90
VI. CONCLUSION	91
6.1 Overview	91
6.2 Field and Laboratory Validation of the Sequential Air Method.....	92
6.3 Determining the Air Void Efficiency of Fresh Concrete Mixtures with the Sequential Air Method.....	92
6.4 Evaluation of the Concrete Mixture Efficiency within Construction Practices	93
6.5 Quantifying Calcium Oxychloride Formation Using Micro-Computed Tomography	94
6.6 Further Research Needed.....	95
REFERENCES	96
APPENDICES	106
APPENDIX A: Supplementary Information for Chapter II	106
APPENDIX B: Supplementary Information for Chapter III	121

LIST OF TABLES

Table	Page
2.1. Oxide analysis of materials used in the study. After [1].	6
2.2. Admixture References. After [1].	6
2.3. SSD Mixture Quantities	7
3.1. Three abstract cross sections of concrete samples with different air void systems.	26
3.2. Type I cement oxide analysis.	27
3.3. Admixture references.	28
3.4. Saturated Surface Dry (SSD) Mixture proportions.	29
4.1. Oxide analysis of cementitious materials.	45
4.2. Admixture information.	45
4.3. Concrete Mixture Designs at SSD.	46
4.4. Test procedures performed.	47
4.5. Concrete Testing Data.	51
5.1. Oxide analysis of cementitious materials.	71
5.2. Admixture information.	72
5.3. Concrete Mixture Designs at SSD.	72
5.4. Mortar samples investigated.	74
5.5. Scans throughout soaking and temperature cycling.	76

Table	Page
5.6. ZEISS XRADIA 410 scan settings.	76
5.7. Images from the grayscale histogram correction process and segmentation of voids for the 20FA M1 sample.	81
5.8. Images from the grayscale histogram correction process and segmentation of voids for the 40FA M1 sample.	82
5.9. Imaging and air volume analysis of 20FA M1 scans 1 through 5.	86
5.10. Imaging and air volume analysis of 40FA M1 scans 1 through 5.	87
A.1. Oklahoma State University Laboratory Concrete Testing Data.....	107
A.2. FHWA Turner Fairbanks Highway Research Center Laboratory Concrete Testing Data...112	
A.3. Field Concrete Testing Data.....114	
B.1. 15 th Quantile Line of SAM Number (Equation (3.1)).....122	
B.2. 85 th Quantile Line of SAM Number (Equation (3.2)).....122	
B.3. Concrete Testing Data.....123	
B.4. FHWA Turner Fairbanks Highway Research Center Laboratory Concrete Testing Data...129	

LIST OF FIGURES

Figure	Page
2.1. SAM testing device and section of SAM device showing top and bottom chambers. The detailed image of the device is after [1].	9
2.2. SAM pressure steps graphically shown for the top and bottom chambers. Image is after [1].	10
2.3. Air Content versus Spacing Factor for 257 laboratory concrete mixtures completed by two different research groups.	13
2.4. Air Content versus Spacing Factor for 231 field concrete mixtures completed by 21 different state DOTs with various aggregates and admixtures.	14
2.5. Air Content versus Spacing Factor for two laboratory mixtures with similar air volume and different air-void qualities. Image after [1].	14
2.6. SAM Number versus Spacing Factor for the two laboratory mixtures previously shown in Figure 2-5. Image after [1].	15
2.7. SAM Number versus air content below 300 μm for 192 laboratory concrete mixtures.	16
2.8. SAM Number versus Spacing Factor for 257 laboratory concrete mixtures completed by two different research groups. The results show 85% agreement.	17
2.9. SAM Number versus air content below 300 μm for 112 field concrete mixtures.	18

Figure	Page
2.10. SAM Number versus Spacing Factor for 231 field concrete mixtures completed by 21 different State DOTs and one Canadian province with various aggregates and admixtures. The results show 70% agreement.	20
2.11. Percent agreement between SAM Number and different Spacing Factors for laboratory and field concrete mixtures.....	21
3.1. SAM Number versus Spacing Factor for 227 laboratory concrete mixtures completed by two different research groups.....	34
3.2. Air Content versus SAM Number for 227 laboratory concrete mixtures completed by two different research groups.....	35
3.3. Efficiency Chart conceptual diagram.....	36
3.4. Air Content versus Spacing Factor for two laboratory mixture designs with different admixtures.	37
3.5. Air Content versus SAM Number for two laboratory mixture designs with different admixtures.	38
3.6. Air Content versus Spacing Factor for two laboratory mixture designs with different types of cement.	39
3.7. Air Content versus SAM Number for two laboratory mixture designs with different types of cement.	40
4.1. Plan View of the pipe network.....	49
4.2. Efficiency Chart with Air Content versus SAM Number for two concrete mixture designs.	52
4.3. Concrete mixtures dropped at different heights versus percent loss in 14 day compression strength. ...	53
4.4. Concrete mixtures dropped at different heights versus percent loss in 28 day compression strength. ...	54
4.5. Concrete mixtures dropped at different heights versus percent loss in air content.	56
4.6. Concrete mixtures dropped at different heights versus percent change in SAM Number.	58
4.7. SAM Number versus Spacing Factor for concrete mixtures dropped at different heights.....	59
4.8. Concrete mixtures dropped at different heights versus percent change in Durability Factor.	60
4.9. SAM Number versus Durability Factor for concrete mixtures dropped at different heights.	61

Figure	Page
4.10. Inefficient concrete mixtures not dropped, dropped at 1.52 meters, pumped with no drop and pumped with a 1.52 meter drop versus percent loss in air content.	63
4.11. Inefficient concrete mixtures not dropped, dropped at 1.52 meters, and pumped then dropped at 1.52 meters versus percent change in SAM Number.....	64
4.12. Inefficient concrete mixtures not dropped, dropped at 1.52 meters, and pumped then dropped at 1.52 meters versus percent change in SAM Number.....	65
4.13. Inefficient concrete mixtures not dropped, dropped at 1.52 meters, and pumped then dropped at 1.52 meters versus percent change in Durability Factor.	66
5.1. Phase diagram of $\text{Ca}(\text{OH})_2\text{-CaCl}_2\text{-H}_2\text{O}$ [12, 98].	70
5.2. Temperature cycling and scanning timeline.	76
5.3. Location and dimension of the investigated volume of interest (VOI).	76
5.4. An example of the Micro-CT dataset with the 3D tomography, a 2D cross-section of the reconstruction image, and the corresponding grayscale histogram for a sample [115].	78
5.5. Length measurement versus percent change.....	80
5.6. Total volume of air per scan for 20 percent and 40 percent fly ash replacement.	83
5.7. Change in the total volume of air over the depth of the 20 percent fly ash sample.	84
5.8. Change in the total volume of air over the depth of the 40 percent fly ash sample.	85
5.9. Cumulative total volume of air in relation to the air void diameter for each scan of sample 20FA M1.	88
5.10. Cumulative total volume of air in relation to the air void diameter for each scan of sample 40FA M1.	89
B.1. Efficiency Chart.....	121

CHAPTER I

INTRODUCTION

1.1 Introduction

This work establishes new ways to measure and examine the air bubble distribution within concrete. This is important to provide freeze thaw durability and resistance to oxychloride formation. These bubbles decrease the fluid pressure on freezing and crystal formation. The Sequential Air Method (SAM), described in AASHTO TP 118, has been shown to be a useful tool to study the air bubble distribution [1, 4-6]; however, more tools are needed to help interpret the results. This work aims to provide practical and useful tools for both research and the concrete industry to be used in the lab and the field with important feedback before the concrete has hardened. This feedback allows the mixture to be modified to improve performance or it can be used to troubleshoot problems in the field.

This work shows that the SAM Number provides a more direct measurement of the air void quality of fresh concrete than the total volume of air, which is important for the freeze-thaw durability of concrete. When concrete becomes critically saturated and experiences a series of freezing and thawing cycles, damage can occur [7, 8]. Concrete pavements have also experienced damage near the joints over time due to the accumulation of deicing salts that have dissolved into water, entered the concrete, and expanded with temperature change [9-14]. This solution can increase the degree of saturation and increase the potential for freezing and thawing

damage [15-19]. However, if the concrete mixture contains a well-distributed air void system with an efficient concrete mixture design, then this damage can be resisted [4, 20-22]. This is typically done by including an air-entraining admixture (AEA) during mixing. This surfactant creates well-spaced air bubbles within concrete that form voids in the hardened concrete. These voids create pressure-relief regions for water movement during freezing [4, 8, 20, 23]. While most specifications require a certain volume of air within the concrete, it is more important to provide a small and well-distributed bubble system in the fresh concrete that in turn creates a void system with the right size and spacing [22, 24, 25].

The quality of the air void distribution is important to maintain from mixing the concrete until it is hardened to ensure durability. If these bubbles are significantly modified or destroyed during construction or are lost over time, then they cannot provide the needed protection. This work studies concrete mixtures immediately after mixing, during placement, after hardening, throughout freezing and thawing cycles, and soaked in chloride solution through temperature changes. The SAM (AASHTO TP 118), Hardened Air Void Analysis (ASTM C), Freeze Thaw Durability Factor (ASTM C666), and Micro computed tomography (Micro-CT) are all utilized to verify and establish the quality of the air void system within concrete mixtures [1-3].

1.2 Research Objectives

Four fundamental tasks can be drawn from this work:

1. Validation of the Super Air Meter through a large-scale field and laboratory study
2. Determining the air void efficiency of fresh concrete mixtures with the Sequential Air Method
3. Evaluation of the concrete mixture efficiency within construction practices
4. Quantifying calcium oxychloride formation using Micro-Computed Tomography

The results will provide new tools to provide higher quality concrete in a more reliable way. This work also provides deeper insights into the behavior of concrete materials in response to these

increased pore pressures from solid formation from ice or crystals. It should be noted that the format for each chapter has been written as individual journal articles.

CHAPTER II

FIELD AND LABORATORY VALIDATION OF THE SEQUENTIAL AIR METHOD

Results presented in this chapter have been published in *Material and Structures (2020) 53:14*. Contributions of the co-authors is greatly acknowledged.

2.1 Introduction

Throughout the world, concrete is a widely used material for infrastructure construction. The quality of modern concrete mixtures is increasingly more important because of the emphasis on long-term durability and improved constructability. However, the tools used to evaluate these materials during design, production, and construction have not evolved to match these higher expectations or the new materials used in modern concrete.

When concrete becomes critically saturated and experiences a series of freezing and thawing cycles, damage can occur [7, 8]. However, if the concrete mixture contains a well-distributed air void system, then this damage can be resisted [4, 20, 21]. This is typically done by including an air-entraining admixture (AEA) during mixing. This surfactant creates well-spaced air bubbles within concrete that form voids in the hardened concrete. These voids create pressure-relief regions for water movement during freezing [4, 8, 20, 23]. While most specifications require a certain volume of air within the concrete, it is more important to provide a small and well-distributed bubble system in the fresh concrete that in turn creates a void system with the right size and spacing [22, 24, 25]. For this work, a term called the quality of the air void system will be used to describe a satisfactory void size and spacing in the hardened concrete.

The most established method to determine the air void quality is to use a hardened air void analysis and determine a parameter called the Spacing Factor [20, 21]. After the concrete has hardened, it is cut, polished, and the surface is inspected under a microscope to quantify the voids. This process can take weeks and so it cannot be used to provide the immediate feedback needed to modify the fresh concrete. While there are other methods that can measure the volume of air in fresh concrete (ASTM C 231, ASTM C 138, ASTM C 173), the volume of air does not necessarily represent the quality of the air void system [26-28].

The concrete industry needs a test method to determine the size and spacing of the air voids within the fresh concrete that can be completed in either the lab or the field. A new test method that measures the concrete response to sequential pressure steps has been developed to address these needs [4]. This test method gives real time results, allowing for production adjustments before concrete placement and is known as the Sequential Air Method or SAM and is described by AASHTO TP 118 [1]. The SAM results show an 88% agreement with the Spacing Factor of 200 μ m and a 90% agreement with a Durability Factor of 70% in rapid freeze-thaw testing (ASTM C 666) [4]. Previous work has suggested that the air volume is adequate to predict the Spacing Factor [29]; however, when a wider range of materials was included the SAM was shown to provide improved performance [4]. The original publications over the SAM used primarily laboratory and only limited field data (241 laboratory and 62 field mixtures) [4]. This work aims to expand that original data set with a special emphasis on gathering field data in a wide array of conditions, with different materials, equipment, and operators. All of the data is combined in this paper to allow stronger conclusions to be gained from a larger dataset and to establish the need for this test method to be used in the field.

2.2 Experimental Methods

2.2.1 Laboratory Materials

Table 2.1. shows the oxide analysis and Bogue calculations for the Type I cement used in all of the laboratory concrete mixtures in this report. These mixtures met ASTM C150 standards.

Crushed limestone and natural sand were the aggregates used from local sources. Some mixtures used a combination of coarse and intermediate sizes. Both aggregates met ASTM C33 standards. The maximum nominal aggregate size of the limestone was 19 mm (3/4 in). *Table 2.2.* shows the admixtures used that met the ASTM C260 and ASTM C494 standards.

Table 2.1. Oxide analysis of materials used in the study. After [4].

Oxide (%)	SiO ₂	Al ₂ O ₃	Fe ₂ O ₃	CaO	MgO	SO ₃	Na ₂ O	K ₂ O	TiO ₂	P ₂ O ₅	C ₃ S	C ₂ S	C ₃ A	C ₄ AF
Cement	21.1	4.7	2.6	62.1	2.4	3.2	0.2	0.3	-	-	56.7	17.8	8.2	7.8
Fly Ash	38.7	18.8	5.8	23.1	5.6	1.2	1.8	0.6	1.5	0.4	-	-	-	-

Table 2.2. Admixture References. After [4].

Abbreviation	Description	Generic Chemical Name
WROS	Wood Rosin	Air-entraining agent
SYNTH	Synthetic chemical combination	Air-entraining agent
PC	Polycarboxylate	Superplasticizer
WR	Triethanolamine	Water reducer

The air-entraining agents (AEAs) in this research are wood rosin (WROS) and synthetic (SYNTH) AEA. These are common commercial AEAs. *Table 2.3.* shows the twenty-three different mixture designs studied for the lab testing. A subset of mixtures was examined with either a polycarboxylate (PC) superplasticizer meeting ASTM C1017, a midrange water reducer (WR) meeting ASTM C494, or a shrinkage reducer (SRA) meeting ASTM C494. The PC dosage fell between 60 and 200 mL/100 kg to adjust the slump of the mixture between 50 mm to 200 mm. Some of the mixture designs used a Class C fly ash replacement for 20% of the cement by weight that met ASTM C618 standards. Each mixture design consisted of four to fourteen dosages of AEA to study air contents from 2% to 10%. This allowed 192 mixtures to be investigated. The details are given in Appendix A.

Table 2.3. SSD Mixture Quantities

w/cm	Cement kg/m ³	Fly-Ash kg/m ³	Paste Volume (%)	Coarse kg/m ³	Fine kg/m ³	Water kg/m ³	Admixture Used
0.45	362	0	29	1098	714	163	WROS
0.45	362	0	29	1098	714	163	SYNTH
0.53	362	0	32	1053	682	192	WROS
0.41	362	0	28	1127	722	148	WROS
0.39	362	0	27	1140	730	141	WROS
0.45	362	0	29	1098	714	163	WROS + PC1
0.45	362	0	29	1098	714	163	SYNTH + PC1
0.45	290	72	30	1089	709	163	WROS
0.45	223	56	23	785/573*	634	126	WROS
0.40	290	72	28	1115	724	145	WROS
0.40	290	72	28	1115	724	145	WROS + PC1
0.35	290	72	28	1127	768	127	WROS + PC1
0.40	290	72	28	1115	724	145	WROS + PC2
0.40	290	72	28	1115	724	145	WROS + PC3
0.40	290	72	28	1115	724	145	WROS + PC4
0.40	290	72	28	1115	724	145	WROS + PC5
0.40	290	72	28	1115	724	145	WROS + WR
0.40	362	0	28	1098	742	145	WROS
0.40	362	0	28	1098	742	145	WROS+PC1
0.45	335	0	27	1142	742	151	WROS
0.45	335	0	27	1142	742	151	WROS+PC1
0.50	335	0	29	1115	724	167	WROS
0.50	335	0	29	1115	724	167	WROS+PC1

* Mixture contained coarse and intermediate aggregates.

The US Federal Highway Administration (FHWA) Turner Fairbanks Highway Research Center laboratory in McLean, Virginia, USA also provided data for this paper to show an independent assessment of the test method with different materials. This work is summarized in other publications [29].

2.2.2 Field Materials

To investigate the field performance of the SAM, testing was completed by either a Department of Transportation or private testing labs from 20 different States and one Canadian Province. Throughout the entire data set, over 15 users completed the SAM test. This data was collected from more than 110 projects. The nine states that provided detailed information used 34 different mix designs. Within those mix designs, there were 62 different aggregates, 19 different cement sources, 20 different fly ash sources and 39 different admixtures. The mixtures investigated consist of approximately 60% pavement mixtures, 20% bridge deck mixtures, and 20% other air-entrained mixtures including self-consolidating, precast, ready mix, and central mix concrete. No lightweight aggregate was investigated in this testing. A single sample was used for hardened air void analysis (ASTM C457) and a single measurement from the SAM device was used. Investigating the performance of the SAM on this wide range of materials allows a large number of variables to be investigated that could not be practically completed in a controlled laboratory setting.

2.2.3 Laboratory Concrete Mixing and Testing Methods

Aggregates from outdoor storage piles were gathered and moved indoors to a controlled temperature of 23°C. After 24 hours, the aggregates were loaded into the mixer and spun. Samples were collected from the mixer for moisture corrections. After moisture corrections were calculated, all of the aggregate and two-thirds of the water was placed in the mixer and spun for three minutes. This time allowed for evenly distributed aggregates and for the aggregates to be closer to saturated surface dry (SSD).

The residual water, cement, and fly ash were added next and mixed for three minutes. While the mixing drum was scraped, the concrete mixture rested for two minutes. Following the rest time, the mixer was spun, and the admixtures were added. The AEA was added 15 to 30 seconds after the PC or WR, then the mixture was spun for three minutes.

One hardened air-void analysis (ASTM C457) sample was made from each concrete mixture for testing. Two 7L samples were tested simultaneously with the SAM by different operators. These were used to find the average SAM Number of a mixture.

2.2.4 Sequential Air Method

The SAM device is similar to the ASTM C231 Type B meter with some modifications. The SAM device uses six restricted clamps to account for increased pressures and a digital pressure gauge for testing. The SAM can be used to test concrete before it hardens, which provides insight into the air void system to help design and evaluate the air void system of the hardened concrete.

The device is shown in *Figure 2.1.*

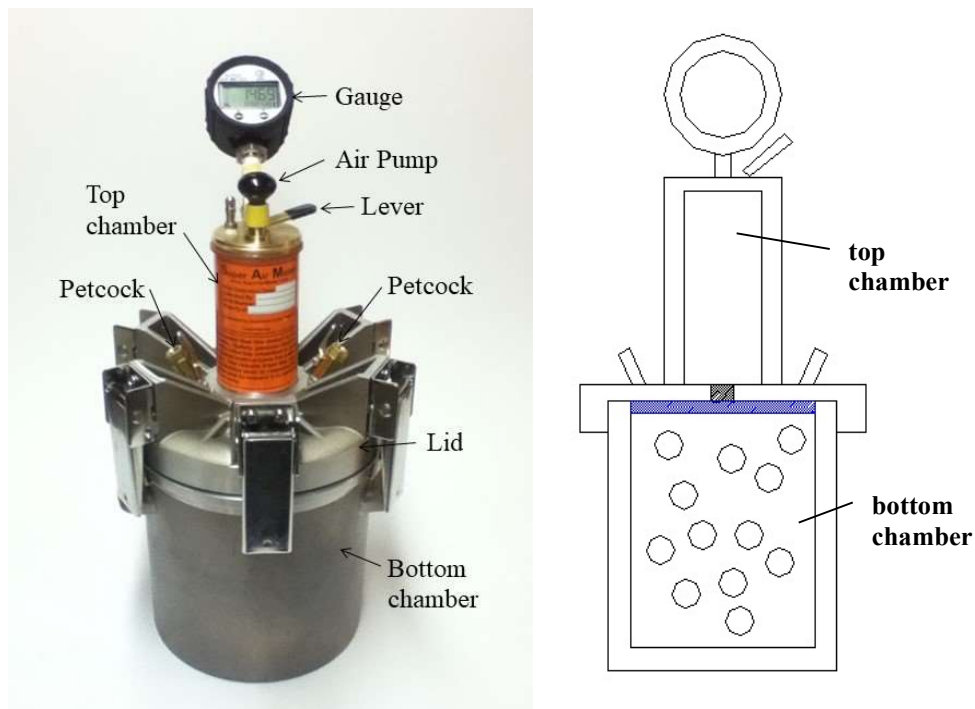


Figure 2.1. SAM testing device and section of SAM device showing top and bottom chambers.

The detailed image of the device is after [4].

The test takes an experienced user between eight to 10 minutes to complete. *Figure 2.2.* shows a typical data set and a video of the test is available [30]. The test applies three sequential pressures to the fresh concrete and the equilibrium pressures are recorded. The pressure is then

released, and the same steps are applied again to the fresh concrete. The SAM Number is calculated by taking the numerical difference between the final pressure steps. The difference between the pressure responses is an indication of the air void size and spacing in the concrete. Further details can be found in other publications [4].

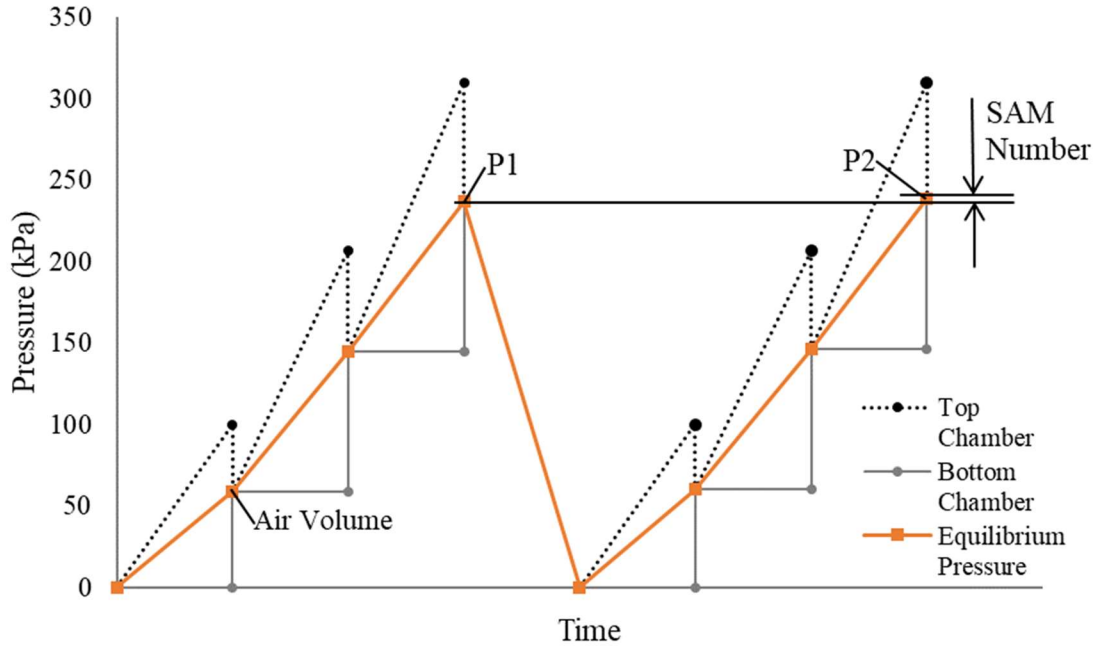


Figure 2.2. SAM pressure steps graphically shown for the top and bottom chambers. Image is after [4].

2.2.4.1 SAM Number Calculations

The SAM Number can be calculated as: $SAM\ Number = (P_2 - P_1)/c$. Where P_1 is the first equalized pressure at 310 kPa (45 psi) and P_2 is the second equalized pressure at 310 kPa (45 psi). The value c is a constant that is 6.90 if the units are in kPa and 1.0 if the units are in psi. More details can be found in Figure 2.2.. The SAM Numbers ranged from 0.03 to 0.78 for the mixtures represented. The SAM Number is an empirical number that has been correlated to the air void size and spacing from empirical relationships [5].

2.2.4.2 Air Content

The total volume of air in the mixtures can be found from the first equilibrium pressure at 100 kPa (14.5 psi) by using Boyle's Law. This procedure is explained in other publications [31-36] and uses the same method and procedure used in the conventional pressure meter (ASTM C231). Previous experiments with similar equipment have shown that the air content found by the SAM agreed with results from the ASTM C231 pressure method [29, 31, 37].

2.2.4.3 Measurement Variability

The variability of the SAM Number is reported to have a standard deviation of 0.049 and a coefficient of variation of 15.2%. The coefficient of variation is lower than the reported values for determining the Spacing Factor and Durability Factor (20.1% and 22.7% respectively) [4].

2.2.5 Sample Preparation for Hardened Air Void Analysis

Concrete samples were cut into 19 mm thick slabs and polished with sequentially finer grits. The surface of the sample was preserved with an acetone and lacquer mixture to strengthen the surface before it was inspected under a stereo microscope. After an acceptable surface was obtained, the sample is cleaned with acetone. The surface was then colored with a black permanent marker, the air voids were filled with less than 1 μm white barium sulfate powder, and the air voids within the aggregates were blackened under a stereo microscope. This process makes the concrete sample black and the voids in the paste white. Sample preparation details can be found in other publications [31, 38]. The sample analyzed with ASTM C457 method C by using the Rapid Air 457 from Concrete Experts, Inc, which uses chord counting. A single threshold value of 185 was used for all samples in this research and the results do not include chords smaller than 30 μm . A traverse length of 2286 mm was used for all samples to satisfy the requirements of ASTM C457. These settings and sample processing methods are similar to methods used in other publications [38-40]. All air voids were used for the volume of chords less than 300 μm [6].

The hardened air-void analysis from Kansas, Iowa, Pennsylvania, and the FHWA Turner Fairbanks Highway Research Center was completed by their staff with methods that may be different from that described above. This accounted for 29% of the lab data and 28% of the field data shown. The hardened air samples that had differences of more than 2% between the fresh and hardened air content were not included in the analysis. This discrepancy could be caused by a fresh air measurement that was not completed correctly, a hardened sample that was not adequately consolidated, or an air-void system that was unstable. An unstable air-void system would cause the fresh concrete to lose air over time. This can cause the fresh air measurements to be higher than the hardened concrete. Regardless of the reason, samples with large differences in the fresh and hardened air content were not used in this study.

2.3 Results and Discussion

2.3.1 Comparing the Spacing Factor and Air Volume

The fresh air content and Spacing Factor is compared for all the mixtures in this study. The laboratory concrete is shown in *Figure 2.3.* and the field concrete in *Figure 2.4.*. A horizontal line is shown with a Spacing Factor of 200 μm as this is the value recommended by ACI 201.2R for freeze-thaw durability [41].

It can be seen in both *Figure 2.3.* and *Figure 2.4.* that the range of air contents needed to provide a Spacing Factor of 200 μm varied from 3.25% to 7.75% air volume. This wide range shows that it is difficult to develop a specification based on the volume of air to provide freeze-thaw durability. For example, to ensure the freeze-thaw durability of some of these mixtures, it would require the air volume in the concrete to be greater than 7.5%. Unfortunately, this would require many mixtures to have much higher air contents than is required. These higher air contents would impact the constructability and the strength of the concrete. This would increase the costs and may reduce the sustainability of a mixture. This reinforces that the air volume and air void quality do not correlate. More insights can be gained by looking at individual mixtures.

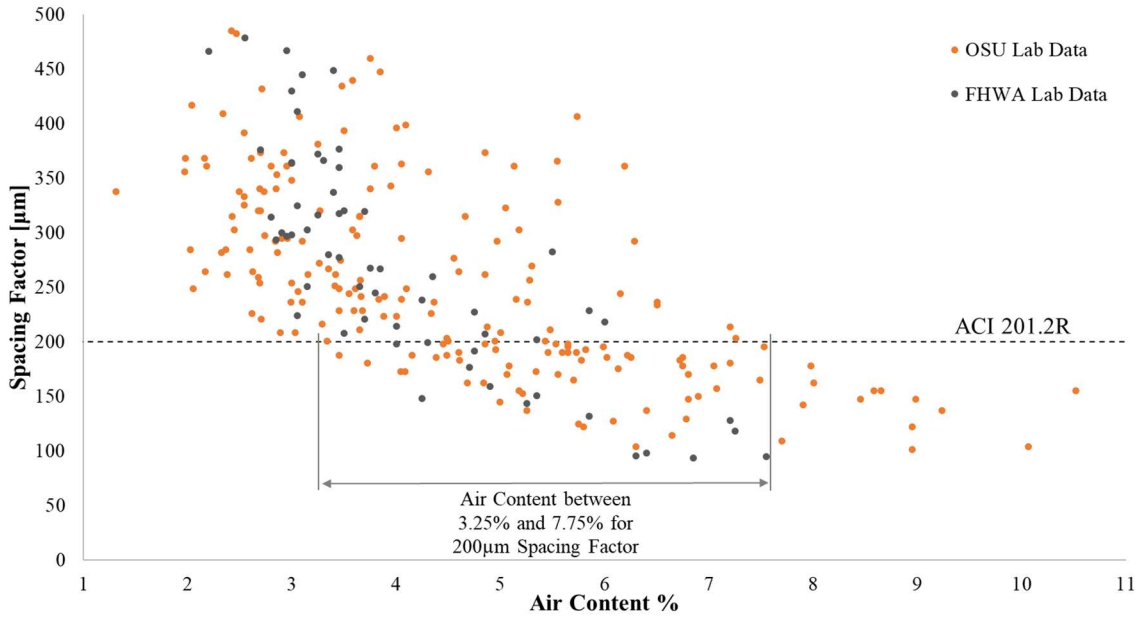


Figure 2.3. Air Content versus Spacing Factor for 257 laboratory concrete mixtures completed by two different research groups.

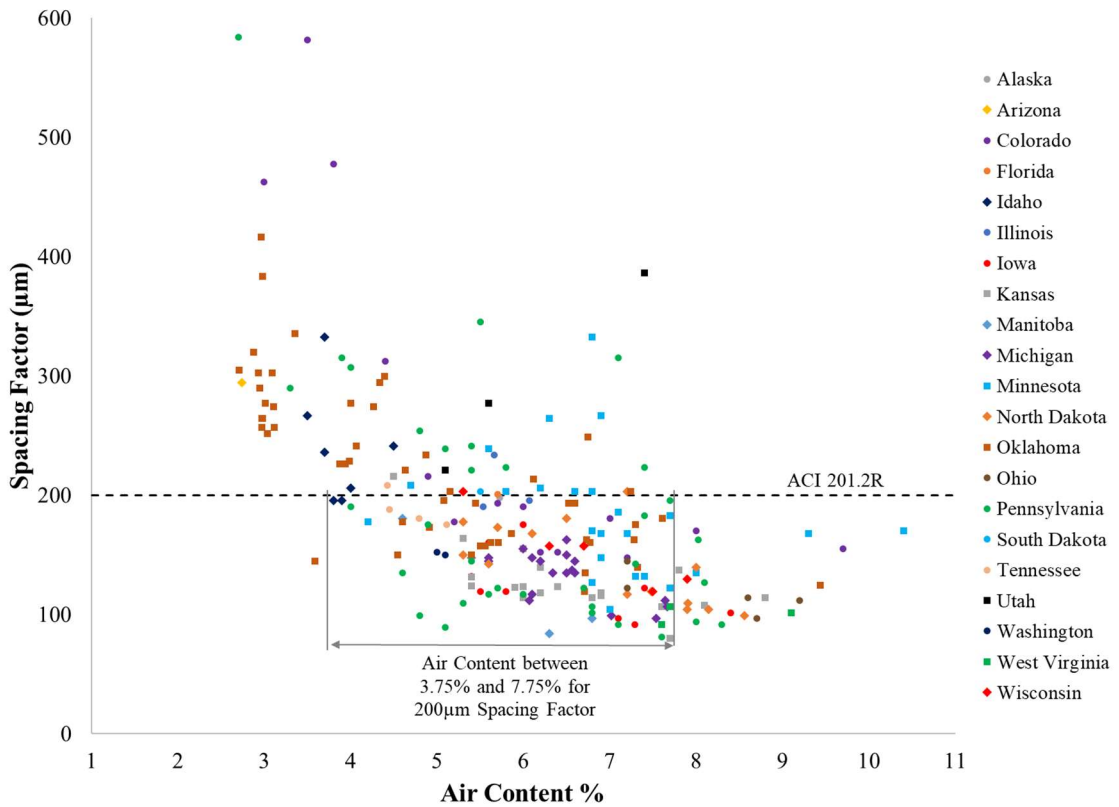


Figure 2.4. Air Content versus Spacing Factor for 231 field concrete mixtures completed by 21 different state DOTs with various aggregates and admixtures.

In the following figures, two series of concrete mixtures are compared to show how the relation between the air content and Spacing Factor and then the Spacing Factor and SAM Number. The only difference between the two series is that one uses a blend of admixtures and the other uses only an AEA. In Figure 2.5, the comparison between air content and Spacing Factor is presented. Linear trend lines are shown for each series. At an air content of 5%, the Spacing Factor is different by almost 200 μm . The series with just an AEA needs approximately 4.5% air to reach a Spacing Factor of 200 μm , while the series with a blend of admixtures needs approximately 7.5% air to reach 200 μm . This highlights that the volume of air cannot be used to determine the quality of the air within the hardened concrete.

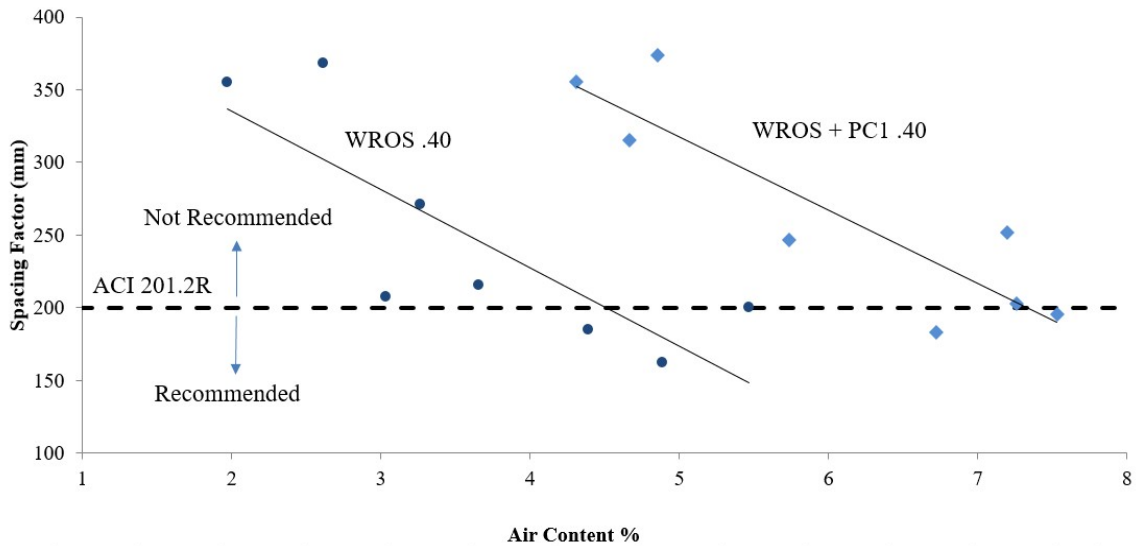


Figure 2.5. Air Content versus Spacing Factor for two laboratory mixtures with similar air volume and different air-void qualities. Image after [4].

2.3.2 Comparing the SAM Number and Spacing Factor

In Figure 2.6., the comparison between SAM Number and Spacing Factor is presented for the same mixtures shown in Figure 2.5.. In this data, the linear trend lines for each mixture are

nearly overlapping. The similarity between the trend lines shows that there is a similar correlation between the SAM Number and Spacing Factor for these two mixtures. This shows that the SAM Number better correlates to the Spacing Factor for these two mixtures than the air volume. This is a large improvement over using the volume of air to specify and evaluate the air void quality of the concrete.

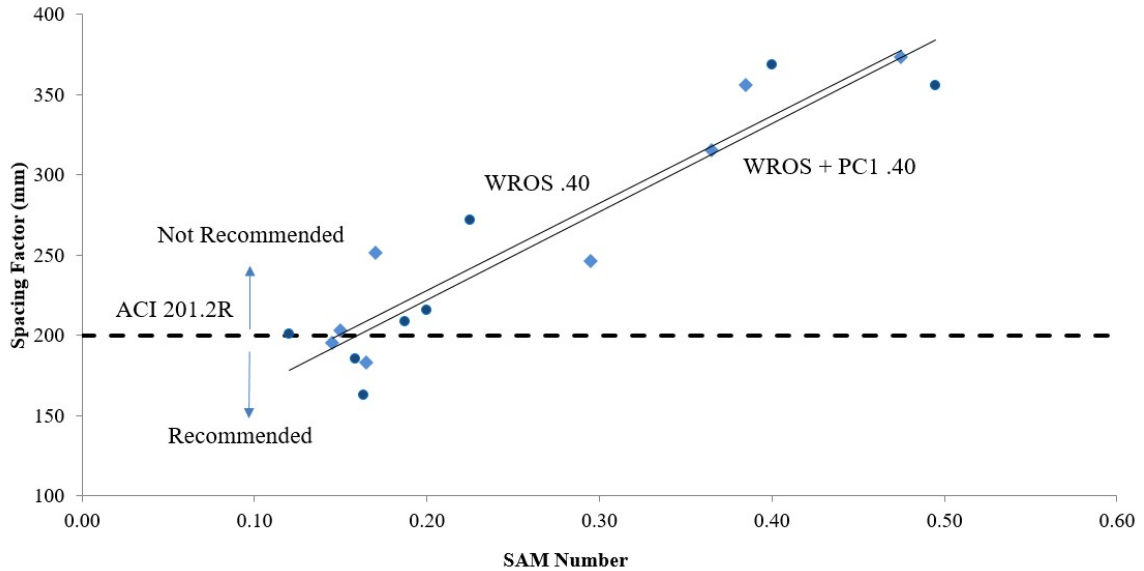


Figure 2.6. SAM Number versus Spacing Factor for the two laboratory mixtures previously shown in Figure 2.5.. Image after [4].

Figure 2.7. shows the relationship between the SAM Number and the air volume of voids less than 300 μm . A SAM Number of 0.33 corresponds to a 1.5% volume of voids less than 300 μm . The results show a cubic and linear relationship between these two parameters below the 0.33 SAM Number and 1.5% air content intersection. Previous research has shown that a SAM Number of 0.32 best corresponded with performance in the ASTM C666 rapid freeze thaw test [4]. The satisfactory agreement shows that the SAM Number is an indication of the small voids in the concrete and that these voids seem to be important for freeze thaw durability. Care should be taken in only using the volume of small air voids as the measurement does not take into account the paste volume in the mixture as is done by the Spacing Factor [21].

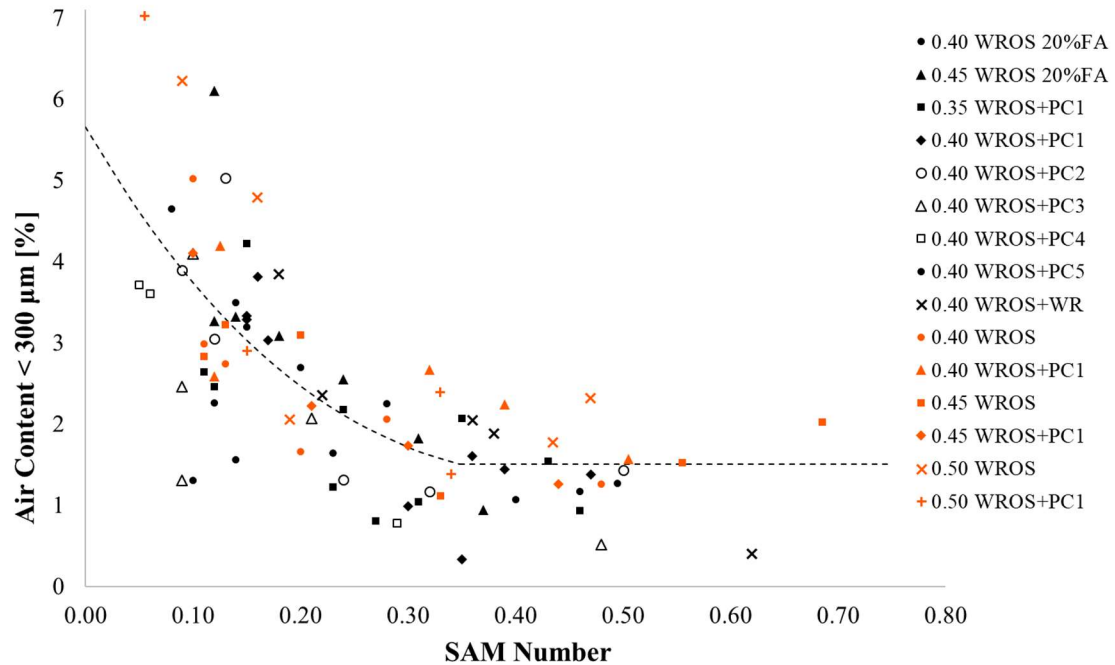


Figure 2.7. SAM Number versus air content below 300 μm for 192 laboratory concrete mixtures.

To further show the utility of the SAM Number, Figure 2.8. shows the relationship between SAM Number and Spacing Factor for 257 laboratory concrete mixtures completed by two different labs. Within this set of data, 75% of the mixtures were completed at Oklahoma State University and 25% of the mixtures were completed at FHWA Turner Fairbanks Highway Research Center [29]. Figure 2.8. shows that as the SAM Number increases then so does the Spacing Factor. Past recommendations for the Spacing Factor have used a single value to determine if a material is recommended for freeze-thaw durability. This has also been beneficial in aiding industry implementation because it is simple and shows if something is above or below the recommended value.

If target values for the SAM Number and Spacing Factor are used, then this will separate the data into four quadrants. The upper right and lower left quadrant show where the SAM Numbers and Spacing Factors agree that the air void system is either satisfactory or unsatisfactory. The upper left and lower right quadrant show where the SAM Number and Spacing Factor do not agree. Past work has suggested that a SAM Number of 0.20 correctly determines if a Spacing Factor is

above or below 200 μm for 88% of the data [4]. For this work, the laboratory data shows that the data in the lower left-hand quadrant and the upper right-hand quadrant represent 85% of the data points, which means the SAM Number and Spacing Factor for this data set shows an 85% agreement.

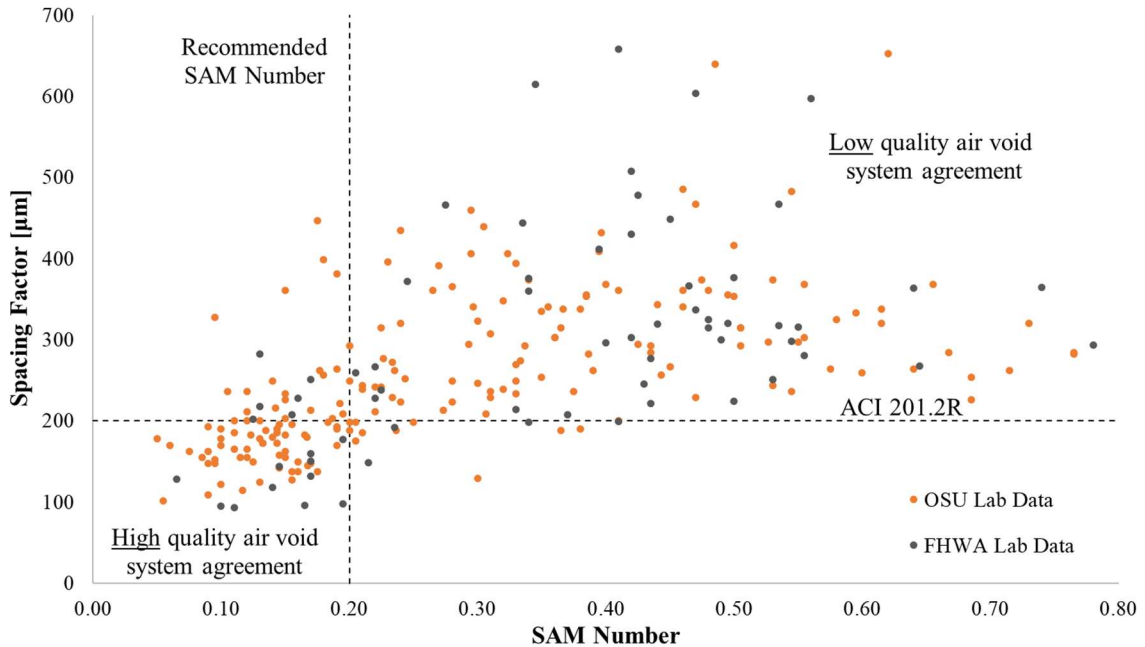


Figure 2.8. SAM Number versus Spacing Factor for 257 laboratory concrete mixtures completed by two different research groups. The results show 85% agreement.

Next, to investigate if the SAM is a useful tool for field usage, the test was used to evaluate field mixtures completed by either a Department of Transportation or private testing lab from 20 different States and one Canadian Province for 231 different concrete mixtures from 110 different projects. A hardened sample was also obtained for ASTM C457 analysis. Figure 2.9. shows the relationship between the SAM Number and the air volume of chords less than 300 μm for field concrete mixtures. The SAM Number and Spacing Factor are plotted together for the field data in Figure 2.10..

Figure 2.9. shows the relationship between the SAM Number and the air volume of chords less than 300 μm for field concrete mixtures. This data set represents 112 comparisons with the same

cubic and linear trend line that was used in *Figure 2.7.* to compare the field data agreement. The field data that was completed by Kansas, Iowa, Pennsylvania, and the FHWA Turner Fairbanks Highway Research Center with other methods was not included in this analysis due to lack of content in the air volume of chords less than 300 μm . Again, the data shows that the SAM Number is a good indicator of the small voids in the concrete. Spacing Factor limit of 200 μm from ACI 201.2R-16 [41] is displayed in *Figure 2.10.* as well as a SAM Number limit of 0.20. The results show 70% agreement for the field data. While this is slightly lower than the laboratory testing, it shows the SAM Number is a useful tool to provide important insights into the quality of the air void system in fresh concrete. This lower agreement may be caused by the increased variability of the field and differences in testing procedures and materials. With the wide range in field users, this new test may also show variability due to unfamiliarity.

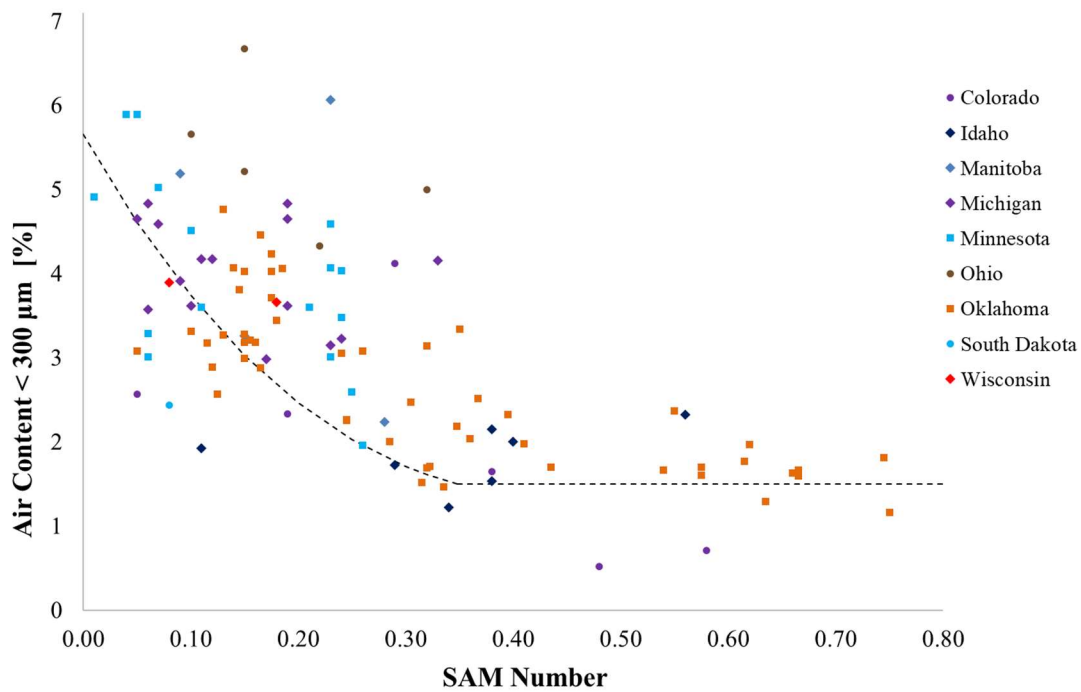


Figure 2.9. SAM Number versus air content below 300 μm for 112 field concrete mixtures.

For this work, the field data plotted in *Figure 2.10.* shows that the data in the lower left-hand quadrant and the upper right-hand quadrant represent 70% of the data points, which means the

SAM Number and Spacing Factor for this data set shows a 70% agreement. As stated in Section 2.2.2, the field data has a diverse set of concrete mixtures from a wide variety of testing locations and users making the data set different than the laboratory data set. The field data points in the upper right-hand quadrant of *Figure 2.10*. represent mixtures that would not be recommended for use in freezing climates and consist of nearly 25% of the data (57 out of 231 mixtures). These projects may show a reduced lifespan if they are exposed to moisture and freezing temperatures. If these mixtures could have been identified by the SAM to have a low-quality air void system, then they could be adjusted. If this adjustment could have increased the lifespan of at least one project, then it would make significant savings to the public. This again highlights the limitation of using the air volume to evaluate concrete.

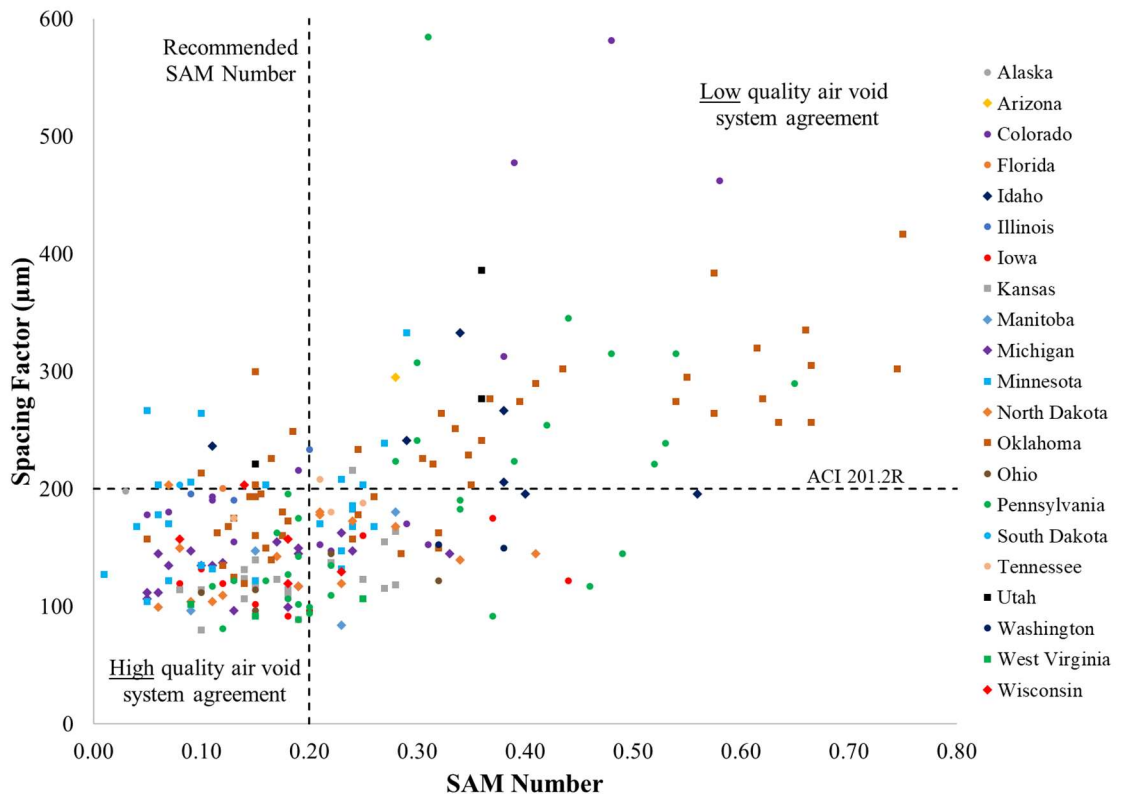


Figure 2.10. SAM Number versus Spacing Factor for 231 field concrete mixtures completed by 21 different State DOTs and one Canadian province with various aggregates and admixtures. The results show 70% agreement.

Based on the data in *Figure 2.8.* and *Figure 2.10.* it is not clear if a SAM Number of 0.20 shows the best correlation with a Spacing Factor of 200 μm . For example, there are a number of data points that are in the lower right quadrant or have a SAM Number greater than 0.20 but a Spacing Factor less than 200 μm in *Figure 2.10.*. If the SAM Number limit was higher, then this might improve the agreement for the field data. To investigate this further a range of SAM Numbers were chosen and compared to a Spacing Factor of 200 μm for both the lab and field data.

Figure 2.11. shows the percentage of data points that fall within either the upper right or lower left quadrants. These results show that a SAM Number near 0.20 has an agreement of close to 85% with a Spacing Factor of 200 μm for the laboratory data. While the data varies for the laboratory data, a value of 0.20 is chosen is recommended because the values do not change drastically in this range, and it is a round number that is conservative but not overly conservative. As the SAM Number increases above 0.22 and below 0.18 there is a decrease in the agreement for the laboratory data. One reason the curve has this shape is that in the laboratory testing the mixtures were designed to have almost equal amounts of low and high-quality air void systems. However, the field mixtures that were sampled did not have many low-quality air void systems as this would not be in the best interest for the durability of the concrete. Because of this, the agreement curve for the field data will not have the same shape. For example, *Figure 2.11.* shows that the correlation of that data may be improved if a higher SAM Number is used. As expected, the agreement curve for the field data does not have the same shape as the agreement curve for the lab data. However, it is important to note that the improvement in agreement for increasing the SAM Number is not significant. Furthermore, it is conservative to use a lower

SAM Number for the design and specification of concrete mixtures. Because of this, a SAM Number of 0.20 remains a satisfactory choice to correlate with a Spacing Factor of 200 μm .

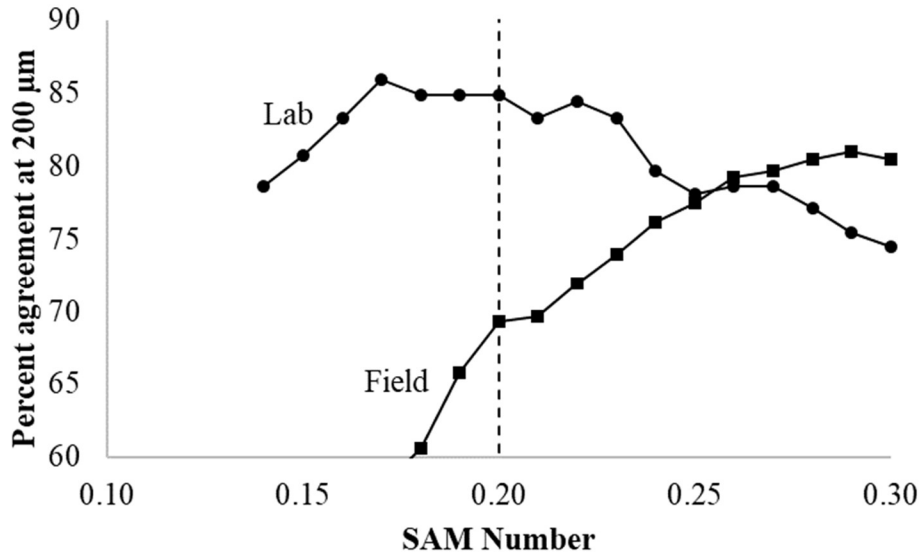


Figure 2.11. Percent agreement between SAM Number and different Spacing Factors for laboratory and field concrete mixtures.

2.4 Practical Implications

Due to shrinking resources and greater demand for long-lasting infrastructure the use of rapid test methods that provide direct measurements of critical parameters in a concrete mixture is in greater demand [42]. The SAM seems to meet these needs and provides a tool that shows great potential to be used as a quality control test where freeze-thaw durable concrete is required.

This work shows that the SAM Number is a more direct measurement of the air void quality in the fresh concrete than using the total air volume. The measurement method has shown good agreement to the Spacing Factor (85% lab, 70% field) for 488 concrete mixtures. The success of this testing with such a wide range of materials, operators, equipment, conditions, and construction procedures is a strong validation of the SAM. Furthermore, as shown in *Figure 2.10*, in the upper right quadrant, 25% of the field data was found to contain Spacing Factors and SAM Numbers that are not recommended. These mixtures were accepted on their projects based

on their air content but then the SAM showed low quality air void systems. This shows the importance in using the SAM to investigate the quality of the air void systems in the concrete before it is placed.

The SAM is a powerful measurement because it can be completed in less than 10 minutes before the concrete has hardened and it provides more insight than the volume of air within the concrete. This testing method also allows the mixtures to be changed before they are placed to ensure that satisfactory freeze-thaw durability is obtained. Furthermore, because this tool is portable, it can provide immediate feedback on how mixture ingredients, construction practices, and changes in temperature impact the quality of the air void system in fresh concrete. This can provide important insights into the performance of these concrete mixtures that were not possible to obtain in the past. In addition, because the SAM Number is a more direct measurement than the total volume of air, it will allow the overdesign of the air content for concrete mixtures to be reduced while ensuring long-term durability. This reduction in overdesign of the air content will allow for improvements in the economy and sustainability of the mixture.

2.5 Conclusion

This work compares the correlation between the SAM Number, Spacing Factor, and air content for 257 laboratory mixtures and 231 field mixtures with various admixtures, aggregates, devices, and users. The reliability of the method across a data set this diverse shows the reliability and robustness of the SAM test method.

These specific findings have been made:

- Air contents between 3% and 8% were needed to obtain a Spacing Factor of 200 μm . This shows the inability of a specific air volume to correlate with air void quality.
- For 257 laboratory mixtures, the correlation between a SAM Number of 0.20 and a Spacing Factor of 200 μm agrees with 85% of the laboratory data comparisons.
- For 231 field mixtures, the correlation between a SAM Number of 0.20 and a Spacing Factor of 200 μm agrees with 70% of the field data comparisons.

- For 231 field mixtures, 25% or 57 of them that were placed based on their air volume were shown by the Spacing Factor and SAM Number to have an air void distribution that is not recommended for freeze thaw durability.

This work shows that the SAM Number provides a more direct measurement of the air void quality of fresh concrete than the total volume of air, which is important for the freeze-thaw durability of concrete. The almost immediate feedback provided by the SAM in the fresh concrete can benefit material suppliers, producers, contractors, and engineers in their quest to build long lasting and economic infrastructure. The implementation of this procedure also shows promise to give new tools to design concrete mixtures, admixture formulation, and construction practices. These are all areas of examples where the SAM is currently being used in the industry. These will be areas of future publications.

2.6 Acknowledgements

The authors would like to acknowledge funding from the Oklahoma Transportation Center and Pooled Fund TPF-5(297) and the supporting states. Special thanks to Jason Weiss for the discussion over this work. We would also like to thank David Porter, Justin Becker, Brad Woodard, Zane Lloyd, Brendan Barns, Jacob Lavey, Chad Stevenson, Jason Toney, Mark Finnell, Muwanika Jdiobe, Megan Buchanan, Tyler Suder, and Lizzie Long for their assistance in preparing samples.

CHAPTER III

DETERMINING THE AIR VOID EFFICIENCY OF FRESH CONCRETE MIXTURES WITH THE SEQUENTIAL AIR METHOD

Results presented in this chapter have been published in *Construction and Building Materials* 288 (2021) 122865. Contributions of the co-authors is greatly acknowledged.

3.1 Introduction

The quality of concrete mixtures affects the constructability and long-term durability of concrete structures. With the wide range of materials and admixtures used in modern concrete, the industry needs tools to evaluate the quality of their concrete mixtures to understand the effects of the combination of different materials. These tools need to be rapid, easily understood, and provide critical feedback for users to help them obtain reliable concrete mixtures. This work introduces a new tool called the Efficiency Chart. The Efficiency Chart determines how different ingredients or changes to the environment impact the volume and spacing of the air void system. This can help producers create more reliable and consistent air void systems that also meet the suggested freeze thaw requirements.

Producing reliable air void systems in fresh concrete is extremely challenging for the concrete industry because there are improvements needed in determining the size and spacing of air bubbles in fresh concrete. Air-entraining admixtures (AEA) are used to achieve well-spaced air bubbles while mixing the concrete. These air voids create pressure-relief regions for water to

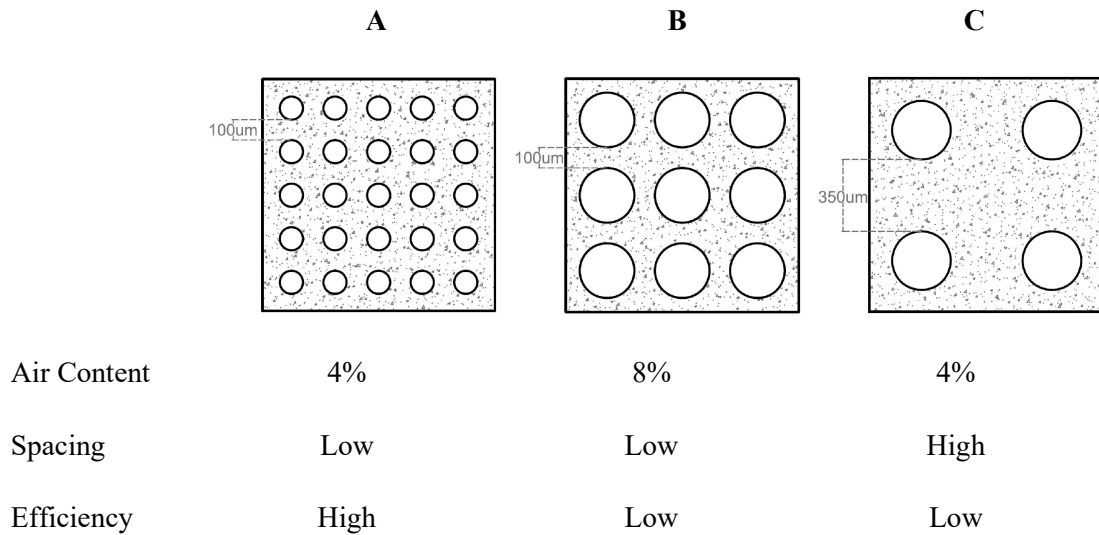
useful tool to study this [4-6] but more tools are needed to help interpret the results. The goal of move to during freezing [4, 8, 20, 23]. It is important to provide well-distributed voids in the hardened concrete [22, 24, 25]. The Sequential Air Method (SAM) has been shown to be this research is to create a new way to relate the both the air volume and bubble spacing in a concrete mixture as measured by the SAM and communicate this information with an easy-to-use chart that can be used for design or troubleshooting air-entrained concrete mixtures.

The air void spacing and air volume in concrete are related. As the air volume is increased, the spacing of the air bubbles will decrease. However, this relationship will depend on the size of the bubbles being stabilized in the concrete mixture. In this work the air void spacing for a given volume will be known as the air void efficiency. The efficiency of the air void system is important to understand because low efficiency mixtures will require higher air volumes to reach the same air void quality. These higher air volumes are harder to manage and reduce the strength of the concrete [32, 36, 43, 44]. This means that mixtures with high efficiency air void systems are more desirable because the smaller bubbles will be spaced closer together, but the industry cannot easily target this because there is no standard against which to measure the efficiency of the air void system.

To better illustrate the efficiency concept, three abstract cross sections of concrete are shown in *Table 3.1*. as A, B, and C. Each concrete has an air content with different sizes and spacing of air voids. The air content, air void spacing, and efficiency are shown below each sample. The air content is expressed in percent by volume of the sample. The air void spacing indicates whether the bubbles inside the concrete sample are close together or far apart. The efficiency of each sample is determined by comparing the volume of air needed to reach a desired spacing between air voids. This means that a low efficiency air void system will require a higher volume of air to reach a desired air void spacing while a high efficiency air void system can achieve a similar spacing at a lower volume of air. As an example, concrete sample A contains 4% air content with

low air void spacing, which creates a high efficiency mixture while sample C contains the same volume of air with a high air void spacing. Despite sample C having the same volume of air as sample A, the air void spacing is higher and so this system will have a lower efficiency. Further, sample B has similar spacing as sample A, but it required a much higher air volume. This higher air volume was needed because sample B has an air void system with low efficiency. While it is desirable for a mixture to have a high efficiency air void system, this parameter is not easily measured in the fresh concrete and so the industry cannot easily determine which variables control the air void efficiency of the concrete. This work aims to solve this issue by using the air volume and bubble spacing measurements from the SAM.

Table 3.1. Three abstract cross sections of concrete samples with different air void systems.



This work uses the air volume and SAM Number, a measurement of air void spacing, from 227 diverse concrete mixtures and a quantile regression analysis is used to separate the data into different categories of air void system efficiency. For example, outcomes near the 15% quantile function have favorable combinations of air volume and bubbles spacing or high efficiency and those near the 85% quantile function have unfavorable combinations and are low efficiency mixtures. If a set of components consistently provides low efficiency, then a producer will know

there is great potential to improve the concrete by changing the mixture of components or the components themselves. Further, several examples are presented with a hardened air void analysis that show how these concepts and tools could be used to evaluate different concrete mixtures. This work aims to provide practical and useful tools for both research and the concrete industry to be used in the lab or the field to provide important feedback before the concrete has hardened. This feedback allows the mixture to be modified to improve performance or it can be used to troubleshoot problems in the field. Ultimately, the Efficiency Chart can help the concrete industry to improve the reliability of air entrained concrete.

3.2 Experimental Methods

3.2.1 Laboratory Materials

All the concrete mixtures in this research used Type I cements that met the requirements of ASTM C150. Both the oxide analysis and Bogue calculations for the three different cements used are shown in *Table 3.2.* The fly ash used in the study was an ASTM C618 Class C and the oxide analysis is provided in *Table 3.2.* The LOI for this fly ash is < 0.5%. The aggregates were locally available crushed limestone and natural sand used in commercial concrete. The crushed limestone had a maximum nominal aggregate size of 19 mm (3/4"). One mixture contained a blend of the coarse and intermediate aggregate as noted in *Table 3.4.* Both the crushed limestone and the sand met ASTM C33 specifications. All the admixtures used are described in *Table 3.3.*, which met the requirements of ASTM C260 and ASTM C494.

Table 3.2. Type I cement oxide analysis.

Oxide (%)	Cement 0 (C0)	Cement 1 (C1)	Cement 2 (C2)	Fly Ash
SiO ₂	21.1	20.6	19.2	38.7
Al ₂ O ₃	4.70	3.76	5.36	18.8
Fe ₂ O ₃	2.60	3.07	2.30	5.80
CaO	62.1	64.9	62.5	23.1
MgO	2.40	3.25	2.99	5.60
SO ₃	3.20	2.09	4.17	1.20
Na ₂ O	0.20	0.08	0.33	1.80
K ₂ O	0.30	0.15	1.06	0.60
TiO ₂	-	-	0.22	1.50
P ₂ O ₅	-	-	0.22	0.40
Mn ₂ O ₃	-	-	0.10	-
SrO	-	-	0.31	-
Cr ₂ O ₃	-	-	0.01	-
ZnO	-	-	0.03	-
C ₃ S	56.7	67.0	57.5	-
C ₂ S	17.8	8.0	11.6	-
C ₃ A	8.20	5.00	10.31	-
C ₄ AF	7.80	9.00	7.01	-

Table 3.3. Admixture references.

Short Hand	Description	Application
WROS	Wood Rosin	Air-entraining agent
SYNTH	Synthetic chemical combination	Air-entraining agent
PC	Polycarboxylate	Superplasticizer
WR	Triethanolamine	Water reducer

The wood rosin (WROS) and synthetic (SYNTH) AEA are two popular commercial AEAs.

Twenty-three different mixture designs were investigated and are shown in *Table 3.4.*. The air content of these mixtures was varied to evaluate the quality and efficiency of the air void system.

A subset of mixtures was investigated with either a polycarboxylate (PC) superplasticizer meeting ASTM C1017, or a midrange water reducer (WR) meeting ASTM C494. A dose of between 60 and 200 mL/100 kg was used for the superplasticizer to increase the slump of the mixture between 50 mm to 200 mm. Between four and fourteen dosages of AEA were investigated for

each mixture to achieve a range of air contents from 2% to 10%. An ASTM C618 Class C fly ash was used in several of the mixtures with a 20% cement replacement by weight.

Table 3.4. Saturated Surface Dry (SSD) Mixture proportions.

w/cm	Cement kg/m ³	Fly-Ash kg/m ³	Paste Volume (%)	Coarse kg/m ³	Fine kg/m ³	Water kg/m ³	Admixture Used
0.45	362	0	29	1098	714	163	WROS
0.45	362	0	29	1098	714	163	SYNTH
0.53	362	0	32	1053	682	192	WROS
0.41	362	0	28	1127	722	148	WROS
0.39	362	0	27	1140	730	141	WROS
0.45	362	0	29	1098	714	163	WROS + PC1
0.45	362	0	29	1098	714	163	SYNTH + PC1
0.45	290	72	30	1089	709	163	WROS
0.45	223	56	23	785/573*	634	126	WROS
0.40	290	72	28	1115	724	145	WROS
0.40	290	72	28	1115	724	145	WROS + PC1
0.35	290	72	28	1127	768	127	WROS + PC1
0.40	290	72	28	1115	724	145	WROS + PC2
0.40	290	72	28	1115	724	145	WROS + PC3
0.40	290	72	28	1115	724	145	WROS + PC4
0.40	290	72	28	1115	724	145	WROS + PC5
0.40	290	72	28	1115	724	145	WROS + WR
0.40	362	0	28	1098	742	145	WROS
0.40	362	0	28	1098	742	145	WROS+PC1
0.45	335	0	27	1142	742	151	WROS
0.45	335	0	27	1142	742	151	WROS+PC1
0.50	335	0	29	1115	724	167	WROS
0.50	335	0	29	1115	724	167	WROS+PC1
0.45	C1: 362	0	29	1098	714	163	WROS
0.45	C2: 362	0	29	1098	714	163	WROS

* Mixture contained coarse and intermediate aggregates.
Cement 0 (C0) was used unless noted otherwise.

Data from the US Federal Highway Administration (FHWA) Turner Fairbanks Highway

Research Center laboratory in McLean, Virginia, USA was included in this study. This research has been summarized in previous publications [29].

3.2.2 Laboratory Concrete Mixture Procedure and Testing

Aggregates were collected from outside storage piles and brought into a temperature-controlled room at 23°C for at least 24 hours before mixing. Aggregates were placed in the mixer and spun, and a representative sample was taken for a moisture correction. At the time of mixing all aggregate was loaded into the mixer along with approximately two thirds of the mixing water. This combination was mixed for three min to allow the aggregates to approach the saturated surface dry (SSD) condition and ensure that the aggregates were evenly distributed.

Next, the cement, fly ash (if used), and the remaining water was added and mixed for three min. The resulting mixture rested for two min while the sides of the mixing drum were scraped. After the rest period, the mixer was started, and the admixtures were added. If the PC or WR was used, then it was added first and allowed to mix for 15 seconds to 30 seconds then the AEA was added. After the admixtures were added, the concrete was mixed for three minutes.

Samples were made for hardened air void analysis (ASTM C457). Two or three 7 L samples were tested with the SAM. These samples were investigated simultaneously by different operators to determine the average SAM Number of a concrete mixture. For the same level of prediction, it is recommended that two SAM tests be used. The SAM test was completed as per AASHTO TP 118. Other publications have shown good correlation with the SAM Number to the Spacing Factor as determined by ASTM C457 and freeze thaw performance by ASTM [4]. Further, the repeatability and reliability of the test has been established in the laboratory and the device has been widely used in the field [4-6]. The standard deviation of the SAM has found to be 0.049 with a coefficient of variation of 15.2% [4].

3.2.3 Sequential Air Method (SAM) and SAM Number

The SAM device is similar to the ASTM C231 Type B meter with some modifications. The SAM device uses six restricted clamps to account for increased pressures and a digital pressure gauge for testing. The test applies three sequential pressures to the fresh concrete and the

equilibrium pressures are recorded. The pressure is then released, and the same steps are applied again. The SAM Number is calculated by taking the numerical difference between the final pressure steps. The difference between the pressure responses is an indication of the air void size and spacing in the concrete. The SAM Number is an empirical number that has been correlated to the air void size and spacing from empirical relationships. Further details can be found in other publications and in a demonstration video of the test [4, 5, 30].

3.2.4 Hardened Air Sample Preparation

To evaluate the accuracy of the Efficiency Chart and SAM, their predictions are compared to predictions of Spacing Factors from a hardened air void analysis. To do this analysis, samples were cut into 19 mm thick slabs, the surface was treated with an acetone and lacquer mixture to harden the surface, and then the samples were lapped with sequentially finer grits. The prepared surface was then inspected under a stereo microscope. After a satisfactory surface was obtained, the hardener was removed with acetone. The sample was then blackened with black permanent marker, the voids were filled with less than 1 μm white barium sulfate powder, and the voids within the aggregates were blackened under a stereo microscope. This process left the surface of the concrete sample black and the voids within the paste white. Sample preparation details can be found in other publications [22, 31]. The Spacing Factor of the surface was then calculated following ASTM C457 method C using the Rapid Air 457 from Concrete Experts, Inc. A single threshold value of 185 was used for all samples in this research and the results do not include chords smaller than 30 μm . These settings have been shown to provide satisfactory results with the materials and instruments used and match the practices by others [22, 39, 40].

The hardened air-void analysis from the FHWA Turner Fairbanks Highway Research Center was completed by their staff with methods that may be different from that described above. This accounted for 29% of the data shown.

3.3 Estimating Air Void Efficiency with a Quantile Analysis

Because the SAM Number is comparable to the Spacing Factor this means that it is an indication of the bubble spacing in fresh concrete as shown in *Table 3.1.* The volume of air is another key indicator of the efficiency of the air void system. Because the SAM can determine both the volume and SAM Number then a single measurement with the device can be used to determine the efficiency of the air void system.

For example, a satisfactory SAM Number or bubble spacing could be obtained with either a low or high volume of air. However, a user may not have the experience to examine the SAM Number and air volume and realize the efficiency of the mixture. This work gathers a large set of data and makes this determination with a quantile based statistical analysis method using XLSTAT statistic software [45]. A quantile analysis is used to separate the data into different groups based on a chosen percentile. For example, a 50th quantile separates the data into two separate groups. For this work an 85th and 15th quantile is used. The 85th quantile gives a line where 15% of the observations lie above and 85% of the observations lie below. This will serve as a guideline for the upper bound estimate of efficiency for the large data set investigated. A lower bound estimate is set with the 15th quantile. Next, an α -quantile regression is used to find the equation that describes the boundary of the 85th and 15th quantile. A cubic equation was found to best fit the data.

These quantile lines are useful guides to highlight the upper and lower limits of the efficiencies for the data set investigated. This allows the air volume and SAM Number to be plotted by the user against these lines and it will indicate if the air void system in the concrete mixture has a high or low efficiency compared to a historic data set. For example, outcomes near the 15% quantile function have favorable combinations of air volume and bubbles spacing or high efficiency and those near the 85% quantile function have unfavorable combinations and are low efficiency mixtures. This can help a user to make an immediate evaluation of the efficiency of

the air void system in the fresh concrete. Using this immediate feedback, users can experiment with different ingredients, construction procedures, or environmental conditions and how they impact the quality of the bubble size and spacing in the concrete.

3.4 Results and Discussion

3.4.1 SAM Number and Spacing Factor Relationship

To confirm the accuracy of the data, the relationship between SAM Number and Spacing Factor is presented for the 227 laboratory concrete mixtures in *Figure 3.1.*. The results show that as the SAM Number increases so does the Spacing Factor. Past recommendations in freeze thaw analysis used a single value to determine if a material is recommended for freeze thaw durability [41]. A common Spacing Factor recommendation is 200 μm [41]. Past work has suggested that a SAM Number of 0.20 correctly determines if a Spacing Factor is above or below 200 μm for 88% of the data [4]. This means that 88% of the data falls in the upper right or lower left quadrants of *Figure 3.1.*. For this work, 84% of the data is correctly determined to be above or below 200 μm . Discussion over the variability of the data can be found in other publications [4, 5]. The Appendix B Table B.3 and B.4 contains the detailed data for the laboratory concrete mixtures.

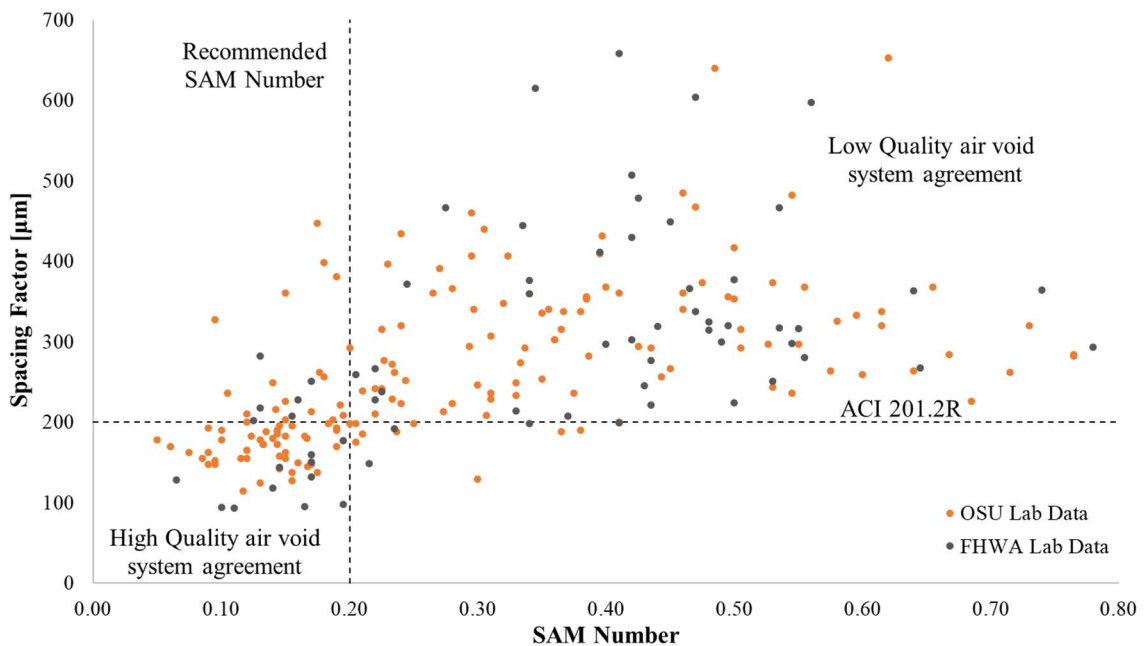


Figure 3.1. SAM Number versus Spacing Factor for 227 laboratory concrete mixtures completed by two different research groups.

3.4.2 SAM Number and Air Content Relationship

The correlation between the SAM Number and the Spacing Factor shows the usefulness of the SAM test. The two parameters that are measured in the SAM test are the air content and the SAM Number. The Efficiency Chart will let users compare their numbers to representative values based on previous data.

The relationship between the air volume and SAM Number is shown in *Figure 3.2.*. This graph of the air content, SAM Number, and the 85th and 15th quantile lines will be known as the Efficiency Chart. The 85th and 15th quantile lines are shown with cubic polynomial functions. These lines show the efficiency of the concrete with a given SAM Number at a given air content. 15% of the data falls below the High Efficiency Line and 85% of the data falls below the Low Efficiency Line. The data used to derive these lines are included on *Figure 3.2.* for easy review. Further, a plot that just has the High and Low Efficiency Lines has been included in the appendix so that it could be used in practice to estimate the efficiency of a concrete mixture.

The Efficiency Chart is based on 227 different concrete mixtures consisting of at least nine different admixture combinations, seven different water cement ratios (w/cm), and a range of 1.3% to 10.5% air contents. The quantile lines are dependent on the mixtures that were investigated. However, the results are helpful because they are based on a large and diverse data set. The estimated quantile functions are

Equation 3.1. High Efficiency Line:

$$\text{SAM Number} = -0.0006 \times (\text{Air Content})^3 + 0.0186 \times (\text{Air Content})^2 - 0.1888 \times (\text{Air Content}) + 0.6804$$

Equation 3.2. Low Efficiency Line:

$$SAM\ Number = 0.0014 \times (Air\ Content)^3 - 0.0102 \times (Air\ Content)^2 - 0.1061 \times (Air\ Content) + 0.9213$$

The standard error for the coefficients in *Equation 3.1.* and *Equation 3.2.* has been provided in the Appendix B, Tables B.1 and B.2. The coefficients within these equations correlate to the 85th and 15th quantile lines respectively.

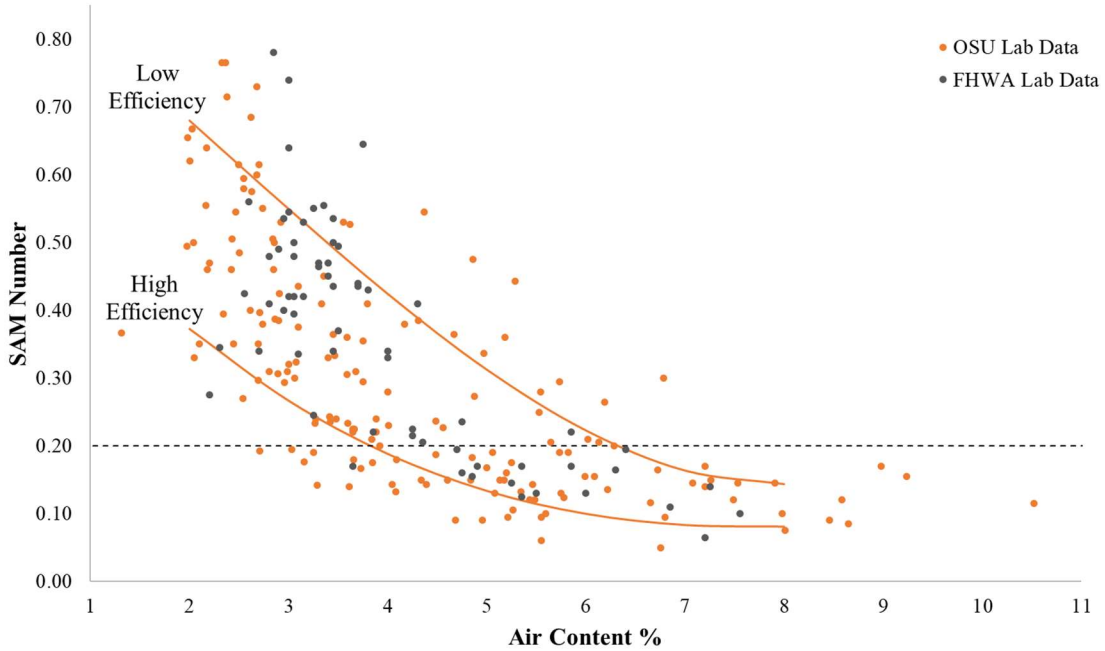


Figure 3.2. Air Content versus SAM Number for 227 laboratory concrete mixtures completed by two different research groups.

3.4.3 Application of the Efficiency Chart

Figure 3.3. shows air content and SAM Number results from the three conceptual concrete cross sections shown in *Table 3.1.*. Mixtures A and C have similar air volumes but different SAM Numbers. Mixtures A and B have similar SAM Numbers but different air volumes. When a mixture has a SAM Number and air volume combination that is close to the High Efficiency Line, this means that the air voids have a much smaller spacing than typical for the given air volume. If the Sam Number and air volume combination is close to the Low Efficiency Line, this means that the air voids have an unusually large spacing for that air volume.

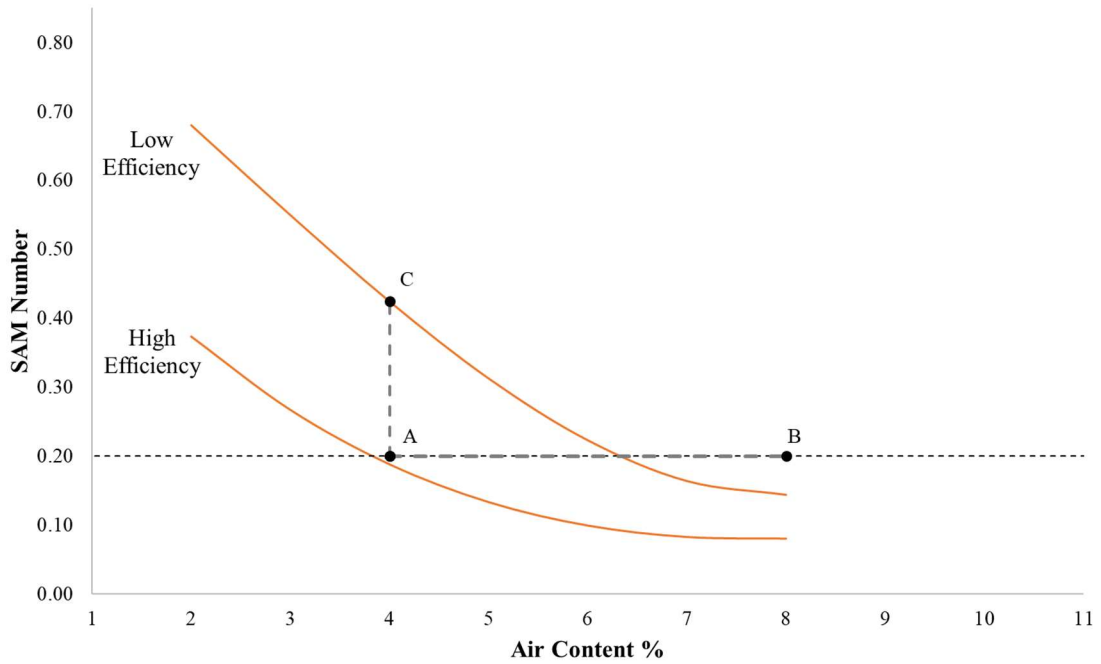


Figure 3.3. Efficiency Chart conceptual diagram.

3.4.4 The Impact of Water Reducers on Air Void Efficiency

In Figure 3.4., the comparison between air content and Spacing Factor is shown for two concrete mixtures with the same mixture proportions and air entraining agent but with and without a water reducer. The individual data points and linear trend lines are drawn for each admixture combination. The mixture containing only air entrainment shows a trend line that passes the Spacing Factor limit of 200 μm at approximately 6% air content. The mixtures that contain water reducers cross the 200 μm limit at approximately 8% air content. This shows the challenge of strictly using air content to obtain a satisfactory Spacing Factor.

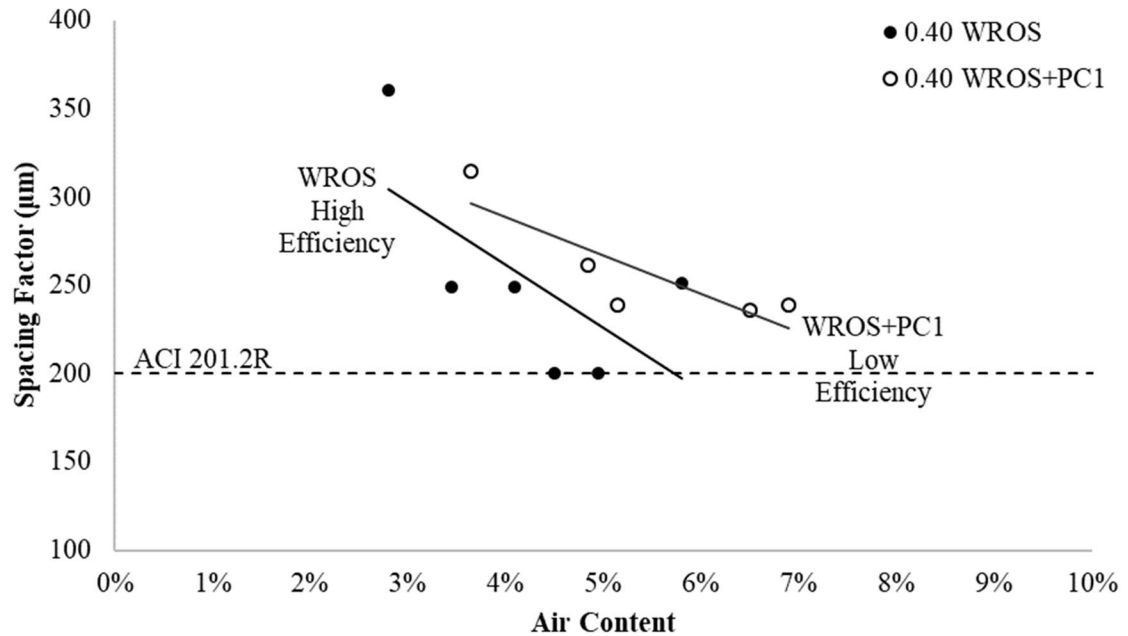


Figure 3.4. Air Content versus Spacing Factor for two laboratory mixture designs with different admixtures.

In Figure 3.5., the Efficiency Chart is shown for these same mixtures. The individual data points and cubic trend lines are drawn for each admixture combination. As can be seen in Figure 3.5., the mixtures showed the same trend as observed in Figure 3.4. or the mixture with the water reducer had a lower efficiency than the mixture without. This shows that the Efficiency Chart can identify how different admixture combinations change the efficiency of the air void system. It is worth emphasizing that a low efficiency air void system can produce a satisfactory Spacing Factor; however, it requires a higher air content. For example, at 6% air content, the mixture with only the air entraining agent, produces a Spacing Factor of 200 µm while the mixture with the blend of admixtures produced a Spacing Factor of 250 µm. This shows that the mixture with the blend of admixtures needs a higher air content to reach the same Spacing Factor and so it has a lower efficiency.

This difference in performance between these two mixtures may be caused by interactions between the admixtures that coarsens the air void system. This has been observed in a number of

previous publications [36, 43, 46, 47]. It should be noted that not all water reducers perform the same and this example was chosen to highlight the usefulness of the Efficiency Chart.

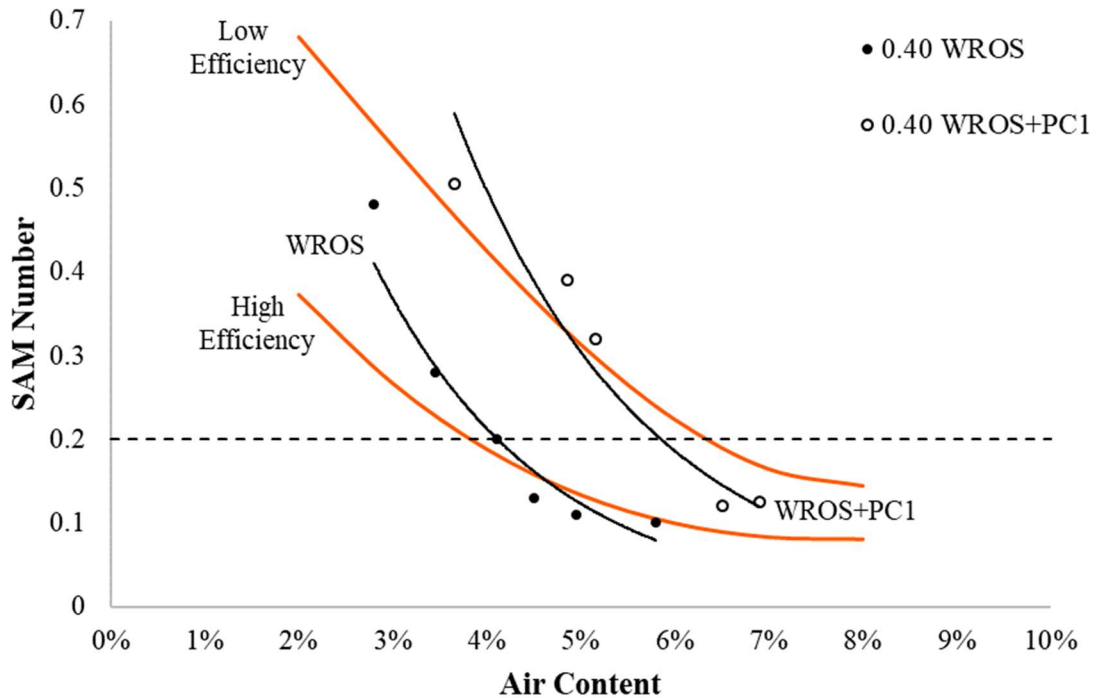


Figure 3.5. Air Content versus SAM Number for two laboratory mixture designs with different admixtures.

3.4.5 The Impact of Cement Type on Air Void Efficiency

Figure 3.6. compares the air content and Spacing Factor for two concrete mixtures with the same design but with different types of cements. The individual data points and linear trend lines are drawn for each mixture. The mixture containing C1 shows a trend line that passes the Spacing Factor limit of 200 μm at approximately 5.5% air content. The mixture containing C2 shows a trend line that passes the Spacing Factor limit of 200 μm at approximately 3.5% air content. This again shows the challenge of strictly using air content to reach a desired Spacing Factor and the differing efficiency that can occur in a mixture with minor changes in the materials.

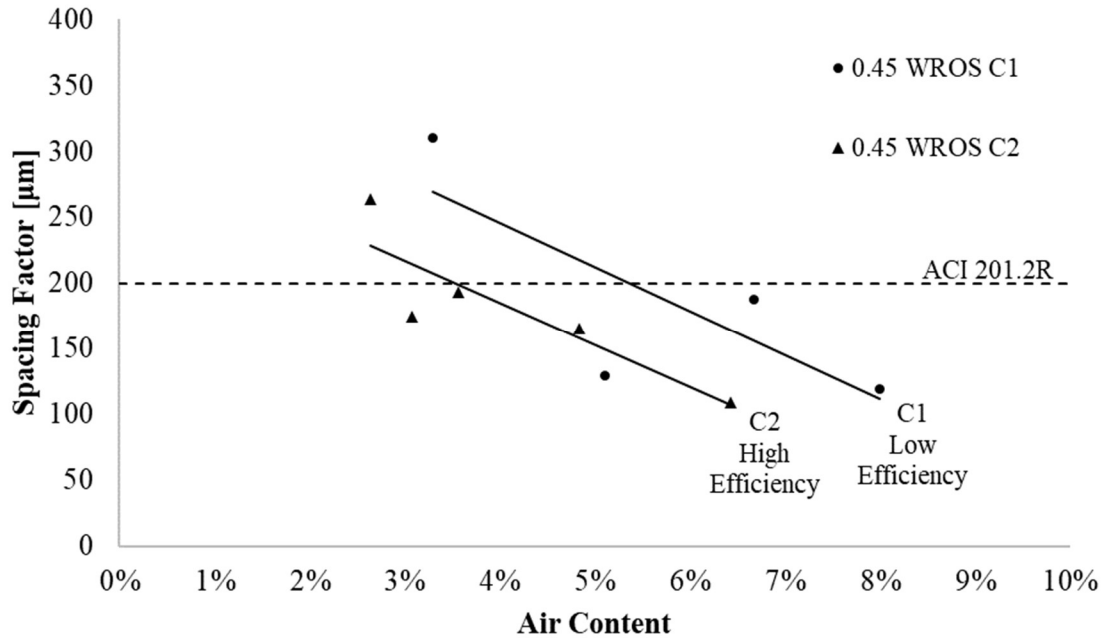


Figure 3.6. Air Content versus Spacing Factor for two laboratory mixture designs with different types of cement.

In Figure 3.7., a comparison between the air volume and SAM Number is shown for the same concrete mixtures. The Efficiency Chart results match those found by comparing the air volume and Spacing Factor. The mixtures containing C2 fall along the High Efficiency Line and the mixtures containing C1 fall closer to the Low Efficiency Line. By using different cements, the air void system quality drastically changes the air content necessary to reach a certain SAM Number and Spacing Factor. For example, the High Efficiency mixtures provide a Spacing Factor of 200 µm with an air content of 3.5% while the Low Efficiency provides a Spacing Factor of 200 µm with an air content of 5.5%. This shows that the mixture with a higher air content is less efficient due to the amount of air volume needed to reach the same Spacing Factor.

While this finding is intriguing it is outside the scope of this work to determine the exact reason for the change in performance between the two cements. There are a number of additives used in the cement production to enhance strength and also reduce the energy for grinding. At this point it is not clear how these additives impact the efficiency of the air void system, but it seems like

they may play a role in the performance, or this difference could be caused by some other factor. This is a subject of ongoing research. However, this shows the value of using the Efficiency Chart to compare how different ingredients change the efficiency of the air void systems as soon as the fresh concrete is tested with the SAM.

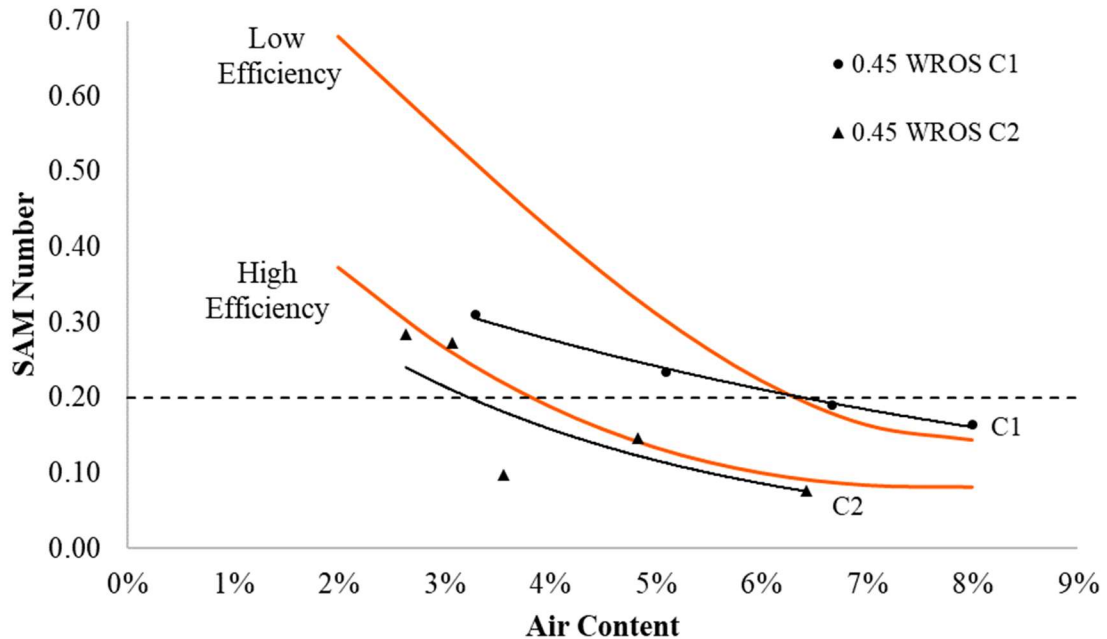


Figure 3.7. Air Content versus SAM Number for two laboratory mixture designs with different types of cement.

3.5 Practical Implications

The Efficiency Chart is valuable because users can complete a few concrete mixtures and determine the efficiency of their air void system in fresh concrete. This means that data that would require weeks to obtain and a significant amount of effort can be found from testing the fresh concrete. This is helpful because it gives immediate feedback to the concrete producer and allows a concrete mixture to be designed with the desired freeze thaw performance at the minimum air content. This will have much less impact on the strength of the concrete mixture and the stability of the air void system.

This is highlighted by the wide variety of data in *Figure 3.2.* at close to 4% air content. The mixtures with highest efficiency all plot near the bottom line and provide a satisfactory spacing factor of 200 μm . The mixtures with moderate and low efficiency all provide unsatisfactory spacing factors at the same air content. This highlights the importance of investigating efficiency in designing mixtures with the lowest possible air content with a satisfactory spacing factor for hundreds of concrete mixtures.

The Efficiency Chart can also be used to compare a number of different ingredients during the mixture design stage to find the best combination for the set of materials that are available.

Examples of this for different admixtures and cements are shown. The Efficiency Chart is also useful to troubleshoot problems as they occur in the field and identify how material or condition changes impacts the quality of the air void system. This feedback can guide changes in the material and determine the variables that impact the reliability of air entrained concrete.

3.6 Conclusion

A tool was created to show High and Low Efficiency Lines using both the SAM Number and air volume that defines the typical range of air void size for a given air volume in fresh concrete mixtures. These curves define the Efficiency Chart and act as guidelines to judge the performance of concrete mixtures. This work also shows that for the 227 mixtures investigated, the SAM test method closely relates to the Spacing Factor or quality of the air void system and can be used to determine the efficiency of the air void system.

These specific findings have been made:

- The cubic quantile lines provide useful boundaries on the Efficiency Chart that can be used to judge the efficiency of bubble spacing in fresh concrete.
- Satisfactory examples for cements and admixtures reinforce the usefulness of the Efficiency Chart in evaluating various concrete mixtures.

- For 227 laboratory mixtures, using thresholds of 0.20 for a SAM Number and 200 μm for Spacing Factor leads to the same classifications for 84% of the laboratory data.

The primary use of the Efficiency Chart is to give practitioners critical information about the quality of concrete mixtures before the material has hardened. Practitioners can change the mixture if it has low efficiency, and the Efficiency Chart gives the user immediate feedback on how the changes in ingredients and practices impacts the efficiency of the air void system in the concrete. The Efficiency Chart promises to be an important tool as researchers make more fundamental investigations of how different parameters impact the air void system in a concrete mixture.

3.7 Acknowledgements

The authors would like to acknowledge funding from the Oklahoma Transportation Center and Pooled Fund TPF-5(297) and the supporting states. Special thanks to Jason Weiss for the discussion over this work. We would also like to thank David Porter, Justin Becker, Brad Woodard, Zane Lloyd, Brendan Barns, Jacob Lavey, Chad Stevenson, Jason Toney, Mark Finnell, Michael Dickey, Braden Boyd, Erinn McArtor, Loren Emerson, Muwanika Jdiobe, Megan Buchanan, Tyler Suder, Lizzie Long, Erin Roark for their assistance in preparing samples.

CHAPTER IV

EVALUATION OF THE CONCRETE MIXTURE EFFICIENCY WITHIN CONSTRUCTION PRACTICES

4.1 Introduction

It is critical for the durability and performance of concrete that the correct properties of the concrete are obtained in the final structure. Concrete is tested during batching and after transport to the jobsite, but little testing is done during the placement of concrete. During placement, concrete is a plastic, and the movement, consolidation, and finishing can inadvertently change the properties of the concrete [48-52].

Changes in air entrained concrete is concerning during construction because air entrained concrete contains air bubbles that are critical for the freeze thaw durability of the concrete. These air bubbles are created during mixing, and to be effective, they must remain suspended within the mixture until the concrete stiffens. If these bubbles are significantly modified or destroyed during construction, then they cannot provide the needed freeze thaw durability.

It is common to limit the drop height of concrete during construction from 0.9 to 1.8 m to not damage the concrete [53-55]. There are concerns that if this drop height is higher, then it could impact the properties of the concrete. This paper focuses on the change in the air void volume, spacing, freeze thaw performance, and compressive strength of the concrete both before and after dropping.

The drop height of concrete measures the free-fall distance between a bucket, the ready mix truck chute or from a conveyor belt and the surface below [53-55]. Different construction methods can be used to reduce the free fall of the concrete by casting the concrete in a tube called a tremie.

The tremie is systematically pulled upward during construction. The tremie will catch the concrete with the walls after it falls and reduces the fall height for the subsequent concrete.

However, techniques to reduce freefall are not always practical, require additional logistics, and does not eliminate the drop height.

This work focuses on dropping concrete from a bucket at a known height onto hardened concrete.

This method was chosen because it simplifies the testing, and it is a worst-case scenario that regularly happens in practice. Despite these limitations, if the concrete mixtures are shown to be resistant to these conditions, then they should perform well in other less strenuous situations.

This work uses concrete mixtures that are designed to have air void systems with high and low air void efficiency. The air void efficiency relates the air void spacing and air volume in the concrete [56]. The air void spacing is the most important parameter to predict the freeze thaw durability of concrete [8, 21]. Mixtures with high air void efficiency will provide a satisfactory air void spacing with a low air content. This means that concrete has a smaller bubble size and so these bubbles are expected to be small and well distributed within the concrete. This means these bubbles are more resistant to being removed during construction. A new tool has been developed called the Efficiency Chart that can quantify the efficiency of the air void system in the fresh concrete. The Efficiency Chart uses both the air volume and SAM Number for the mixture and compares it to statistically derived limits that highlight high and low efficiency based on previous mixtures [56].

This work measures the air volume, air void distribution, freeze thaw durability, strength, and slump of concrete mixtures before and after drop heights of 1.52 m, 3.05 m, and 6.1 m. The Efficiency Chart will be a helpful tool in this study to compare different air void systems and how

they are impacted by dropping the concrete. In addition, a limited number of tests are done to concrete that is pumped and then dropped to see how this construction sequence impacts the air void system. Pumping is the preferred concrete placement method for many jobsite applications due to the increased efficiency, versatility, and economic benefits. This work is done because previous research shows that pumping may temporarily modify the air void system that may ultimately change the response to dropping the concrete.

4.2 Experimental Methods

4.2.1 Concrete Materials and Mixture Designs

Table 4.1. shows the oxide analysis and Bogue calculations for the cementitious materials used in all the concrete mixtures. The cement met Type I Portland cement as per ASTM C150 standards. Crushed limestone and natural sand were the aggregates used from local sources. Some mixtures used a combination of coarse and intermediate sizes noted in *Table 4.3.* All aggregates met ASTM C33 standards. The maximum nominal aggregate size of the limestone was 19 mm (3/4 in). *Table 4.2.* shows the admixtures used that met the ASTM C260 and ASTM C494 standards.

Table 4.1. Oxide analysis of cementitious materials.

Oxide (%)	SiO ₂	Al ₂ O ₃	Fe ₂ O ₃	CaO	MgO	SO ₃	Na ₂ O	K ₂ O	TiO ₂	P ₂ O ₅	SrO	C ₃ S	C ₂ S	C ₃ A	C ₄ AF
Cement	21.1	4.7	2.6	62.1	2.4	3.2	0.2	0.3	-	-	-	56.7	17.8	8.2	7.8
Fly Ash	25.3	19.3	5.2	32.5	7.8	2.6	3.4	0.6	1.1	1.9	0.3	-	-	-	-

Table 4.2. Admixture information.

Abbreviation	Description	Generic Chemical Name
WROS	Wood Rosin	Air-entraining agent
PC	Polycarboxylate	Superplasticizer

The air-entraining agent (AEA) in this research is a wood rosin (WROS) AEA. This is a common commercial AEA. *Table 4.3.* shows the three different mixture designs studied for the laboratory testing. A subset of mixtures was examined with a polycarboxylate (PC) superplasticizer meeting

ASTM C1017. The PC dosage was 138 and 162 mL/kg to achieve a 150mm and 200mm slump of the mixture respectively. Some of the mixture designs used a Class C fly ash replacement for 20% of the cement by weight that met ASTM C618 standards. Each mixture design consisted of three to eight dosages of AEA to study air contents from 3% to 10%. This allowed 29 mixtures to be investigated.

Table 4.3. Concrete Mixture Designs at SSD.

Mixture	w/cm	Cement kg/m ³	Fly-Ash kg/m ³	Paste Volume (%)	Coarse kg/m ³	Intermediate kg/m ³	Fine kg/m ³	Water kg/m ³	Admixture Used
1	0.45	489	122	29	1835	0	1195	275	WROS
2	0.45	564	0	26	1155	770	1250	254	WROS+PC
3	0.45	489	122	28	1113	552	1494	275	WROS+PC

4.2.2 Laboratory Concrete Mixing

Aggregates from outdoor storage piles were gathered and moved indoors to a controlled temperature of 23°C. After 24 hours, the aggregates were loaded into the mixer and spun. Samples were collected from the mixer for moisture corrections. After moisture corrections were calculated, all the aggregate and two-thirds of the water were placed in the mixer and spun for three minutes. This time allowed for evenly distributed aggregates and for the aggregates to be closer to saturated surface dry (SSD).

The residual water, cement, and fly ash were added next and mixed for three minutes. While the mixing drum was scraped, the concrete mixture rested for two minutes. Following the rest time, the mixer was spun, and the admixtures were added. The AEA was added 15 to 30 seconds after the PC and then the mixture was spun for three minutes.

4.2.3 Drop Height and Concrete Sampling Procedure

Immediately after mixing the concrete, slump (ASTM C143) and unit weight were measured [26]. One hardened air-void analysis (ASTM C457) sample was made from each concrete mixture for testing [2]. Two 7L samples were tested simultaneously with the SAM (AASHTO

TP 118) by different operators [1]. These were used to find the average SAM Number of a mixture. Two Freeze Thaw Durability (ASTM C666) beam samples were made to find the average Durability Factor of a mixture [3]. The remaining concrete was transferred from the wheelbarrow into a one-third cubic yard hopper. Wooden barricades were set around the bucket roughly ten feet on each side to contain any flying debris and protect workers. The hopper was then lifted to the test height using an overhead crane. The height was verified with a tape measure attached to the hopper. One technician held the tag line to reduce side sway when the concrete was dropped, while another pulled the rope attached to the handle on the hopper. This ensured the concrete would land in a controlled area.

Immediately after dropping the concrete, the concrete was tested with the same procedures used prior to dropping. These testing procedures are outlined in *Table 4.4.* The dropped concrete was gathered into a single pile to begin testing. It took approximately 25 minutes between initially sampling the concrete until sampling began after dropping the concrete.

As a control, several replicate concrete mixtures were tested without dropping the concrete. This allowed the changes in the concrete to be quantified without dropping. To mimic the timing of the dropped mixtures, the concrete was sampled immediately after mixing and then again after 25 minutes. During this period the concrete sat undisturbed. This is summarized in *Table 4.4.*

Table 4.4. Test procedures performed.

		Slump	Unit Weight	Hardened Air Void Analysis	Super Air Meter	Freeze Thaw Durability Beams	Compression Strength Cylinders
Dropped Mixtures	Prior to Dropping	1	2	1	2	2	12
	After Dropping	1	2	1	2	2	12
Not Dropped Mixtures	0 minutes	1	2	1	2	2	12
	After 25 minutes	1	2	1	2	2	12

4.2.4 Concrete Testing

4.2.4.1 Sequential Air Method (SAM)

The SAM testing is defined in AASHTO 118 [1]. The SAM device applies three sequential pressures to the fresh concrete and the equilibrium pressures are recorded. After the first pressure step, the air content is found [28]. The pressure is then released, and the same steps are applied again to the fresh concrete. The SAM Number is calculated by taking the numerical difference between the final pressure steps. The difference between the pressure responses is an indication of the air void size and spacing in the concrete. Further details can be found in other publications [32]. The SAM can be used to test concrete before it hardens, which provides insight into the air void system to help design and evaluate the air void system of the hardened concrete.

4.2.4.2 Hardened Air Void Analysis Sample Preparation

Concrete samples were cut into 19 mm thick slabs and polished with sequentially finer grits. The surface of the sample was preserved with an acetone and lacquer mixture to strengthen the surface before it was inspected under a stereo microscope. After an acceptable surface was obtained, the sample is cleaned with acetone. The surface was then colored with a black permanent marker, the air voids were filled with less than 1 μm diameter white barium sulfate powder, and the air voids within the aggregates were blackened under a stereo microscope. This process makes the concrete sample black and the voids in the paste white. Sample preparation details can be found in other publications [31, 38]. The sample analyzed with ASTM C457 method C using Rapid Air 457 from Concrete Experts, Inc, which uses chord counting. A single threshold value of 185 was used for all samples in this research and the results do not include chords smaller than 30 μm . A traverse length of 2286 mm was used for all samples to satisfy the requirements of ASTM C457. These settings and sample processing methods are like methods used in other publications [38-40].

4.2.4.3 Freeze-Thaw Durability

Concrete samples were tested based on the ASTM C666 standard test method for rapid freeze thaw durability [3]. Each sample was 406 mm long with a cross section of 76.2 mm by 101.6 mm. The beam samples were cured for 14 days prior to testing. Immediately after curing, samples were cycled through freezing and thawing temperatures. After approximately 36 cycles, each sample was measured for mass, length, and relative dynamic modulus of elasticity. The Durability Factors, shown in *Table 4.5*, were calculated accordingly [3].

4.2.5 Pumping and Dropping Concrete Mixtures

4.2.5.1 Pumping and Dropping Method

The pump and drop testing used a standard pipe network shown in *Figure 4.1*. The pipe network consists of a 1 m long single wall steel pipe reducer that reduces the 127 mm I.D. output of the pump to 102 mm. After the reducer, there is 9 m of 102 mm I.D. steel pipe with two 0.5 m radius 90° bends. At the end of the steel pipe network a 2 m, 102 mm I.D. pipe was inclined to create a 1.52 m drop distance for the concrete to free fall. The total volume of the pipe network was approximately 0.1 cubic meters.

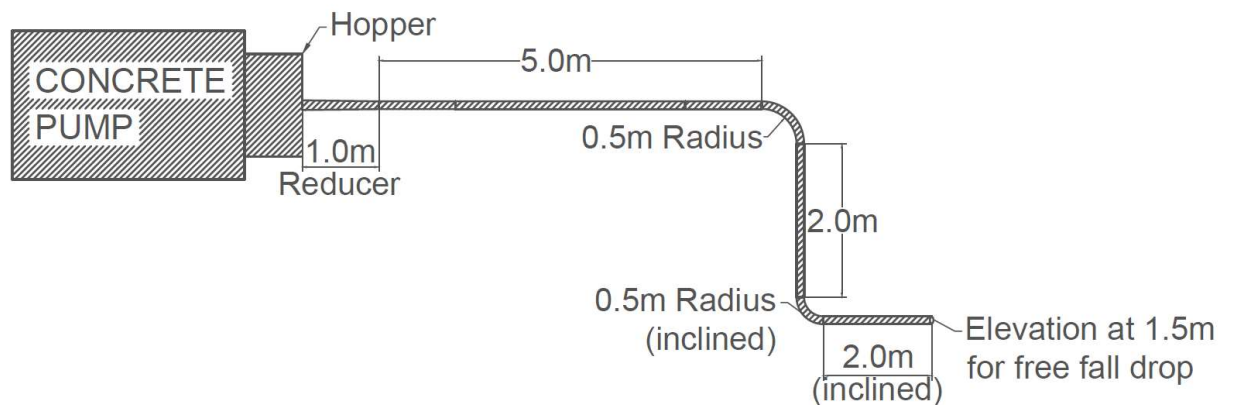


Figure 4.1. Plan View of the pipe network.

4.2.5.2 Pumping Mechanisms that Impact Air Void Distribution

It is common to lose up to 50% of the air volume during pumping. Three primary mechanisms impact the volume change during pumping. These mechanisms are vacuum, impact, and pressure. The literature suggests that these variables likely play a key role in the bubble size, distribution, and volume in a concrete mixture [57-59].

When concrete overcomes the frictional resistance in the pipe network and free falls to a 90 degree bend, when concrete free falls from excessive heights while being placed, or when concrete is poured into the hopper of the pump, air content can be lost from the mixture [57, 60].

Typical concrete pumps can apply pressure ranging from 2068 kPa to 3447 kPa [59, 61, 62].

Research has shown that when the concrete is under pressure it will cause air bubbles in the concrete to dissolve. This dissolution of air is controlled by Henry's Law [59, 61]. The smaller bubbles are observed to dissolve first. This is caused by the smaller bubbles having a higher pressure according to the Young-Laplace equation [57, 61]. However, once the pressure is released, the dissolved air will return to a gas. Measurements on 30 laboratory and 60 field mixtures show that the air returns to the concrete at a similar spacing factor and freeze thaw durability [58, 59].

4.3 Results

4.3.1 Efficient and Inefficient Concrete Mixture Designs

Table 4.5. shows the data set for all the concrete mixtures studied prior to and after dropping the concrete.

Table 4.5. Concrete Testing Data.

Mix	Drop Height (m)	Time of Test	Slump (mm)	AASHTO TP 118		ASTM C457			ASTM C666	ASTM C39		
				Air Content (%)	SAM Number	Hard Air (%)	Spacing Factor (µm)	Specific Surface (mm ²)	Durability Factor	14 days	28 days	
1	0	Prior	198	4.2%	0.20	3.2%	239	25.37	92%	4771	4907	
		After	-	3.5%	0.22	4.4%	251	21.01	96%	4534	5258	
		Prior	191	5.1%	0.16	3.1%	196	21.54	96%	3689	4286	
		After	-	4.5%	0.13	6.4%	155	24.69	94%	3619	4419	
		Prior	203	6.6%	0.11	5.3%	145	33.48	94%	3827	3456	
		After	-	5.7%	0.13	4.6%	173	29.67	91%	3836	4137	
	3.05	Prior	188	4.0%	0.18	3.7%	213	27.37	95%	5036	5708	
		After	74	2.8%	0.23	3.5%	286	22.81	92%	5402	6003	
		Prior	165	6.1%	0.13	7.7%	124	30.65	99%	4434	5086	
		After	74	4.4%	0.15	4.2%	196	25.67	97%	5007	5694	
		Prior	124	4.0%	0.17	4.2%	241	23.42	98%	4415	4806	
		After	41	2.7%	0.24	3.4%	362	17.71	94%	4680	5236	
	6.10	Prior	114	5.4%	0.17	3.5%	191	31.17	100%	4198	4675	
		After	46	3.2%	0.23	4.2%	254	21.23	98%	4498	5156	
		Prior	165	6.8%	0.06	4.8%	160	32.03	96%	3605	3916	
		After	71	4.4%	0.15	3.1%	246	25.32	96%	4362	4353	
		Prior	122	8.2%	0.11	7.8%	127	29.25	96%	5279	5927	
		After	38	5.8%	0.12	4.6%	226	22.97	95%	5613	6081	
	2	0	Prior	51	3.1%	0.40	3.9%	378	14.77	1%	5301	5365
			After	-	2.6%	0.35	4.5%	279	18.69	3%	5430	5630
			Prior	203	5.3%	0.48	4.9%	224	10.85	15%	3765	4863
			After	-	3.5%	0.43	5.4%	345	13.33	4%	4168	5075
			Prior	165	8.2%	0.10	8.0%	152	21.66	96%	4593	4862
			After	-	5.7%	0.11	-	-	-	89%	4805	4717
1.52		Prior	64	3.3%	0.51	3.4%	295	19.22	9%	5286	5896	
		After	25	2.6%	0.36	2.8%	351	17.52	15%	5303	5933	
		Prior	114	5.2%	0.16	6.3%	201	20.90	89%	4880	5243	
		After	46	3.7%	0.35	4.3%	244	20.91	57%	4721	5884	
		Prior	76	6.4%	0.06	6.3%	191	22.02	96%	4862	5359	
		After	46	4.2%	0.15	4.5%	277	17.99	91%	5230	5877	
3.05		Prior	203	3.9%	0.46	4.0%	333	15.92	11%	5827	6172	
		After	58	2.8%	0.41	2.9%	419	14.74	2%	5848	6549	
		Prior	236	5.8%	0.32	6.4%	345	12.13	44%	5424	5680	
		After	84	3.2%	0.43	3.1%	340	17.33	28%	5436	6283	
		Prior	224	6.3%	0.16	6.7%	224	15.92	90%	5010	5528	
		After	79	3.8%	0.28	3.8%	297	18.87	63%	5592	6052	
3*		0	Prior	229	6.7%	0.15	6.5%	178	23.83	96%	-	-
			After	178	7.5%	0.08	7.7%	164	22.09	94%	-	-
		1.52	Prior	224	5.8%	0.31	6.9%	272	15.28	56%	3714	3918
			After	178	5.2%	0.19	-	-	-	100%	4151	4473
			Prior	224	8.0%	0.06	8.3%	152	22.72	96%	4619	4862
			After	173	6.1%	0.15	7.0%	234	17.34	94%	4904	5134
	Prior		191	10.4%	0.04	10.9%	99	26.08	96%	3980	4361	
	After		165	8.8%	0.07	8.4%	140	23.92	98%	4250	4509	

* concrete mixtures were pumped

4.3.2 Efficiency Chart

Figure 4.2. shows the Efficiency Chart with the relationship between the air content and SAM Number of two different concrete mixture designs [56]. These data points represent the measurements before the concrete was dropped. The top Efficiency Line represents low efficiency, and the bottom line is high efficiency. The closer a concrete mixture falls to the high

efficiency line, the more efficient the mixture design will be. The orange data points represent mixtures from an efficient mixture design and the blue data points represent mixtures from an inefficient mixture design. In *Figure 4.2.*, the set of inefficient mixtures move toward the high efficiency line when the air content reaches 6.5 percent. The material combination for this mixture design creates an inefficient air void system because it takes far greater amounts of air to reach an efficient system than the efficient mixture design. The efficiency of the air void system will be an important parameter in understanding the performance of the concrete from impact.

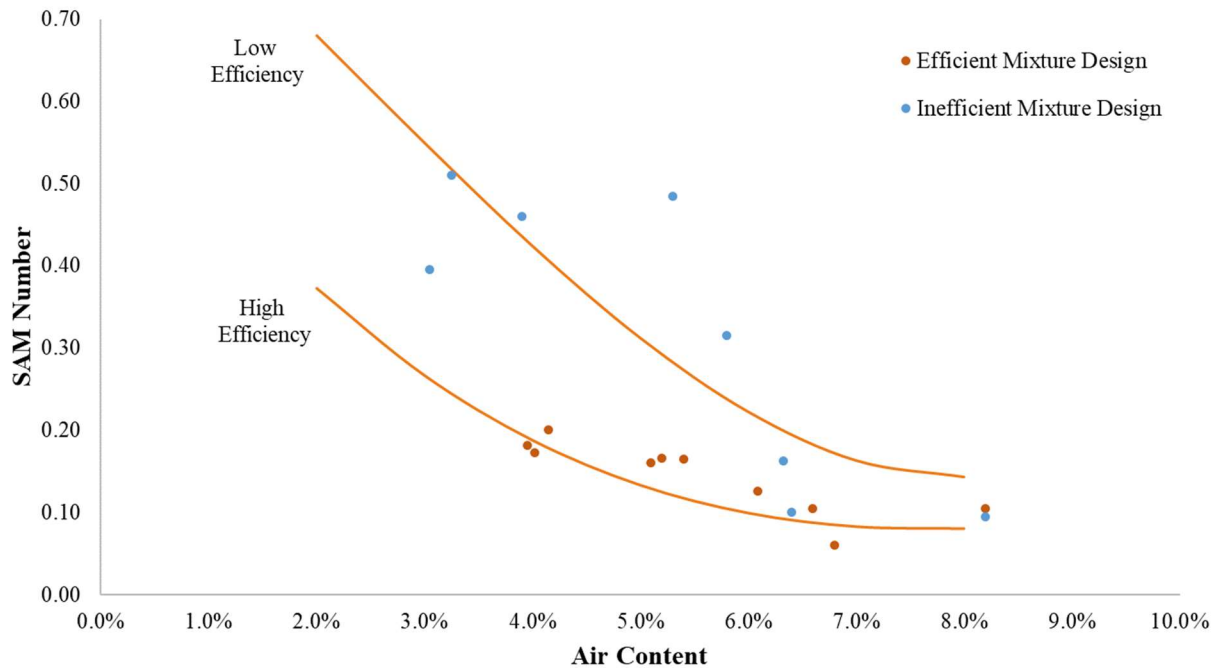


Figure 4.2. Efficiency Chart with Air Content versus SAM Number for two concrete mixture designs.

4.3.3 Compressive Strength Change

Figure 4.3. and *Figure 4.4.* shows the percentage change in compressive strength for mixtures that were dropped at various heights and control mixtures there were not dropped. The results are grouped by mixtures with efficient and inefficient air void systems. The percentage of change in

14-day and 28-day compressive strength shown in *Figure 4.3.* and *Figure 4.4.* is the compressive strength after drop minus the compressive strength prior to drop divided by the compressive strength prior to drop. For example, if the mixture starts with 34722 kPa prior to drop and then after drop achieves 37246 kPa, the percent change in strength would be 7.3 percent.

The percent change on average for efficient and inefficient mixtures does not exceed 10.2 percent for both 14-day and 28-day compressive strength. This means that no matter the drop height or mixture design for this study, the compressive strength did not show a significant change.

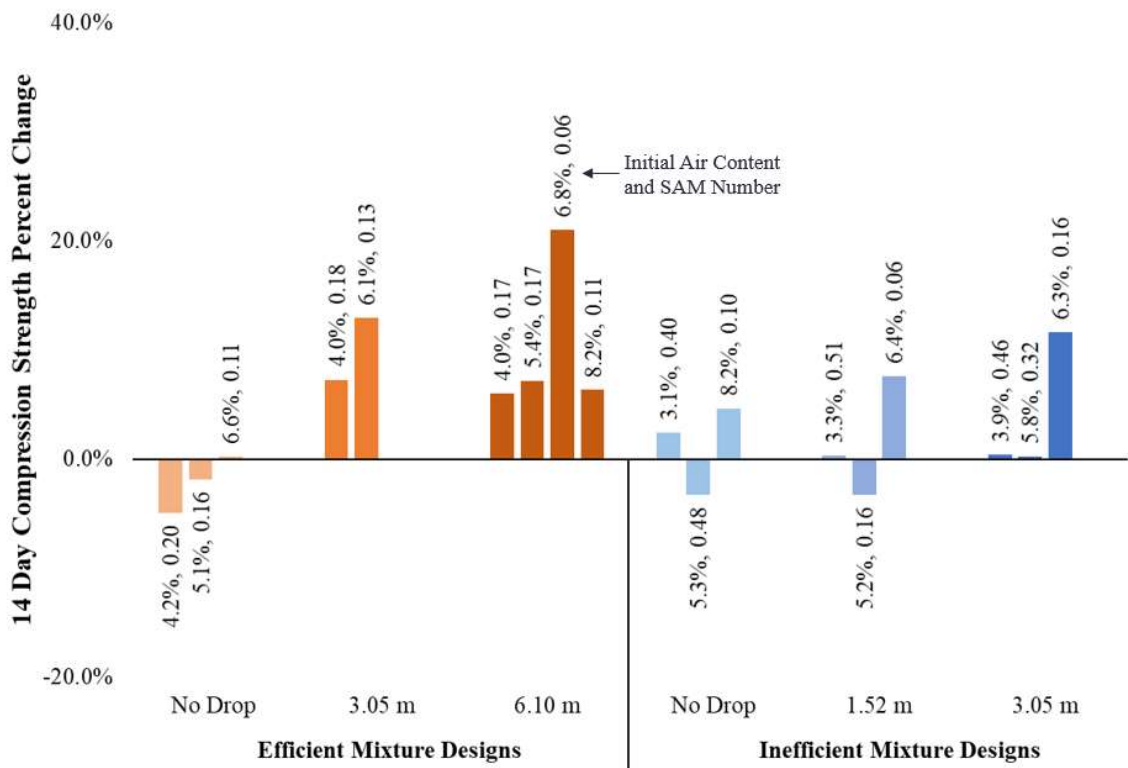


Figure 4.3. Concrete mixtures dropped at different heights versus percent loss in 14 day compression strength.

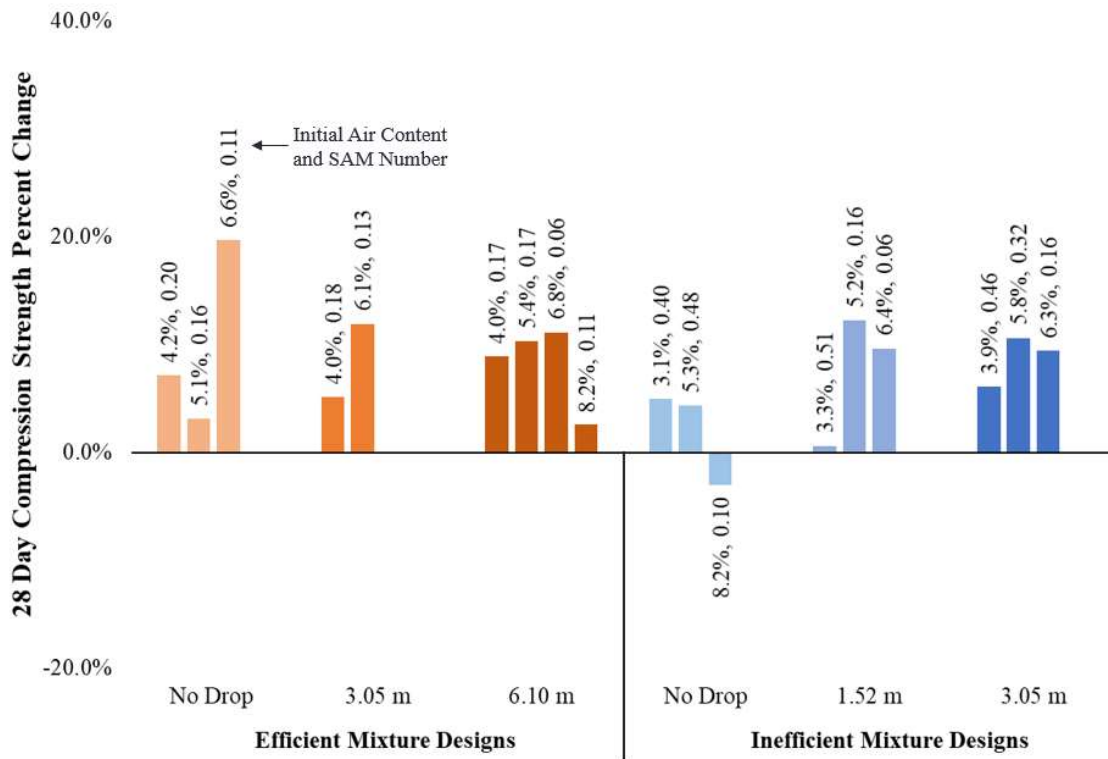


Figure 4.4. Concrete mixtures dropped at different heights versus percent loss in 28 day compression strength.

4.3.4 Air Content Change

Figure 4.5. shows the percentage change in air content for mixtures that were dropped at various heights and control mixtures that were not dropped. The results are grouped by mixtures with efficient and inefficient air void systems. The percentage of air content lost shown in Figure 4.5. is the air content prior to drop minus the air content after drop divided by the air content prior to drop. For example, if the mixture starts with 6 percent air prior to drop and then after drop contains 4 percent air, the percent loss of air would be 33 percent.

Efficient mixtures that were not dropped, labeled “No Drop,” lost on average 14 percent air, while the inefficient mixtures that were not dropped lost on average 27 percent air. This shows the difference of the air void efficiency on mixtures that are not disturbed. This may be caused by the larger air voids contained in the inefficient mixtures.

As the concrete impacts the ground, the air content changes depending on the air void efficiency. The concrete mixtures with efficient air voids lost air; however, the air that was lost seemed to be the larger air voids. This will be shown in the following sections with the SAM Number data. The efficient air voids are expected to be small and well distributed. This may have also helped to minimize the air loss because there are fewer large air voids within the air void system. This performance is deemed to be satisfactory and so additional testing was done with a 6.10 m drop height. The efficient mixtures dropped at 6.10 m lost on average 20% more air than the mixtures that were not dropped. While this seems like a large reduction in air content, the small air voids that are important for freeze thaw durability will prove to not be impacted in the following sections.

The concrete mixtures with inefficient air voids at 3.05 m had a 38% reduction in the air content. The inefficient mixtures have larger air voids that are more buoyant and so these are expected to be easier to escape. Because of the unacceptable behavior, the drop height was decreased to 1.52 m. At this height, the percentage of air content lost was on average 27 percent and for the “No Drop” mixtures there was on average 29 percent lost. This is a very small difference between the two mixture sets.

After performing the statistical, student t test, there was major discrepancies when comparing the percent changes of the data. Initial values for air content, SAM Number, Spacing Factor, and Durability Factor before the drop were not held constant due to the variability of concrete. It was not possible to hold all of the test results constant prior to drop; therefore, this statistical analysis was not helpful in studying the results.

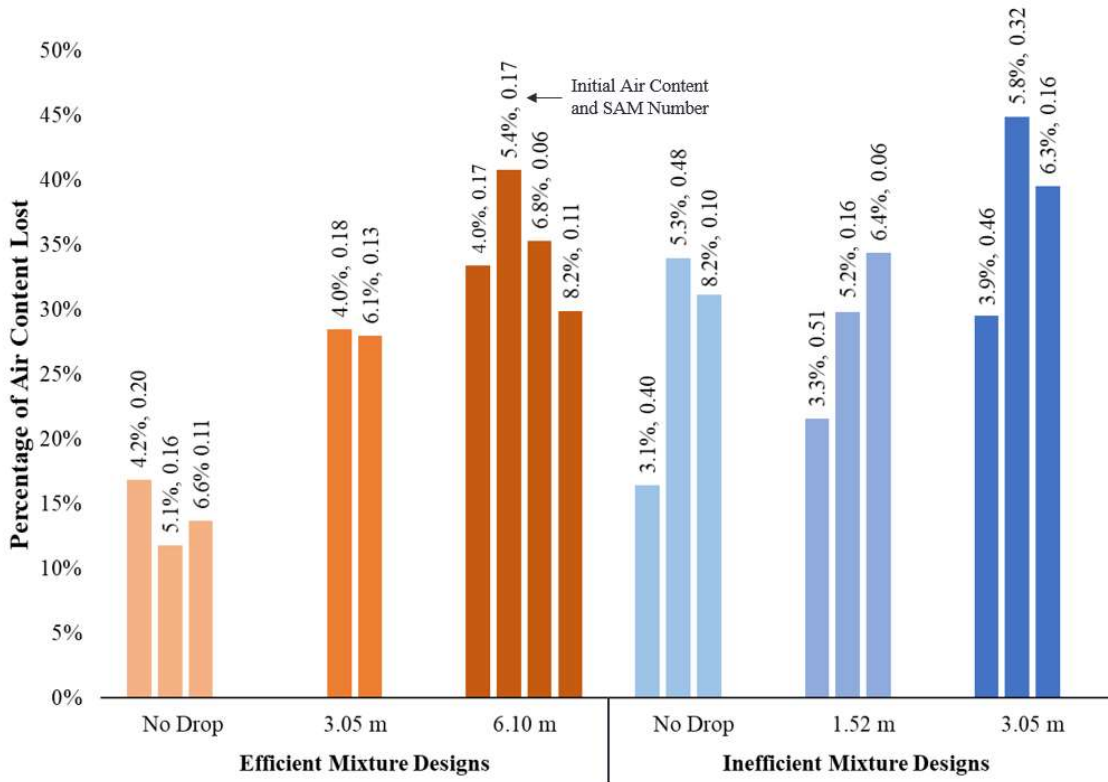


Figure 4.5. Concrete mixtures dropped at different heights versus percent loss in air content.

4.3.5 SAM Number Change

Figure 4.6. shows the percent change in SAM Number. The SAM Number percent change is the SAM Number after drop minus the SAM Number prior to drop divided by the SAM Number prior to drop. An increase in SAM Number or a positive percent change in SAM Number, means that the air void spacing increases. If the SAM Number decreases after the drop, the air void spacing decreases. For example, if the mixture starts with a 0.17 SAM Number prior to drop and then after the drop it has a 0.23 SAM Number, the percent change would be 36 percent and the air void spacing increased.

In Figure 4.6., the efficient mixtures that were not dropped show similar change in SAM Number to mixtures that were dropped at 3.05 m and 6.10 m except one mixture. The one mixture with the higher percent change started with a very low SAM Number of 0.06, which resulted in a larger percent change. All the other efficient mixtures had a less than 40 percent change in SAM

Number. This means that the drops did not significantly impact the small air voids after the impact of the mixture. The efficient air void system mixtures that were dropped at 6.10 m were slightly higher change in SAM Number, but all passed freeze thaw durability testing.

The inefficient mixtures that were not dropped show less change in SAM Number than mixtures that were dropped at 1.52 m and 3.05 m. The mixtures dropped at 1.52 m show a change in SAM Number that is 70 times larger than the mixtures that were not dropped. Mixtures with an initial air content around 5 percent have a less stable air void system than those starting at a higher air content. This can be expected because according to the efficiency chart, low air volumes for this mixture provide coarser air void systems. This has been observed in several previous publications [36, 43, 46, 47]. These changes in SAM Numbers are the result of a change in air void distribution. Larger SAM Numbers represent higher spacing of bubbles within the concrete [4, 5, 56]. This explains why the inefficient mixtures show a higher change in SAM Number at the 3.05 m drop than the 1.52 m drop.

Efficient mixtures dropped at 6.10 m changed 57 percent, while inefficient mixtures that were dropped at 1.52 m changed on average 71 percent. The efficient mixture that was dropped 6.10 m lost a similar amount of air volume as the inefficient mixture that was dropped 1.52 m.

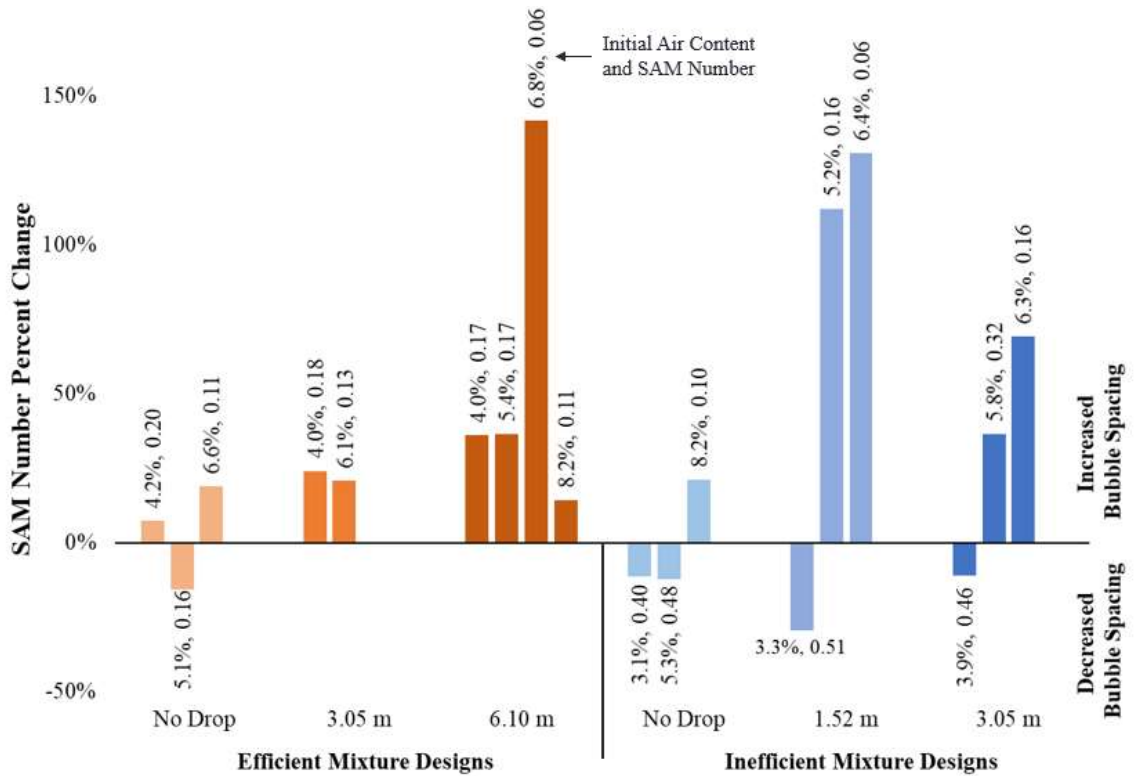


Figure 4.6. Concrete mixtures dropped at different heights versus percent change in SAM Number.

4.3.6 Spacing Factor Change

Figure 4.7. shows the same set of concrete mixtures with the Spacing Factor and SAM Number results. The results show that as the SAM Number increases so does the Spacing Factor. The two recommendation limits, 200 microns for Spacing Factor and 0.20 for SAM Number, for each measurement are shown with dashed lines [4, 5, 41]. In Figure 4.7., the relationship between SAM Number and Spacing Factor shows an 83 percent agreement. This means that 83% of the data falls in the upper right or lower left quadrants of the plot. This percent agreement is similar to that of previous studies [4, 5, 56]. This shows that the change in the spacing factor and SAM Number are correlated, even in concrete that has been dropped.

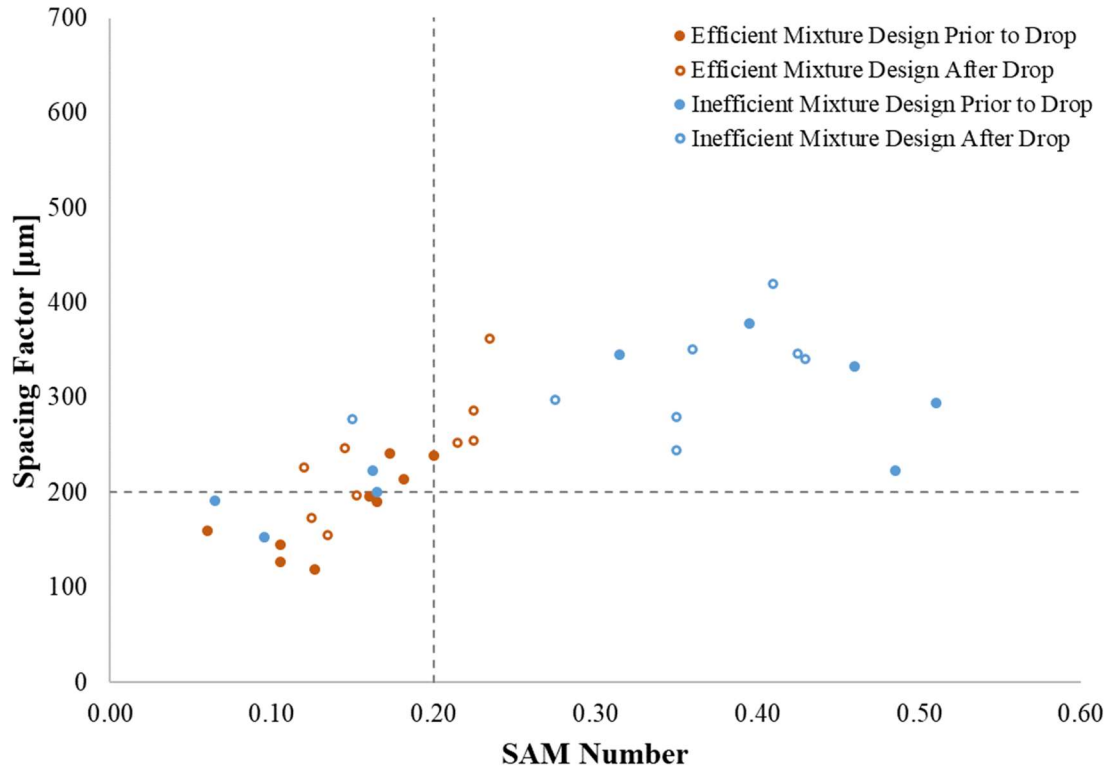


Figure 4.7. SAM Number versus Spacing Factor for concrete mixtures dropped at different heights.

4.3.7 Durability Factor Change

Figure 4.8. shows the percent change in Durability Factor. All the efficient mixtures have a passing freeze thaw durability performance (Durability Factor > 70%) before and after the drop and most of the inefficient mixtures did not pass the freeze thaw durability testing (Durability Factor < 70%) after the drop.

The efficient set of mixtures show on average a 2 percent change in Durability Factor this shows the impact of the drop had little impact on the freeze thaw performance of the concrete. This is a large contrast to the inefficient mixtures that show on average a 34 percent change.

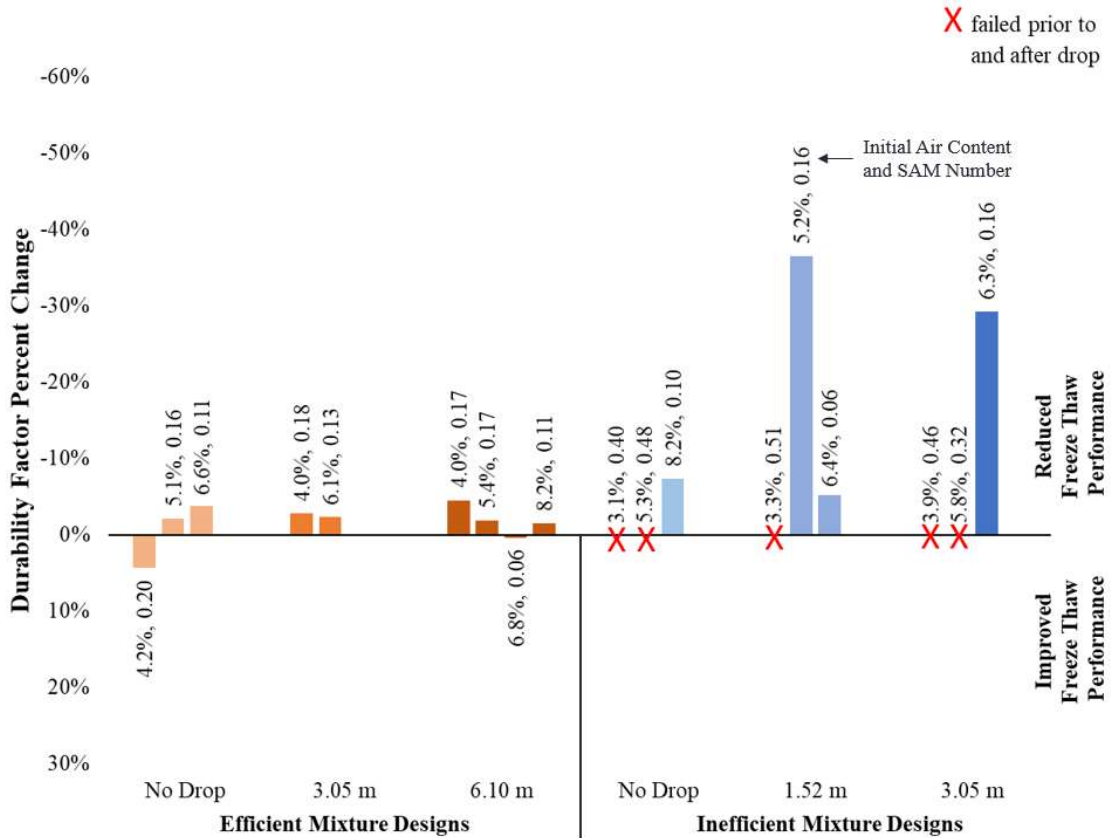


Figure 4.8. Concrete mixtures dropped at different heights versus percent change in Durability Factor.

To compare the correlation of the SAM Number to the Durability Factor, Figure 4.9. compares the results of these two measures. The two recommendation limits, 70 percent for Durability Factor and 0.32 for SAM Number, for each measurement are shown with dashed lines [4]. The results show that at a SAM Number of 0.32, the Durability Factor dramatically decreases. In Figure 4.9., The SAM Number relationship to the Durability Factor shows a 94% agreement prior to and after the drop. This means that 94% of the data falls in the upper left or lower right quadrants of the plot. This means that the SAM Number is a useful tool to predict the freeze thaw durability of the concrete before and after it is dropped.

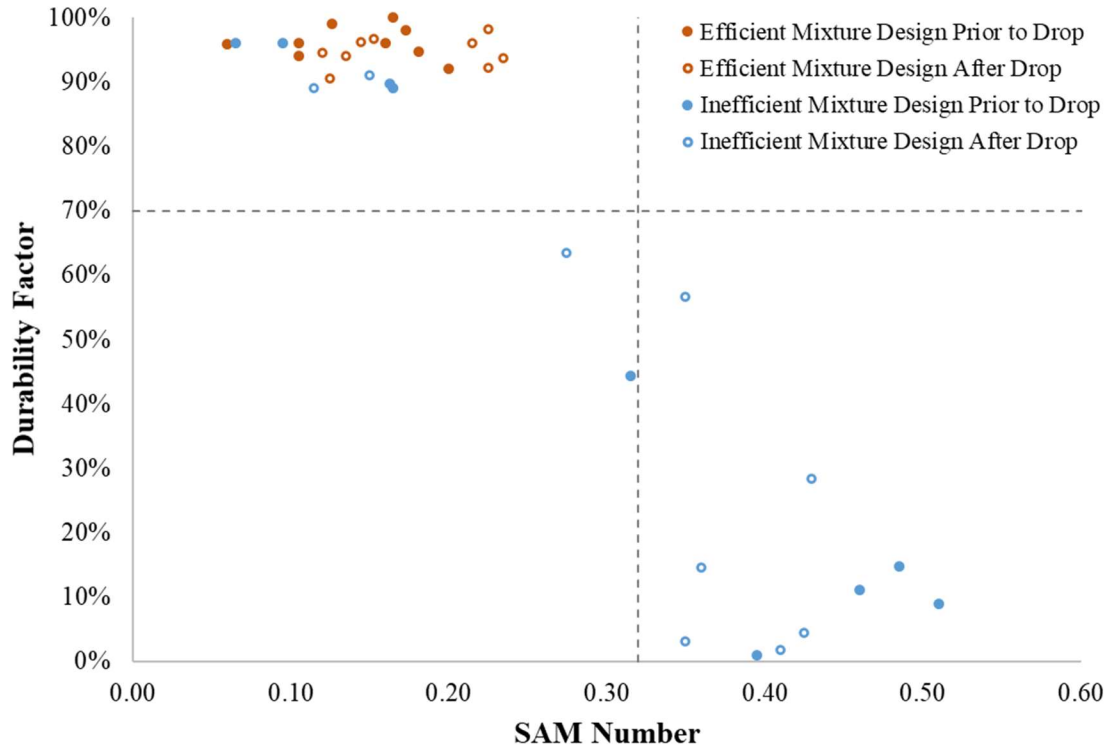


Figure 4.9. SAM Number versus Durability Factor for concrete mixtures dropped at different heights.

4.4 Discussion

Overall, the efficient mixtures could show up to 40 percent change in air content without significant changes in SAM Number, Spacing Factor, or Durability Factor. The inefficient mixtures with an initial air content less than 5 percent showed a significant change in the SAM Number, Spacing Factor, and Durability Factor when they were dropped. This poor performance even occurred at a drop height of 1.52 m. The SAM Number, Spacing Factor, and Durability Factor results agree in comparison between efficient and inefficient mixtures. This means that SAM Number measurements in the field are a useful way to determine how the impact of the drop will change the quality of the air void system.

4.5 Pump and Drop Comparison

4.5.1 Air Content Change

Figure 4.10. shows the percent loss in air content for inefficient concrete mixture designs not dropped, dropped at 1.52 m, pumped with no drop, and pumped with a 1.52 m drop. All mixture designs provided inefficient air void systems. The mixtures that were not pumped show a greater percentage or air content loss than the mixtures that were pumped. Dropping concrete after pumping shows a smaller change in air content than mixtures that were not pumped. This reduced air loss could be caused by the pumping causing a portion of the air voids to dissolve in solution as shown in previous work [58, 59, 61, 62]. This means these air voids would not be lost by the impact.

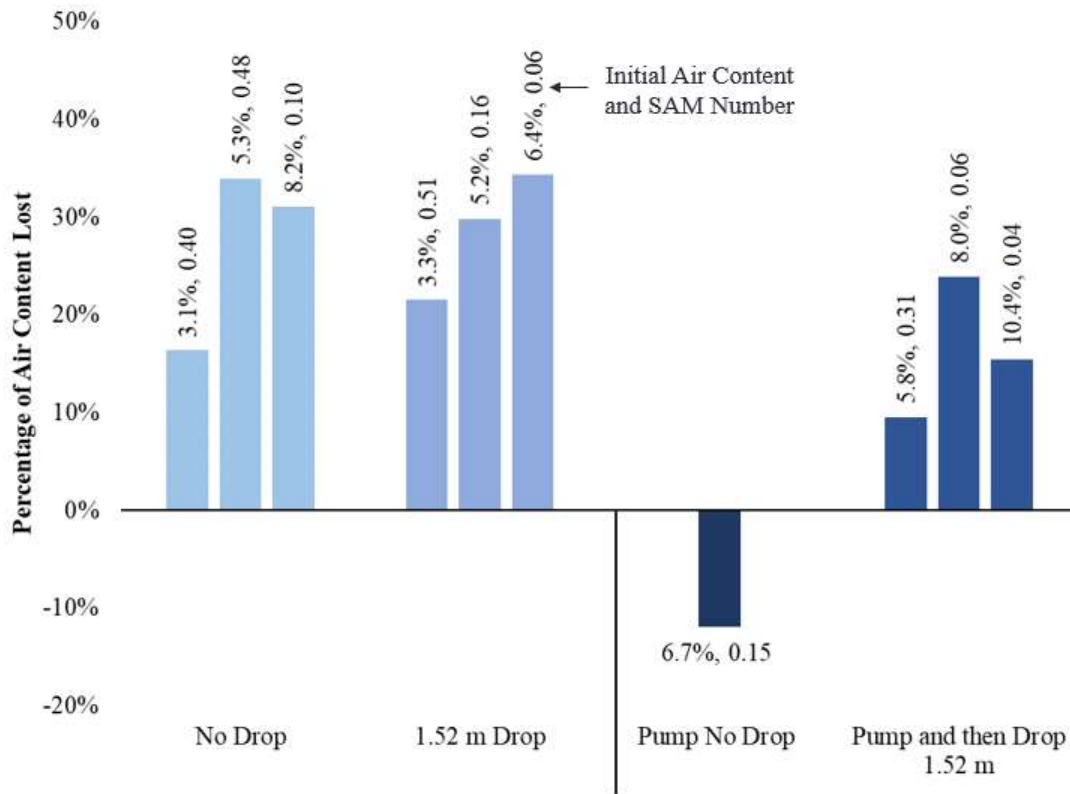


Figure 4.10. Inefficient concrete mixtures not dropped, dropped at 1.52 meters, pumped with no drop and pumped with a 1.52 meter drop versus percent loss in air content.

4.5.2 Sequential Air Method Change

Figure 4.11. shows the percent loss in SAM Number for the same mixtures discussed in the previous section. Mixtures that were not pumped show similar changes in SAM Number as mixtures that were pumped. However, "Pump Drop 1.52 m" mixture with 5.8% air content shows a significant drop in SAM Number. This could be due to air voids dissolving into solution before impacting the surface at the drop [57, 62]. Those air voids are not able to be affected during the 1.52 m drop.

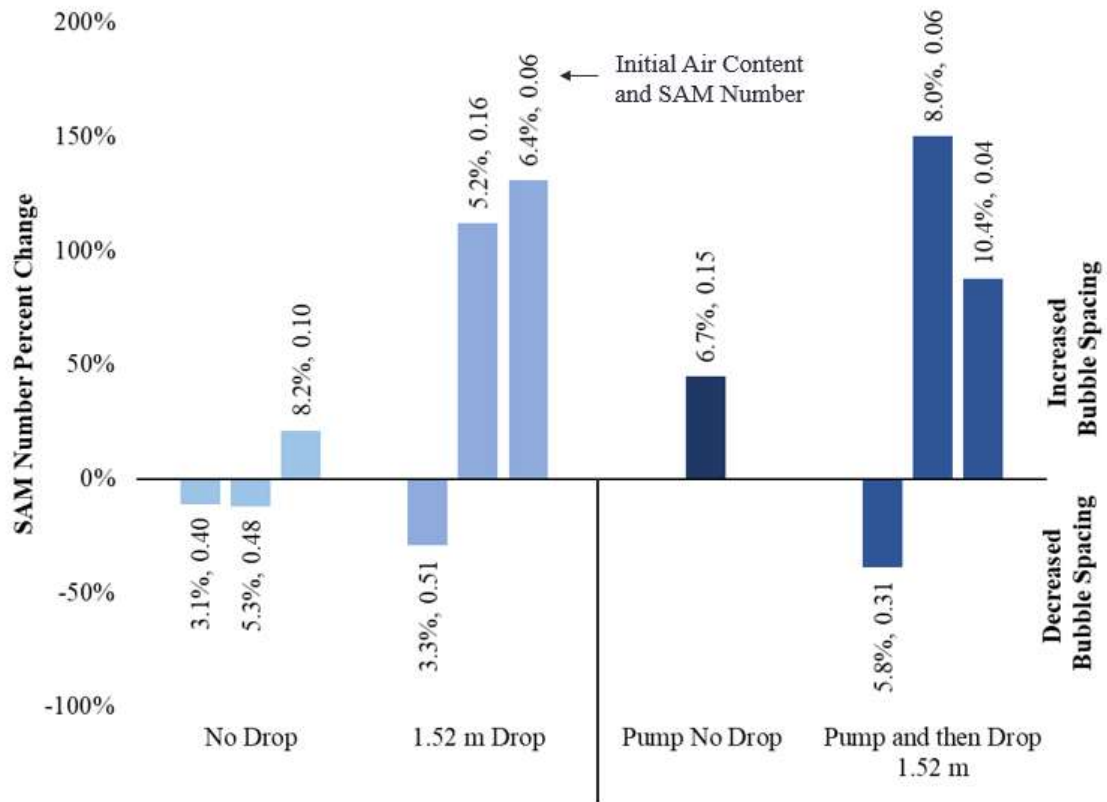


Figure 4.11. Inefficient concrete mixtures not dropped, dropped at 1.52 meters, and pumped then dropped at 1.52 meters versus percent change in SAM Number.

4.5.3 Spacing Factor Change

Figure 4.12. shows the same set of concrete mixtures as discussed in the last two sections with results from the percent change in Spacing Factor. Due to the higher unit values of the Spacing Factor measurements, the percent changes are smaller than those shown in the SAM Number changes. The changes shown in Figure 4.12. shows that mixtures that were dropped show a higher change in Spacing Factor than those that were not dropped whether they were pumped or not.

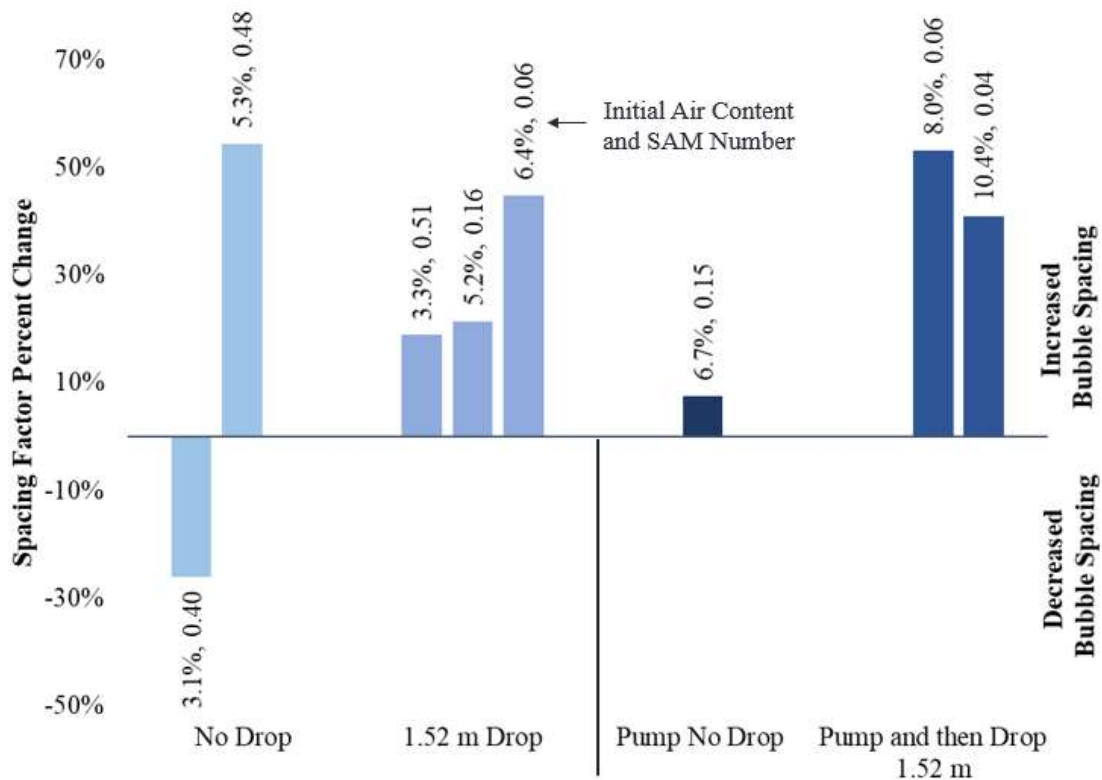


Figure 4.12. Inefficient concrete mixtures not dropped, dropped at 1.52 meters, and pumped then dropped at 1.52 meters versus percent change in SAM Number.

4.5.4 Durability Factor Change

Figure 4.13. shows the percent loss in Durability Factor for mixture designs previously discussed. Mixtures that were not pumped show larger changes in Durability Factor than mixtures that were pumped. This shows the mixtures with an air content less than 5.5 percent showed worse freeze thaw performance over time regardless of if they are dropped. However, the mixtures that were pumped all showed satisfactory performance regardless of the air content. This could mean that pumping inefficient mixtures could remove the concern of losing the air bubbles over time or from an impact. More work is needed to with a wider arrange of materials to understand this.

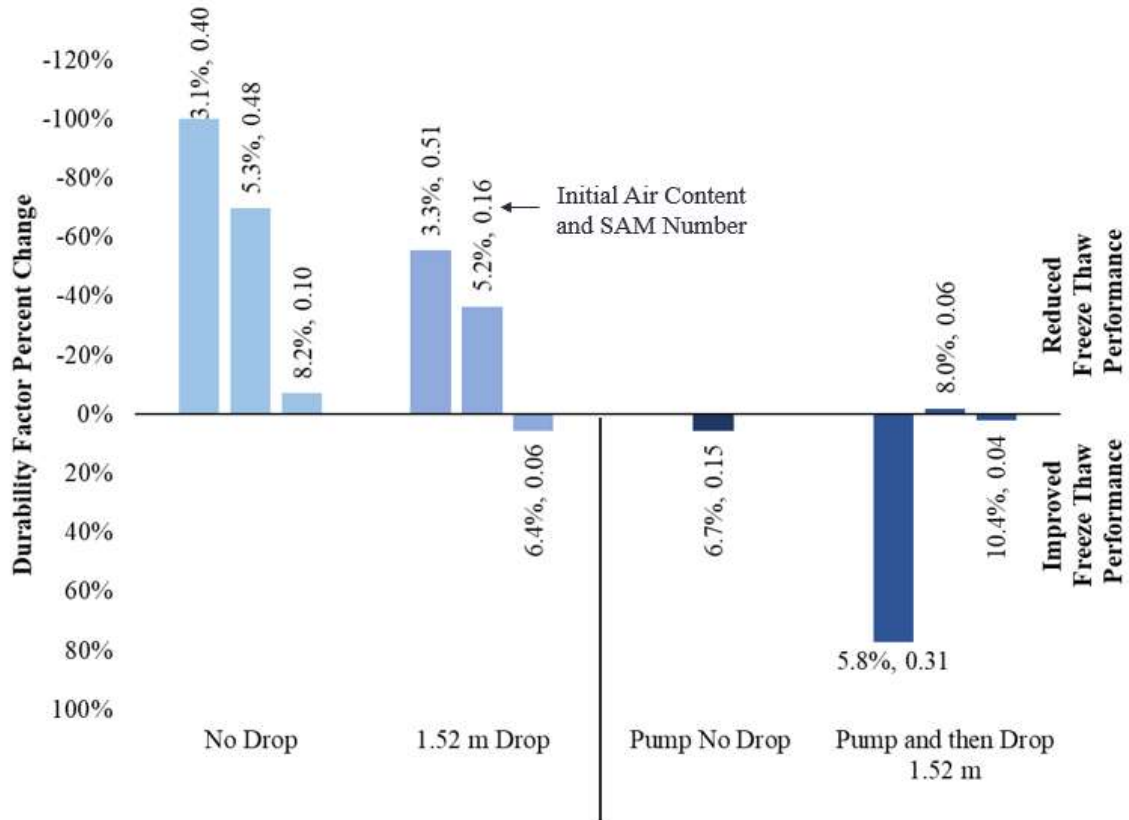


Figure 4.13. Inefficient concrete mixtures not dropped, dropped at 1.52 meters, and pumped then dropped at 1.52 meters versus percent change in Durability Factor.

4.5.5 Differences in Drop Height Impact on Pumped and Non-Pumped Concrete

After pumping and dropping, the mixture with 5.8% air content shows a significant drop in SAM Number and Durability Factor. This could mean that pumping inefficient mixtures could improve the quality of air void system by dissolving the smaller bubbles into solution before impact. If the pressure mechanism drives the bubbles into solution before the mixture is dropped, the bubbles are less likely to get ‘knocked out’ of the system by the impact [57, 60, 62]. More mixtures should be studied to see if this phenomenon could be repeated.

4.6 Practical Significance

This study shows that drop height effects on air void distribution depends on the efficiency of the concrete mixture. Efficient mixtures can sustain greater drop heights while maintaining the

quality of the air void distribution. For example, in *Figure 4.8*, all the efficient mixtures passed freeze thaw durability no matter the drop height. Using an efficient mixture would give contractors less restrictions on concrete drop heights if the in-place air void distribution is close to that measured before dropping. However, dropping inefficient mixtures had a significant impact on the air void distribution. Looking at *Figure 4.8*, again, the inefficient mixtures show major changes in durability factors throughout. It should be advised that efficient mixtures should be used when dropping concrete to ensure the quality of the hardened concrete.

In addition, pumping inefficient concrete did not have a negative impact on the air void efficiency. Therefore, contractors can pump and drop concrete without concern of losing air void efficiency. The possible dissolving of the small bubbles prior to impact due to pumping, ensures they cannot be “knocked out” at impact. This would allow contractors to increase drop height limits when pumping and may allow easier construction in certain situations, reducing the time and cost of certain projects.

The SAM Number continues to be a useful tool to evaluate the air void distribution in concrete and to learn more about different construction techniques. The SAM Number could be used to investigate concrete before and after dropping to gain important insights into the impact on the Spacing Factor and the Durability Factor of the concrete.

4.7 Conclusions

An efficient concrete mixture design is less likely to be affected by free fall impact if the quality of the air void system is higher prior to drop. The compression strength shows less than 10.2 percent change throughout the mixtures. All the mixtures lost air after dropping; however, the efficient mixtures did not lose the high-quality air void system. The SAM Number, Spacing Factor, and Durability Factor results agree in comparison between efficient and inefficient mixtures.

After pumping and dropping, the mixture with 5.8% air content shows a significant drop in SAM Number and Durability Factor. This could mean that pumping inefficient mixtures could improve the quality of air void system by dissolving bubbles into solution prior to drop. If the pressure mechanism drives the bubbles into solution before the mixture is dropped, the bubbles are less likely to get 'knocked out' of the system [57, 60, 62]. More mixtures should be studied to see if this phenomenon could be repeated more.

- Efficient mixtures that were not dropped lost on average 13 percent less air than inefficient mixtures that were not dropped.
- Efficient mixtures dropped at 6.10 m lost similar air amounts to inefficient mixtures that were dropped at 1.52 m.
- Efficient mixtures dropped at 6.10 m changed 14 percent less in SAM Number on average than inefficient mixtures that were dropped at 1.52 m.
- Efficient mixtures dropped at 6.10 m show less change in Durability Factor than inefficient mixtures dropped at 1.52 m.
- The Efficiency Chart can help identify concrete mixtures that may be susceptible to change in air void distribution after larger drop heights.
- The mixtures containing PC show a less efficient air void system when the air content is less than 6 percent.

CHAPTER V

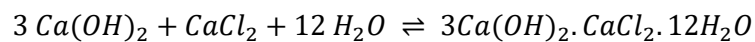
QUANTIFYING CALCIUM OXYCHLORIDE FORMATION USING MICRO-COMPUTED TOMOGRAPHY

5.1 Introduction

Concrete pavements have experienced damage near the joints due to the accumulation of deicing salts that have dissolved into water and entered the concrete [9-14]. This solution can increase the degree of saturation and increase the potential for freezing and thawing damage when the chloride concentration is low [15-19]. As the salt concentration increases, the accumulating fluid can result in the formation of several solid phases such as Friedel's salt (FS), Kuzel's salt, and calcium oxychloride (CaOXY) [63-75].

When portland cement reacts with water, one of the hydrated particles that is formed is calcium hydroxide Ca(OH)_2 . The salt solution ($\text{CaCl}_2 + \text{H}_2\text{O}$) reacts with Ca(OH)_2 to form CaOXY [76-87]. This chemical reaction is shown in *Equation 5.1*. represents a common form of CaOXY that has been associated with concrete deterioration [15, 16, 64, 66, 70-72, 88-98].

Equation 5.1. Formation of CaOXY:



Equation 5.1. is a reversible phase change that depends on the temperature and the CaCl_2 content as illustrated in Figure 5.1. [14, 98]. Figure 5.1. shows that when the temperature is above the liquidus line, the $\text{Ca}(\text{OH})_2 + \text{H}_2\text{O} + \text{CaCl}_2$ solution is a fluid without CaOXY present. When the temperature is below the liquidus line, a phase change occurs and solid CaOXY begins to form. For this study it should be noted that this phase change occurs above freezing temperatures.

Figure 5.1. shows that at 20 percent CaCl_2 and 20°C , solid CaOXY is present within the solution.

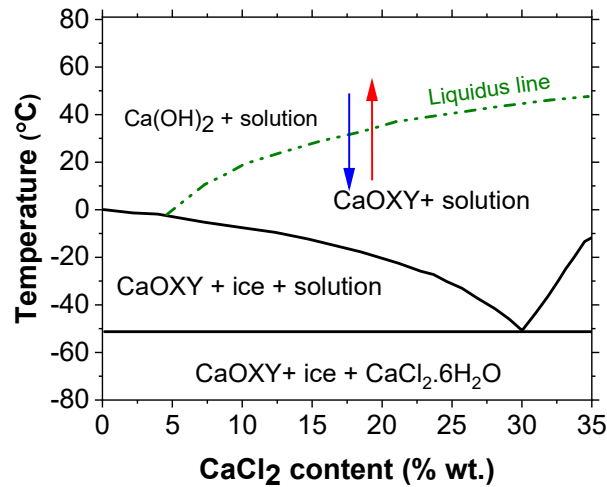


Figure 5.1. Phase diagram of $\text{Ca}(\text{OH})_2\text{-CaCl}_2\text{-H}_2\text{O}$ [14, 98].

The form of CaOXY shown in Figure 5.1. causes an increase in volume of 303 percent from $\text{Ca}(\text{OH})_2$ [90, 92, 94]. The growth of products from this volume change will create pressure inside the concrete that may cause damage [66, 75, 99-101]. Studies have shown that the volume of CaOXY formation can vary throughout the different temperature changes [98, 102]. More information is needed about the distribution of CaOXY growth and damage.

For this study, mortar samples will be examined using Micro computed tomography (Micro-CT). Micro-CT is a non-destructive x-ray tool that can be used to investigate the three-dimensional microstructure of materials. It has been widely used in medical science to investigate biological organisms [103-105]. This method has also been used to study construction materials to analyze

crack propagation [106-108] and air void distribution [109-112]. The Micro-CT captures a series of radiographs from different angles. These radiographs can be used to build a three-dimensional model of the structure called a tomograph. This tomograph can be then used for qualitative and quantitative analyses [113-118]. Each sample can be scanned by the Micro-CT multiple times because of the non-destructive test. This allows samples to be scanned at various times throughout the process. Previous work has studied the microstructure of concrete and mortar samples that have been exposed to freezing and thawing cycles [118-122]. However, for this study, the samples will not be exposed to freezing temperatures to ensure that the damage shown is caused by CaOHY growth without freeze-thaw damage. Micro-CT will be used to quantify the volume growth of product change in air voids and crack formation within each sample at a high level of Degree of Saturation (DOS).

5.2 Experimental Methods

5.2.1 Concrete Materials and Mixture Designs

Table 5.1. shows the oxide analysis and Bogue calculations for the cementitious materials used in all the concrete mixtures. The cement met Type I Portland cement as per ASTM C150 standards. Each mixture contained Class C fly ash as per ASTM C618. Crushed limestone and natural sand were the aggregates used from local sources. Mixture designs are noted in *Table 5.3.*. Both aggregates met ASTM C33 standards. The maximum nominal aggregate size of the limestone was 19 mm (3/4 in).

Table 5.2. shows the admixtures used that met the ASTM C260 and ASTM C494 standards.

Table 5.1. Oxide analysis of cementitious materials.

Oxide (%)	SiO ₂	Al ₂ O ₃	Fe ₂ O ₃	CaO	MgO	SO ₃	Na ₂ O	K ₂ O	C ₃ S	C ₂ S	C ₃ A	C ₄ AF	LOI
Cement	21.1	4.7	2.6	62.1	2.4	3.2	0.2	0.3	56.7	17.8	8.2	7.8	2.7
Fly Ash	27.0	18.1	4.6	30.5	6.4	2.6	2.7	1.1	-	-	-	-	0.12

Table 5.2. Admixture information.

Abbreviation	Description	Generic Chemical Name
WROS	Wood Rosin	Air-entraining agent
PC	Polycarboxylate	Superplasticizer

The air-entraining agent (AEA) in this research is wood rosin (WROS) AEA. This is a common commercial AEA. Table 5.3. shows the two different mixture designs studied for the laboratory testing. All the mixture designs used a Class C fly ash replacement of 20% or 40% of the portland cement by weight. Each fly ash replacement also contained an air content of about 2.5% and 6%. This created four different mixtures.

Table 5.3. Concrete Mixture Designs at SSD.

Mixture	w/cm	Cement kg/m ³	Fly-Ash kg/m ³	Paste Volume (%)	Coarse kg/m ³	Fine kg/m ³	Water kg/m ³	Admixture Used
20FA	0.45	202	36	21	981	971	125	WROS
40FA	0.45	218	145	29	1098	712	163	WROS

5.2.2 Concrete Mixing

Aggregates from outdoor storage piles were gathered and moved indoors to a controlled temperature of 23°C. After 24 hours, the aggregates were loaded into the mixer and spun. Samples were collected from the mixer for moisture corrections. After moisture corrections were calculated, all the aggregate and two-thirds of the water were placed in the mixer and spun for three minutes. This time allowed for evenly distributed aggregates and for the aggregates to be closer to saturated surface dry (SSD).

The residual water, cement, and fly ash were added next and mixed for three minutes. While the mixing drum was scraped, the concrete mixture rested for two minutes. Following the rest time, the mixer was spun, and the admixtures were added.

5.2.3 Concrete and Mortar Sampling and Testing

5.2.3.1 Sampling of Concrete and Mortar

Immediately after mixing the concrete was completed, slump (ASTM C143) and unit weight (ASTM 138) were measured [26, 123]. One hardened air-void analysis (ASTM C457) sample was made from each concrete mixture for testing [2]. Two 7L samples were tested simultaneously with the SAM (AASHTO TP 118) by different operators [1]. These were used to find the average SAM Number of a mixture. Two Freeze Thaw Durability (ASTM C666) beam samples were made to find the average Durability Factor of a mixture [3].

After the concrete samples were made, mortar samples were taken from the same concrete mixture [124]. A 9.5 mm sieve was used to remove the coarse aggregate from the concrete. Two mortar cylinders were made in 102 mm by 203 mm molds. Further testing was completed on these samples that will be discussed in section 2.3.

5.2.3.2 Sequential Air Method (SAM)

The SAM testing is defined in AASHTO 118 [1]. The SAM device applies three sequential pressures to the fresh concrete and the equilibrium pressures are recorded. After the first pressure step, the air content is found like the Type B meter [28]. The pressure is then released, and the same steps are applied again to the fresh concrete. The SAM Number is calculated by taking the numerical difference between the final pressure steps. The difference between the pressure responses is an indication of the air void size and spacing in the concrete. Further details can be found in other publications [32]. The SAM can be used to test concrete before it hardens, which provides insight into the air void system to help design and evaluate the air void system of the hardened concrete.

5.2.3.3 Hardened Air Void Analysis Sample Preparation

Concrete samples were cut into 19 mm thick slabs and polished with sequentially finer grits. The surface of the sample was preserved with an acetone and lacquer mixture to strengthen the surface before it was inspected under a stereo microscope. After an acceptable surface was

obtained, the sample is cleaned with acetone. The surface was then colored with a black permanent marker, the air voids were filled with less than 1 μm white barium sulfate powder, and the air voids within the aggregates were blackened under a stereo microscope. This process makes the concrete sample black and the voids in the paste white. Sample preparation details can be found in other publications [31, 38]. The sample analyzed with ASTM C457 method C using Rapid Air 457 from Concrete Experts, Inc, which uses chord counting. A single threshold value of 185 was used for all samples in this research and the results do not include chords smaller than 30 μm . A traverse length of 2286 mm was used for all samples to satisfy the requirements of ASTM C457. These settings and sample processing methods are like methods used in other publications [38-40]. All air voids were used for the volume of chords less than 300 μm [6].

5.2.4 Mortar Testing

5.2.4.1 Coring and Saturation of Samples

After curing, the mortar samples were demolded and cut using a water-cooled diamond saw into slabs before being cored to cylinders with 10 mm diameter and 30 mm heights [98]. These cylinders edges were then trimmed using a precision diamond saw that was water cooled in order to have parallel surfaces as described in [125]. The final dimensions of the cylindrical cores are 10 mm in diameter and 20 mm in height. The cores were thereafter exposed to 60°C temperature until reaching a constant mass (mass evolution over 24 hours is less than 0.01%). The samples were then vacuum saturated with lime-water solution under a vacuum pressure of 6 Torr according to AASHTO 1.6a. The mortar cores were immersed in lime solution for an additional 24 hours at $23 \pm 2^\circ\text{C}$. They were then kept immersed in lime solution at $50 \pm 1^\circ\text{C}$ for an additional 24 hours.

Table 5.4. Mortar samples investigated.

Sample ID	% Fly Ash	Fresh Concrete Properties		Hardened Mortar Properties	
		Air Content	SAM Number	Initial Mass [g]	Initial Length [mm]
20FA M1	20	5.4%	0.16	3.40	19.16
40FA M1	40	5.9%	0.10	3.70	21.45

5.2.4.2 Temperature Cycling of Samples

Figure 5.2. outlines the process of temperature cycling and scanning timeline that each sample experienced. After the samples were removed from the lime solution, they were scanned (Scan1) using the Micro-CT. After, they were placed directly in 20% CaCl₂ solution that was equilibrated at 50 ± 1°C for an additional 24 hours then scanned (Scan2) again using the Micro-CT. The amount of solution was three times the volume of the sample to ensure proper soaking. The immersion in salt solution at 50°C was to allow the saturation of the pores of the mortar cores with chloride ions without the formation of CaOXY [98, 102]. After scanning the sample, it was placed in a temperature-controlled chamber to be cycled through a series of temperatures: 5°C for 12 hours, 23°C for 10 hours, and 50°C for 30 minutes. This cycle time was chosen to match the timing from a previous study [98]. The scanning timeline is shown in Figure 5.2. to reference each scan at a specific cycle.

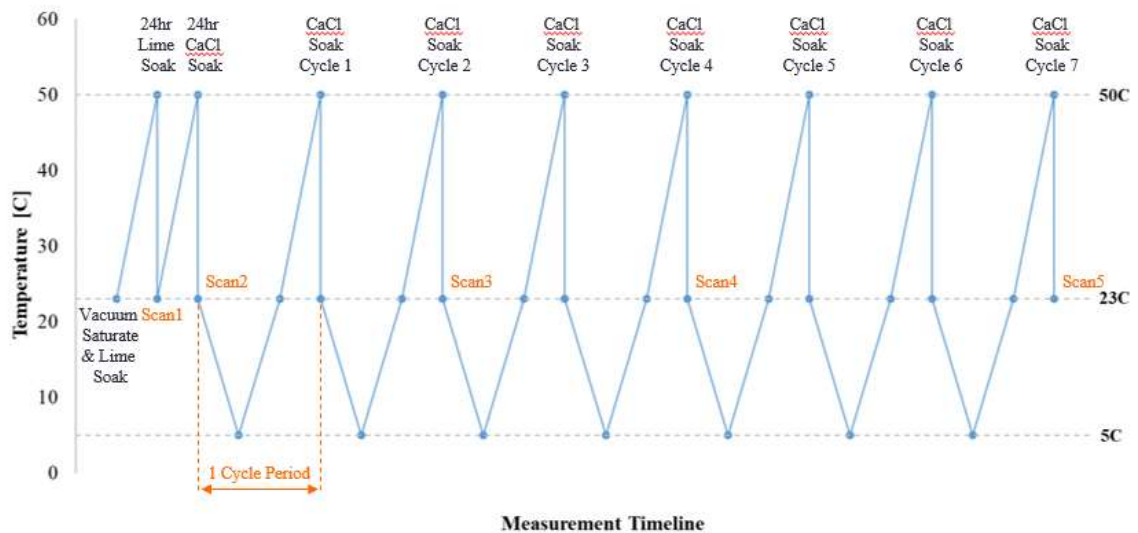


Figure 5.2. Temperature cycling and scanning timeline.

The mortar samples were scanned with the Micro-CT at different stages throughout the process.

These stages are listed in Table 5.5.

Table 5.5. Scans throughout soaking and temperature cycling.

Sample ID	% Fly Ash	Micro-CT Scans				
		24hr Lime Soak @ 50C	24hr CaCl Soak @ 50C	CaCl Soak for 2 cycles	CaCl Soak for 5 cycles	CaCl Soak for 7 cycles
20FA M1	20	1	1	1	1	1
40FA M1	40	1	1	1	1	1

5.2.5 Micro Computed Tomography (Micro-CT)

Each sample was scanned initially and throughout temperature cycles by a ZEISS XRADIA 410 with a photon energy of 90 keV at a resolution of 4.97 $\mu\text{m}/\text{pixel}$. The volume of the interest (VOI) was a cylinder 5.0 mm in diameter and 5.0 mm in height located near the surface of the sample as shown in Figure 5.3. The Micro-CT x-ray settings for each scan is shown in Table 5.6.

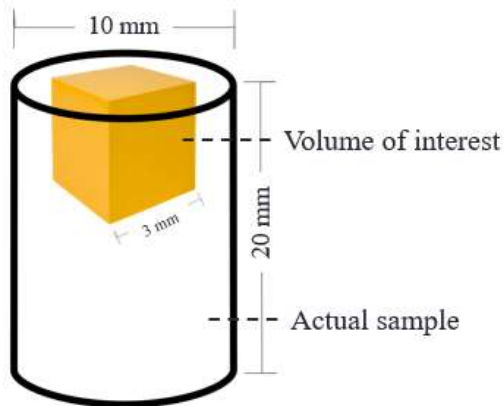


Figure 5.3. Location and dimension of the investigated volume of interest (VOI).

Table 5.6. ZEISS XRADIA 410 scan settings.

Resolution	4.97 $\mu\text{m}/\text{pixel}$
Source Energy	90 keV
Optical Magnification	4X
Exposure Time	8.5 seconds
Number of Projections	2100
Total Exposure Time	5.5 hours

The images captured by the machine must go through a reconstruction process. This process was performed by XMReconstructor to create a library of 2D cross-sectional images. These images can be stacked in such a way that they become a 3D image of the entire scan. An example of this dataset is shown in *Figure 5.4.* with the Micro-CT dataset with the 3D tomography, a 2D cross-section of the reconstruction image, and the corresponding grayscale histogram for a sample [115]. Each 16-bit image consists of pixels with gray values ranging from 0 to 255 corresponding to x-ray absorption which is a function of density and composition of the material [126, 127].

The range in gray values can be used to separate the sample into different elemental phases by an image segmentation process [106, 110, 128]. The main mortar components are air voids, paste, and aggregates. The x-ray absorption for air voids is the lowest because they are the least dense. The lower the density of the element, the darker the voxels in the reconstructed images. The aggregates and un-hydrated cement particles have higher densities, which makes them appear lighter gray to nearly white. The paste of the sample falls somewhere between the air void and aggregate gray values. This can all be observed in *Figure 5.4.*

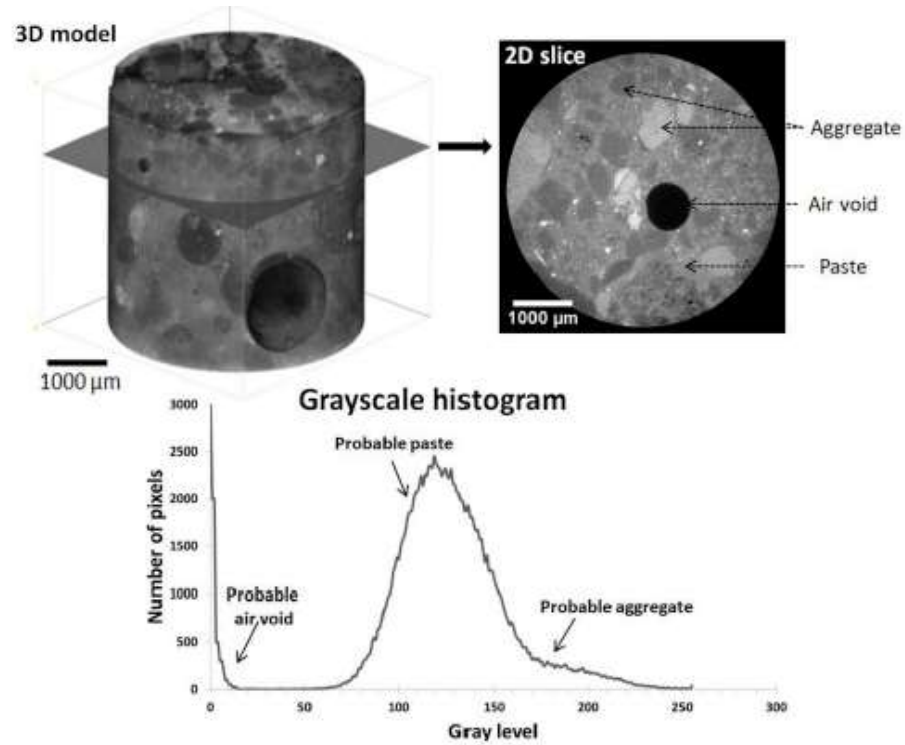


Figure 5.4. An example of the Micro-CT dataset with the 3D tomography, a 2D cross-section of the reconstruction image, and the corresponding grayscale histogram for a sample [115].

5.2.5.1 Image Processing and Analysis

All images were processed, investigated, and visualized using ImageJ software and MATLAB codes. These techniques were used to provide quantitative and qualitative data from the Micro-CT images. Each set of images were aligned with the initial set of images. This alignment would improve accuracy for segmentation and phase identification of each set.

5.2.5.2 Alignment of Micro-CT Datasets

For each set of images, 16-bit reconstruction images were created. To compare each sample from one scan to another, alignment was necessary. Before aligning the images, a histogram shift was used to match the grayscales in the images [111, 115, 118]. This would correct any grayscale shift in values between scans due to automatic normalization during reconstruction. Matlab coding was then used to align the Micro-CT image datasets from one cycle to another. The

alignment algorithm used the first CaCl scan, Scan2, as the reference scan for the subsequent scans. In this process, some identifiable feature regions such as void clusters or high-density sand grains were handpicked throughout all scans, and their coordinates were used to find the 3D affine transformation matrices to align the following scans with the reference scan. Details of the technique can be found in other publications [106, 129, 130]. However, this alignment technique did not fully account for the rigid body movement of the sample between the scans. If the regions of the sample were moved in different directions caused by the damages from the freeze-thaw cycles and the formation of cracks, it is difficult to find a single affine matrix that could consider those individual movements. That makes the full region of the sample difficult to align using this technique. Although there are many other alignment techniques able to solve this problem, a simple solution could be focusing on the alignment for a smaller region. Since the relative movements of the region are small within a small region., the rigid body movement could be able to align those small regions despite the changes and cracks. Thus, for quantitative analyses, some small regions with some identifiable features with the dimensions of 1 mm x 1 mm x 1 mm were cropped and aligned individually to compare between different scans.

5.2.5.3 Segmentation

Segmentation of Micro-CT imaging was used to find quantitative data. In this study, a threshold value was chosen to segment the regions of voids. The threshold value was adjusted and then chosen when the overall void percentage of the full image set of the first scan matched the percent air measured from the concrete sample at the fresh state. Next, the segmented voids were compared with those in the first scan. The regions of voids were labeled as “air voids” if the regions were originally voids in the first scan. The region was labeled as “cracks” if the regions were newly formed voids that did not exist in the first scan. The regions were labeled as “product growth” when they were initially voids in the first scan and later filled in the following scans.

5.3 Results

5.3.1 Mortar Sample Mass and Length Changes

All the samples were measured for length using a micrometer with accuracy of 0.00254 mm.

Figure 5.5. shows the results from the measurements for the 20FA M1 sample and the 40FA M1 sample. Each percent change in length measurement is labeled by the cycle time and scan. The percent change in length is the length minus the initial length divided by the initial length. The figure shows that the 40 percent sample stays below 0.50 percent change, while the 20 percent sample steadily increases in length after cycle 2. The increase in length could be internal damage from the growth of CaOXY as well as cracks forming due to expansion within the cylinder. This damage will be discussed more later in the paper. At cycle 7, the sample was visibly damaged with crumbling particles falling off the edges of the sample.

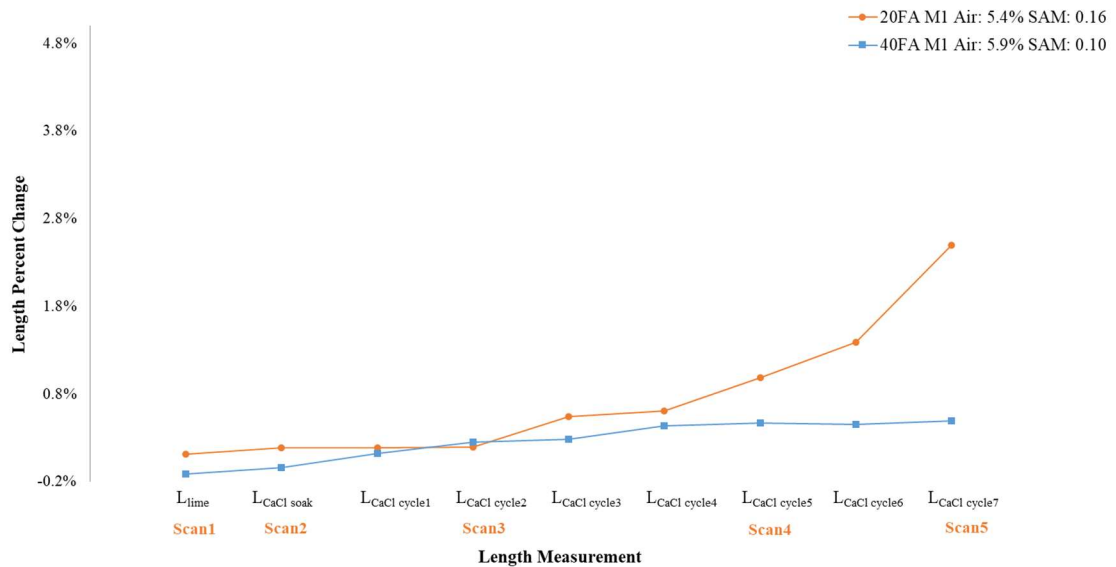


Figure 5.5. Length measurement versus percent change.

5.3.2 Micro-CT Imaging Analysis

5.3.3 Micro-CT Imaging Compared to Segmentation of Voids

To analyze the damaged caused by soaking samples in 20 percent CaCl solution throughout the temperature cycling, the voids were segmented from the Micro-CT scanned images. *Table 5.7.* shows the 3 mm square scan from the interior VOI displayed in *Figure 5.3.* *Location and dimension of the investigated volume of interest (VOI).* for the 20FA M1 mixture. This is the sample that showed expansion in *Figure 5.5.*. The first row of images shown are from after the gray value histogram correction for each cycle in the timeline. The second row of images shown are after the segmentation of voids. The black represents the solids within the sample and the white represents air. The segmentation of the voids shows a decrease in the volume of the air voids and an increase in cracking at CaCl cycle 5. CaCl cycle 7 shows further damage to the sample. The cracks primarily form around the aggregates in the transition zone. The cracks may form here because the transition zone is reported to have higher concentrations of $\text{Ca}(\text{OH})_2$ and is likely weaker than the other parts of the structure.

Table 5.7. Images from the grayscale histogram correction process and segmentation of voids for the 20FA M1 sample.

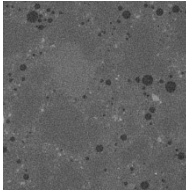
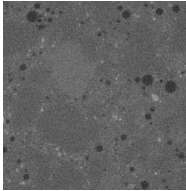
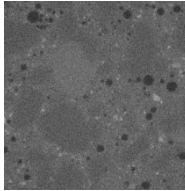
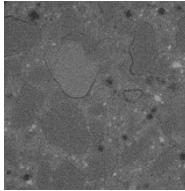
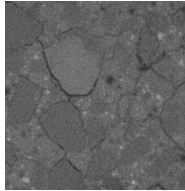
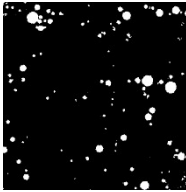
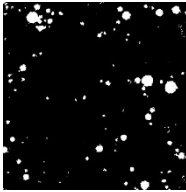
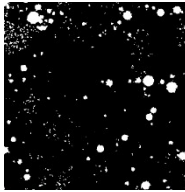
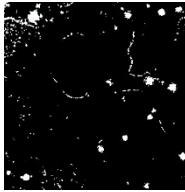
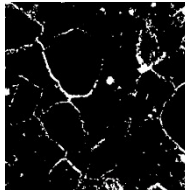
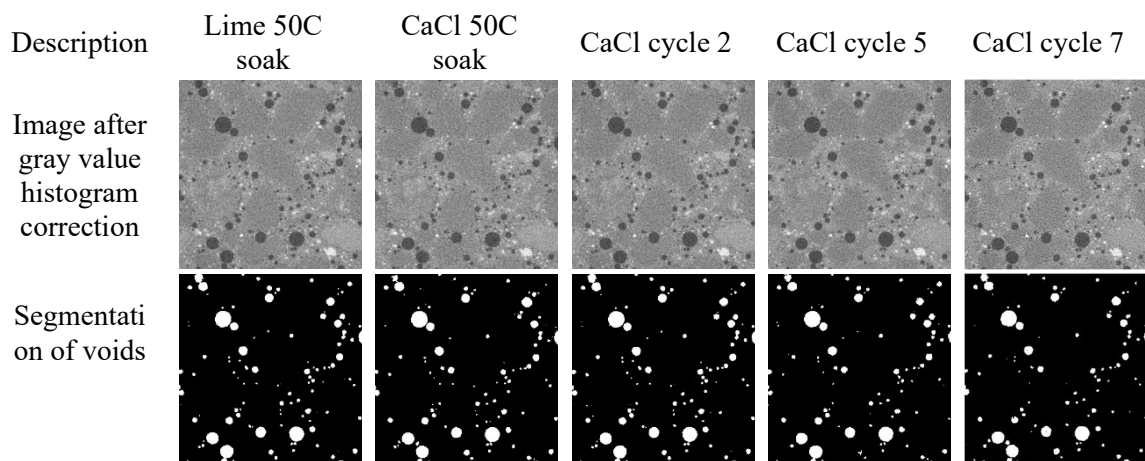
Description	Lime 50C soak	CaCl 50C soak	CaCl cycle 2	CaCl cycle 5	CaCl cycle 7
Image after gray value histogram correction					
Segmentation of voids					

Table 5.8. shows the 3 mm square scan from the interior VOI displayed in Figure 5.3. for 40FA M1 mixture. This is the sample that did not show expansion in Figure 5.5.. The first and second row of images shown are after gray value correction and after segmentation of voids, similar to those in Table 5.7.. The voids are not changing in size and there is not cracking observed. The lack of damage is due to the higher fly ash replacement, which decreases the level of $\text{Ca}(\text{OH})_2$ within the mixture [131, 132].

Table 5.8. Images from the grayscale histogram correction process and segmentation of voids for the 40FA M1 sample.



5.3.4 3.1.2 Quantifying Damage within Samples

To quantify the damage within the sample throughout each scan, the total volume of air was measured by calculating the volume of the voids and adding the volume of the cracks formed. In Figure 5.6., the 20FA M1 sample shows an increase in the volume of air and the cracks. Since the CT scan will observe any space then this means it will observe the voids from the air entrained voids and the volume of the cracks. This increase can be seen to begin at CaCl cycle 2. This agrees with the visual changed observed in Table 5.7.. The 40FA M1 sample shows a consistent total volume of air within the sample throughout the process. This result agrees with the images shown in Table 5.8..

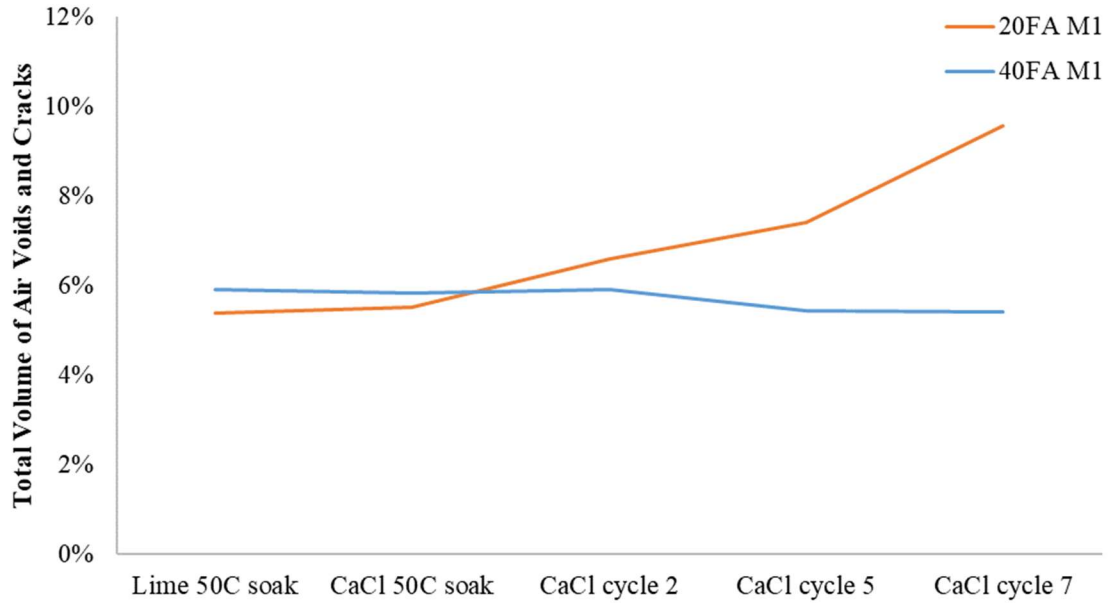


Figure 5.6. Total volume of air per scan for 20 percent and 40 percent fly ash replacement.

To analyze the total volume of air throughout the sample, the scans were evaluated from the surface of the sample to the depth of 3.8 mm. The plot shown in *Figure 5.7.* shows the change in total volume of air voids and volume of cracks and two slices at depths of 0.0 mm and 3.0 mm from cycle 7 for the 20FA M1 sample. The lime soak at 50°C was used as the baseline to see how each scan varied throughout cycling. For example, the total volume of air and cracks at the surface (0.0 mm) for CaCl cycle 7 was 7.3 percent greater than the total volume of air and cracks at the surface for the lime soak. This large increase in volume can be seen in the slice image for cycle 7 at the surface, shown to the right of the plot in *Figure 5.7.*. There are several large cracks visible around the aggregates in the image. This change in total volume of voids is noticeable starting at cycle 2. However, for each scan, the change in total volume of air decreases at a depth of 3.0 mm. The change of volume for cycle 7 at 3.0 mm depth was 1.5 percent volume of air and cracks. This is 5.8 percent less void volume than at the surface. This means that the surface of the sample shows more damage than the interior of the sample. The surface of the sample was in direct contact with the CaCl solution, which was the first location for the CaOXY to start

forming. Over time, the solution enters the concrete and continues to damage the exterior of the sample. Therefore, the surface of the sample sees more damage than the interior.

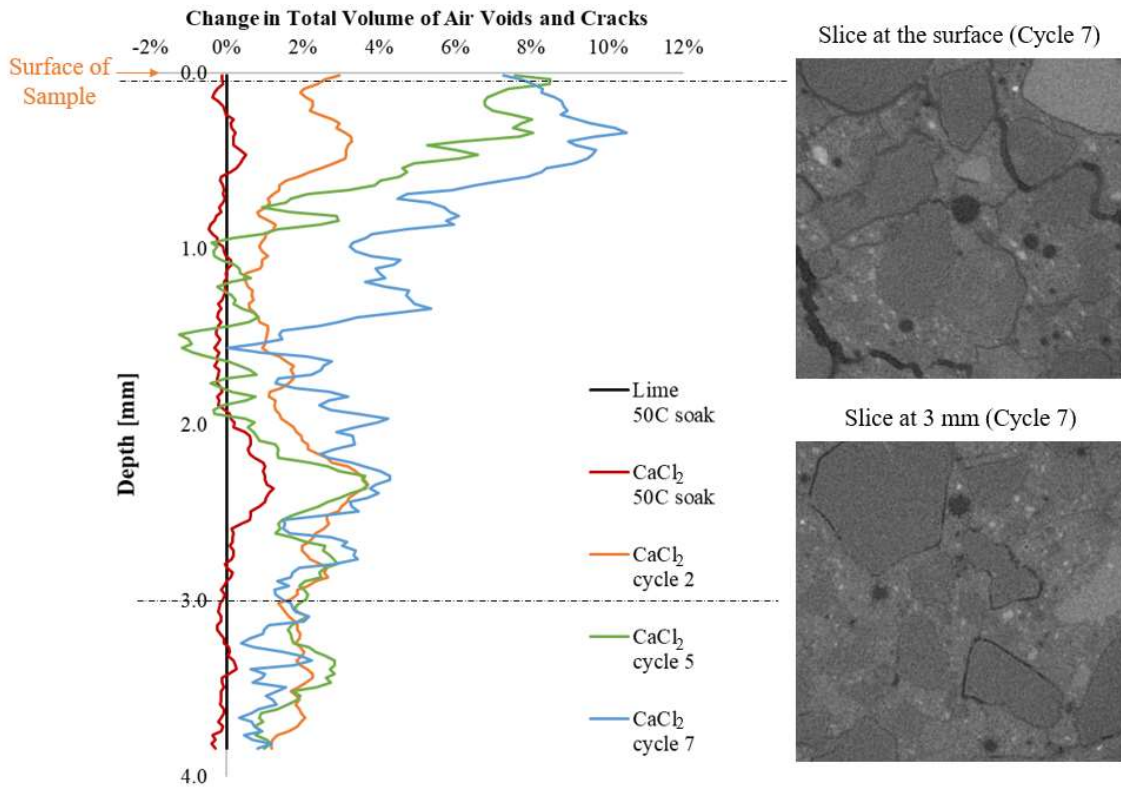


Figure 5.7. Change in the total volume of air over the depth of the 20 percent fly ash sample.

Figure 5.8. shows the same plot and slices as Figure 5.7., but for the 40 percent fly ash sample to compare the 20 percent fly ash sample. There was minimal change in total volume of air for each cycle compared to the lime soak at 50°C. The images to the right do not show any damage to the sample at the surface or at a depth of 3.0 mm.

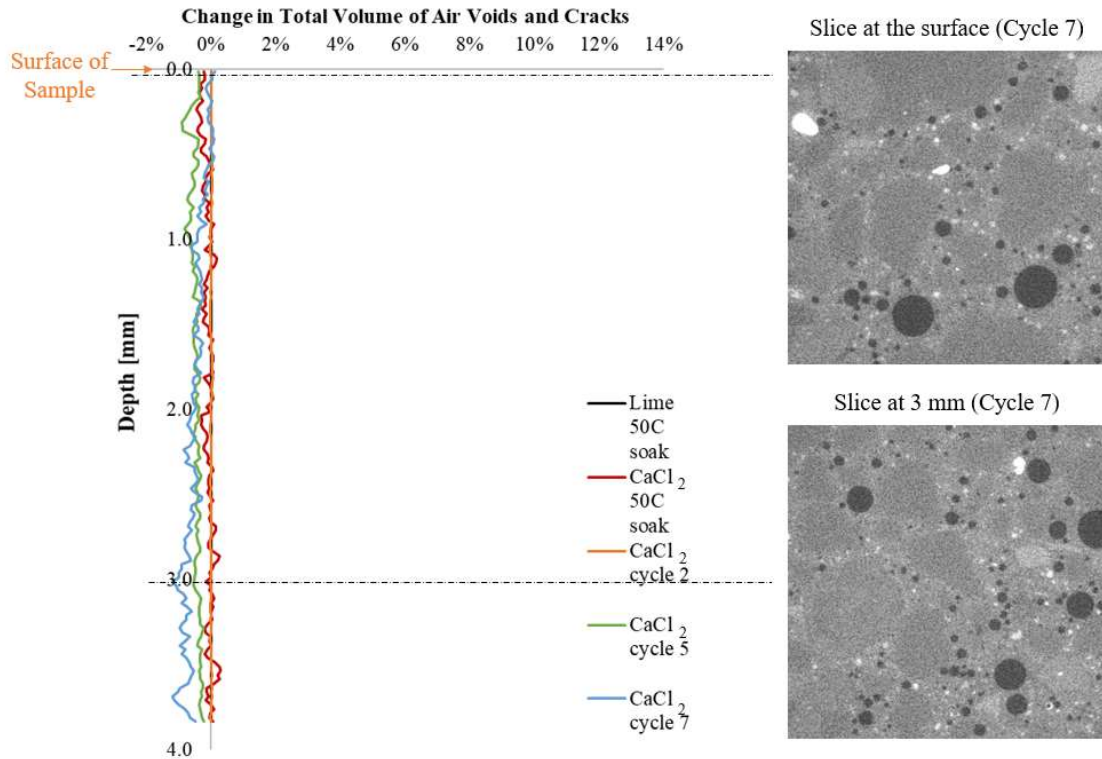


Figure 5.8. Change in the total volume of air over the depth of the 40 percent fly ash sample.

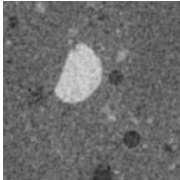
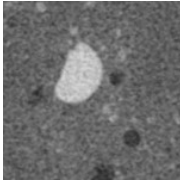
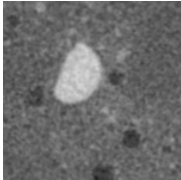
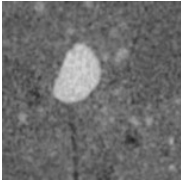
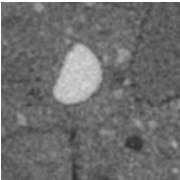
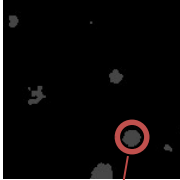
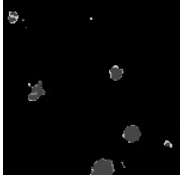
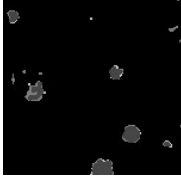
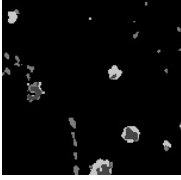
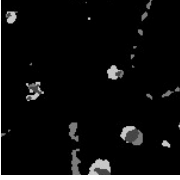
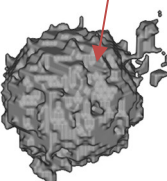
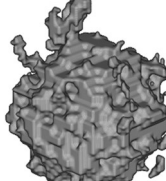
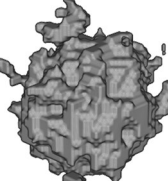
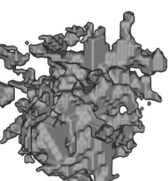
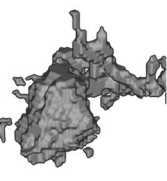
5.3.5 Micro-CT Imaging of Individual Voids

Smaller regions of the sample were investigated to follow the changes of individual voids. In Table 5.9., a raw scan from each cycle for sample 20FA M1 is shown along with a segmented version of the image, a 3D model of an individual air void, the volume of that air void, and the change in measured volume compared to the initial scan. Each image represents a 1 mm cube within the 3 mm cube previously studied.

The segmentation of voids shows air voids filling and cracks forming as the sample was cycled through temperature changes. The 3D model shows how the volume of a single air void changed over time, which is circled in the segmented image. The percent of initial void starts at 100 percent for the lime soak at 50°C. By cycle 5, the volume of air void has reduced to 66 percent of the initial void volume and by cycle 7, it has reduced to 43 percent of the initial air volume. These air voids filled with solids over time. The CaCl is reacting with Ca(OH)₂ to form solid

CaOXY. This increases the pore pressure in the sample and causes cracking in the sample [98]. If the air voids are filled over time by solids, then these voids can no longer protect the concrete from this increase in pore pressure or from damage caused by ice formation during freezing. Although this study did not examine the chemical makeup of the material in the voids, this could be a future area of research to study.

Table 5.9. Imaging and air volume analysis of 20FA M1 scans 1 through 5.

Description	Lime 50C soak	CaCl 50C soak	CaCl cycle 2	CaCl cycle 5	CaCl cycle 7
Image after gray value histogram correction					
Segmentation of voids					
3D void model					
Volume of void [μm^3]	1171125	1129250	1152125	768750	501750
Percent of initial void	100%	96%	98%	66%	43%

In Table 5.10., each cycle for sample 40FA M1 is shown that mirrors Table 5.9.. Each image represents a 1 mm cube within the 3 mm cube previously studied.

The segmentation shows very little filling of air voids and no cracks forming as the sample was cycled through temperature changes. The 3D model shows a consistent volume of air void

volume. There was not much product growth, and no cracks were observed. This occurs because no CaOXY is formed during the different cycles.

Table 5.10. Imaging and air volume analysis of 40FA M1 scans 1 through 5.

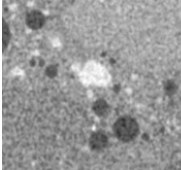
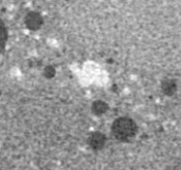
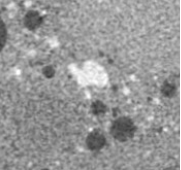
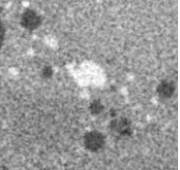
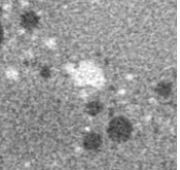



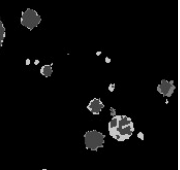
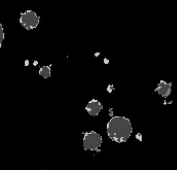
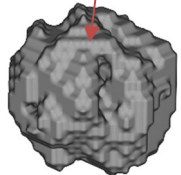
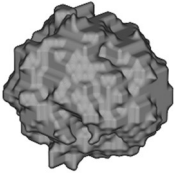
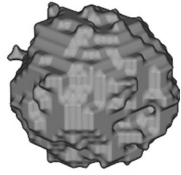
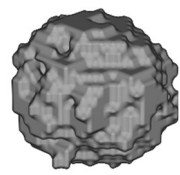
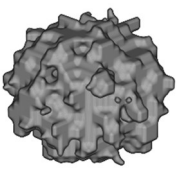
Description	Lime 50C soak	CaCl 50C soak	CaCl cycle 2	CaCl cycle 5	CaCl cycle 7
Image after gray value histogram correction					
Segmentation of voids					
3D void model					
Volume of void [μm^3]	441500	434875	440375	454375	427250
Percent of initial void	100%	98%	100%	103%	97%

Figure 5.9. shows the cumulative volume of air compared to the diameter of the air void for the 20FA M1 sample. The line for Lime 50°C soak shows the initial distribution of the air voids. The CaCl 50°C soak and CaCl cycle 2 lines are only slightly lower than the initial air volume. This shows there is little change air void systems for these cycles; however, cycle 5 and 7 are significantly lower than the previous lines. The overall sum of the volume of air decreases throughout cycling. This means that air voids are filling between cycle 2 and 5. The air void filling also continues between cycle 5 and 7. Cycle 7 shows that the air voids that are greater than

50 μm have decreased by 30% and the voids smaller than 50 μm fill at 18%. This shows the significance of the filling of the air voids that occurs.

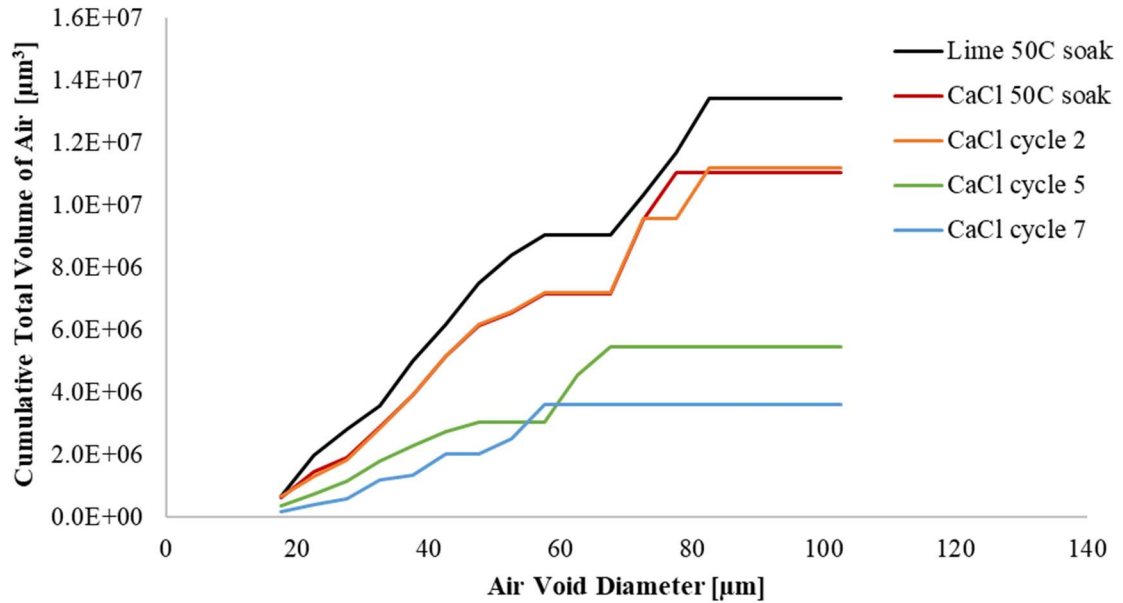


Figure 5.9. Cumulative total volume of air in relation to the air void diameter for each scan of sample 20FA M1.

Figure 5.10. shows the cumulative volume of air compared to the diameter of the air void for the 40FA M1 sample. The air void distribution does not change for the different cycles. This means that the air voids are not filling nearly as much as the sample with 20 percent fly ash replacement. This occurs because there is significantly less CaOXY that forms in this sample.

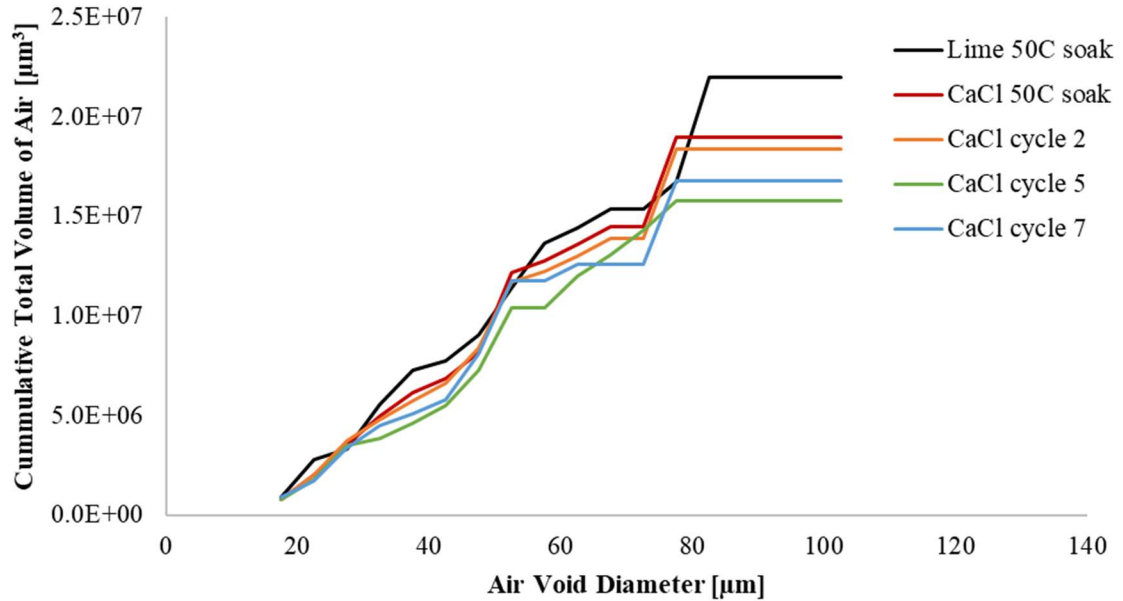


Figure 5.10. Cumulative total volume of air in relation to the air void diameter for each scan of sample 40FA M1.

5.4 Practical Significance

This study shows that when 20% fly ash replacement was used, the sample expands and there is internal cracking and air void filling that occurs. The cracks primarily occur in the transition zone between the aggregates and the paste. Also, the cracks are more prevalent at the surface of the sample and decrease in volume at 3mm from the surface of the sample. The sample with 40% fly ash replacement doesn't show any damage. The difference in performance it caused by the decrease in $\text{Ca}(\text{OH})_2$ when 40% fly ash replacement was used.

The 20% fly ash sample also showed significant air void filling between two and five temperature cycles while the air entrained voids in the 40% fly ash sample did not fill. This decreased the volume and quality of the air void system. This likely impacts the freeze thaw resistance of the concrete.

There is little known about the progression of cracking within the concrete from CaOXY. The formation of cracks at the exposed surface of the sample shows why damage from CaOXY is so

prominently observed in sawed joints in a pavement. These joints can hold moisture and will also have aggregates with exposed transition zones that can react with the salt solution. Once these cracks form, this will allow more moisture to penetrate the sample. This will accelerate the damage of the concrete.

5.5 Conclusions

For this study, two mortar samples were examined using Micro-CT imaging. One sample with 20% fly ash replacement and the other with 40% fly ash replacement. Throughout the study it shows that the sample with 20% replacement experiences more air void filling and cracks than the 40% fly ash sample. The following can be observed from this work:

- For the 20% fly ash sample, the length change steadily increased by 2.50% between temperature cycle 2 and 7, while there was only 0.50% length change for the 40% fly ash sample.
- The cracks were primarily observed in the transition zone around the aggregates. This may be because of the higher amount of $\text{Ca}(\text{OH})_2$ in these regions that may form CaOXY .
- There was an 8% increase in volume that is attributed to cracks at the exposed surface of the 20% fly ash replacement sample that decreased to 2% at 3mm from the surface. There was no cracking observed in the 40% replacement sample.
- The volume of the air voids uniformly decreased by 18% for CaCl soak and cycle 2, 56% for cycle 5, and 70% for cycle 7.

This work provides fundamental insights into the change in the microstructure and air voids caused by the formation of CaOXY . This is an issue that has caused significant destruction and these observations provide more information about the mechanisms and how CaOXY formation may reduce the freeze thaw durability of concrete.

CHAPTER VI

CONCLUSION

6.1 Overview

The main tasks of this research were to:

1. Show that the SAM Number provides a more direct measurement of the air void quality of fresh concrete than the total volume of air, which is important for the freeze-thaw durability of concrete. The almost immediate feedback provided by the SAM in the fresh concrete can benefit material suppliers, producers, contractors, and engineers in their quest to build long lasting and economic infrastructure.
2. Establish the primary use of the Efficiency Chart to give practitioners critical information about the quality of concrete mixtures before the material has hardened. Practitioners can change the mixture if it has low efficiency, and the Efficiency Chart gives the user immediate feedback on how the changes in ingredients and practices impacts the efficiency of the air void system in the concrete.
3. Determine whether the efficiency of a mixture can provide insight into the construction practices of placing concrete on a job site and if there should be a limitation based on these factors.

4. Evaluate the change in the microstructure and air voids caused by the formation of CaOXY. This is an issue that has caused significant destruction and these observations provide more information about the mechanisms and how CaOXY formation may reduce the freeze thaw durability of concrete.

6.2 Field and Laboratory Validation of the Sequential Air Method

This work compares the correlation between the SAM Number, Spacing Factor, and air content for 257 laboratory mixtures and 231 field mixtures with various admixtures, aggregates, devices, and users. The reliability of the method across a data set this diverse shows the reliability and robustness of the SAM test method.

These specific findings have been made:

- Air contents between 3% and 8% were needed to obtain a Spacing Factor of 200 μ m. This shows the inability of a specific air volume to correlate with air void quality.
- For 257 laboratory mixtures, the correlation between a SAM Number of 0.20 and a Spacing Factor of 200 μ m agrees with 85% of the laboratory data comparisons.
- For 231 field mixtures, the correlation between a SAM Number of 0.20 and a Spacing Factor of 200 μ m agrees with 70% of the field data comparisons.
- For 231 field mixtures, 25% or 57 of them that were placed based on their air volume were shown by the Spacing Factor and SAM Number to have an air void distribution that is not recommended for freeze thaw durability.

6.3 Determining the Air Void Efficiency of Fresh Concrete Mixtures with the Sequential Air Method

A tool was created to show High and Low Efficiency Lines using both the SAM Number and air volume that defines the typical range of air void size for a given air volume in fresh concrete mixtures. These curves define the Efficiency Chart and act as guidelines to judge the performance of concrete mixtures. This work also shows that for the 227 mixtures investigated, the SAM test

method closely relates to the Spacing Factor or quality of the air void system and can be used to determine the efficiency of the air void system.

These specific findings have been made:

- The cubic quantile lines provide useful boundaries on the Efficiency Chart that can be used to judge the efficiency of bubble spacing in fresh concrete.
- Satisfactory examples for cements and admixtures reinforce the usefulness of the Efficiency Chart in evaluating various concrete mixtures.
- For 227 laboratory mixtures, using thresholds of 0.20 for a SAM Number and 200 μm for Spacing Factor leads to the same classifications for 84% of the laboratory data.

6.4 Evaluation of the Concrete Mixture Efficiency within Construction Practices

An efficient concrete mixture design is less likely to be affected by free fall impact if the quality of the air void system is higher prior to drop. The compression strength shows less than 10.2 percent change throughout the mixtures. All the mixtures lost air after dropping; however, the efficient mixtures did not lose the high-quality air void system. The SAM Number, Spacing Factor, and Durability Factor results agree in comparison between efficient and inefficient mixtures.

After pumping and dropping, the mixture with 5.8% air content shows a significant drop in SAM Number and Durability Factor. This could mean that pumping inefficient mixtures could improve the quality of air void system by dissolving bubbles into solution prior to drop. If the pressure mechanism drives the bubbles into solution before the mixture is dropped, the bubbles are less likely to get 'knocked out' of the system [57, 60, 62]. More mixtures should be studied to see if this phenomenon could be repeated more.

- Efficient mixtures that were not dropped lost on average 13 percent less air than inefficient mixtures that were not dropped.

- Efficient mixtures dropped at 6.10 m lost similar air amounts to inefficient mixtures that were dropped at 1.52 m.
- Efficient mixtures dropped at 6.10 m changed 14 percent less in SAM Number on average than inefficient mixtures that were dropped at 1.52 m.
- Efficient mixtures dropped at 6.10 m show less change in Durability Factor than inefficient mixtures dropped at 1.52 m.
- The Efficiency Chart can help identify concrete mixtures that may be susceptible to change in air void distribution after larger drop heights.
- The mixtures containing PC show a less efficient air void system when the air content is less than 6 percent.

6.5 Quantifying Calcium Oxychloride Formation Using Micro-Computed Tomography

For this study, two mortar samples were examined using Micro-CT imaging. One sample with 20% fly ash replacement and the other with 40% fly ash replacement. Throughout the study it shows that the sample with 20% replacement experiences more air void filling and cracks than the 40% fly ash sample. The following can be observed from this work:

- For the 20% fly ash sample, the length change steadily increased by 2.50% between temperature cycle 2 and 7, while there was only 0.50% length change for the 40% fly ash sample.
- The cracks were primarily observed in the transition zone around the aggregates. This may be because of the higher amount of Ca(OH)_2 in these regions that may form CaOXY .
- There was an 8% increase in volume that is attributed to cracks at the exposed surface of the 20% fly ash replacement sample that decreased to 2% at 3mm from the surface. There was no cracking observed in the 40% replacement sample.

- The volume of the air voids uniformly decreased by 18% for CaCl soak and cycle 2, 56% for cycle 5, and 70% for cycle 7.

6.6 Further Research Needed

Automated systems to analyze and establish the efficiency of a concrete mixture without user discretion would highly benefit the industry usage of the Super Air Meter. An algorithm has been established to help with determining high quality air void systems that can be implemented into the Efficiency Chart process.

Determining the chemical properties of the product growth within the fly ash samples would help determine what is filling the voids and damaging the concrete. This can be done using Micro X-ray Fluorescence or similar equipment.

REFERENCES

1. *AASHTO TP 118 LRFD Bridge Design Specifications*, A.A.o.S.H.a.T. Officials, Editor. 2017: Washington, D.C.
2. *ASTM C457/C457M-16 Standard Test Method for Microscopical Determination of Parameters of the Air-Void System in Hardened Concrete*, A. International, Editor. 2016: West Conshohocken, PA.
3. *ASTM C666/C666M-15 Standard Test Method for Resistance of Concrete to Rapid Freezing and Thawing*, A. International, Editor. 2015: West Conshohocken, PA.
4. Ley, M.T., et al., *Determining the air-void distribution in fresh concrete with the sequential air method*. *Construction and Building Materials*, 2017. **150**: p. 723-737.
5. Hall, H., M. Tyler Ley, David Welchel, Jacob Peery, Jake Leflore, Morteza Khatibmasjedi, Jagan M. Gudimetlla, and Michael Praul, *Field and Laboratory Validation of the Sequential Air Method*. *Materials and Structures*, 2020. **53**(14).
6. Dąbrowski, M., et al., *Validation of sequential pressure method for evaluation of the content of microvoids in air entrained concrete*. *Construction and Building Materials*, 2019. **227**: p. 116633.
7. Kosmatka, S.H. and M.L. Wilson, *Design and control of concrete mixtures*. 2016: Portland Cement Assoc.
8. Pigeon, M. and R. Pleau, *Durability of concrete in cold climates*. 1995: CRC Press.
9. Del Mar Arribas-Colón, M., et al., *Investigation of Premature Distress Around Joints in PCC Pavements: Parts I & II*. 2012, Joint Transportation Research Program, Indiana Department of Transportation and Purdue University, West Lafayette, Indiana: Publication FHWA/IN/JTRP-2012/25 & FHWA/IN/JTRP-2012/26.
10. Jones, W., et al., *An Overview of Joint Deterioration in Concrete Pavement: Mechanisms, Solution Properties, and Sealers*. 2013: West Lafayette, Indiana.

11. Castro, J., et al., *Durability of saw-cut joints in plain cement concrete pavements*. 2011, Purdue University. Joint Transportation Research Program.
12. Graveen, C., et al., *Performance Related Specifications (PRS) for Concrete Pavements in Indiana, Volume 2: Technical Report*. 2009.
13. Olek, J., M. Radlinski, and M. del Mar Arribas. *Premature deterioration of joints in selected Indiana portland cement concrete pavements*. 2007.
14. Qiao, C., P. Suraneni, and J. Weiss, *Phase diagram and volume change of the $\text{Ca}(\text{OH})_2\text{-CaCl}_2\text{-H}_2\text{O}$ system for varying $\text{Ca}(\text{OH})_2/\text{CaCl}_2$ molar ratios*. Journal of Materials in Civil Engineering, 2018. **30**(2): p. 04017281.
15. Jones, C., et al., *Calcium oxychloride: a critical review of the literature surrounding the formation, deterioration, testing procedures, and recommended mitigation techniques*. Cement and Concrete Composites, 2020. **113**: p. 103663 %@ 0958-9465.
16. Smith, S., et al., *Service-life of Concrete in Freeze-Thaw Environments: Critical Degree of Saturation and Calcium Oxychloride Formation*. Cement and Concrete Research, Under review.
17. Cai, H. and X. Liu, *Freeze-thaw durability of concrete: ice formation process in pores*. Cement and Concrete Research, 1998. **28**: p. 1281-1287.
18. Tanesi, J. and R. Meininger, *Freeze-thaw resistance of concrete with marginal air content*. Transportation research record, 2007. **2020**(1): p. 61-66 %@ 0361-1981.
19. Janssen, D.J. and M.B. Snyder, *Resistance of concrete to freezing and thawing*. 1994.
20. Backstrom, J., et al., *Void spacing as a basis for producing air-entrained concrete*. ACI Journ., 1954. **4**: p. 760-761.
21. Powers, T.C. and T. Willis. *The air requirement of frost resistant concrete*. in *Highway Research Board Proceedings*. 1950.
22. Ley, M.T., *The effects of fly ash on the ability to entrain and stabilize air in concrete*, in *Civil, Architectural, and Environmental Engineering*. 2007, University of Texas at Austin
23. Scherer, G.W. and J. Valenza, *Mechanisms of frost damage*. Materials science of concrete, 2005. **7**(60): p. 209-246.
24. Kleiger, P., *Studies of the Effect of Entrained Air on the Strength and Durability of Concrete made with Various Maximum Sizes of Aggregate*. 1952: Portland Cement Association.
25. Kleiger, P., *Further Studies on the Effect of Entrained Air on Strength and Durability of Concrete with Various Sizes of Aggregates*. 1956: Portland Cement Association.

26. *ASTM C138/C138M-17a Standard Test Method for Density (Unit Weight), Yield, and Air Content (Gravimetric) of Concrete*, A. International, Editor. 2017: West Conshohocken, PA.
27. *ASTM C173/C173M-16 Standard Test Method for Air Content of Freshly Mixed Concrete by the Volumetric Method*, A. International, Editor. 2016: West Conshohocken, PA.
28. *ASTM C231/C231M-17a Standard Test Method for Air Content of Freshly Mixed Concrete by the Pressure Method*, A. International, Editor. 2017: West Conshohocken, PA.
29. Tanesi, J., et al., *Super Air Meter for Assessing Air-Void System of Fresh Concrete*. *Advances in Civil Engineering Materials*, 2016. **5**(2): p. 22-37.
30. LeFlore, J. *Super Air Meter Test Video*. 2016; Available from: https://www.youtube.com/watch?v=xAcHqMz_m3I.
31. Welchel, D., *Determining the Size and Spacing of Air Bubbles in Fresh Concrete*. 2014, Oklahoma State University.
32. Hover, K.C., *Analytical investigation of the influence of air bubble size on the determination of the air content of freshly mixed concrete*. *Cement, concrete and aggregates*, 1988. **10**(1): p. 29-34.
33. Klein, W. and S. Walker. *A method for direct measurement of entrained air in concrete*. in *Journal Proceedings*. 1946.
34. M.T. Ley, K.J.F., K.C. Hover, *Observations of Air-Bubbles Escaped From Fresh Cement Paste*. *Cement Concrete Research* 2009.
35. M.T. Ley, R.C., M. Juenger, K.J. Folliard, *The Physical and Chemical Characteristics of the Shell of Air-Entrained Bubbles in Cement Paste*. *Cement Concrete Research* 2009.
36. Felice, R., J.M. Freeman, and M.T. Ley, *Durable Concrete with Modern Air-Entraining Admixtures*. *Concrete international*, 2014. **36**(8): p. 37-45.
37. Ley, M.T. and B. Tabb. *A test method to measure the freeze thaw durability of fresh concrete using overpressure*. in *T&DI Congress 2014: Planes, Trains, and Automobiles*. 2014.
38. Ley, M.T., *The effects of fly ash on the ability to entrain and stabilize air in concrete*. 2007: ProQuest.
39. Jakobsen, U., et al., *Automated air void analysis of hardened concrete—a Round Robin study*. *Cement and Concrete Research*, 2006. **36**(8): p. 1444-1452.

40. Peterson, K., L. Sutter, and M. Radlinski, *The practical application of a flatbed scanner for air-void characterization of hardened concrete*, in *Recent Advancement in Concrete Freezing-Thawing (FT) Durability*. 2010, ASTM International.
41. 201.2R, A.C. *Guide to Durable Concrete*. 2016. American Concrete Institute.
42. W.J. Weiss, M.T.L., O.B. Isgor, *Toward Performance Specifications for Concrete Durability: Using the Formation Factor for Corrosion and Critical Saturation for Freeze-Thaw*. Transportation Research Board, 2017(17-02543).
43. Freeman, J.M., *Stability and quality of air void systems in concretes with superplasticizers*. 2012, Oklahoma State University.
44. Lian, C., Y. Zhuge, and S. Beecham, *The relationship between porosity and strength for porous concrete*. Construction and Building Materials, 2011. **25**(11): p. 4294-4298.
45. Addinsoft, *XLSTAT Statistical and Data Analysis Solution*. 2019: Long Island, NY, USA.
46. Plante, P., M. Pigeon, and C. Foy, *The influence of water-reducers on the production and stability of the air void system in concrete*. Cement and Concrete Research, 1989. **19**(4): p. 621-633.
47. Whiting, D.A. and M.A. Nagi, *Manual on control of air content in concrete*. 1998.
48. Kovler, K. and N. Roussel, *Properties of fresh and hardened concrete*. Cement and Concrete Research, 2011. **41**(7): p. 775-792.
49. De Larrard, F., *Concrete mixture proportioning: a scientific approach*. 1999: CRC Press.
50. Banfill, P.F., *The rheology of fresh mortar*. Magazine of concrete research, 1991. **43**(154): p. 13-21.
51. Murata, J., *Flow and deformation of fresh concrete*. Materiaux et Construction, 1984. **17**(2): p. 117-129.
52. Otsubo, Y., S. Miyai, and K. Umeya, *Time-dependent flow of cement pastes*. Cement and Concrete Research, 1980. **10**(5): p. 631-638.
53. Koel, L., *Concrete Formwork*. 1988, Illinois: American Technical Publishers Inc.
54. Smith, R.C.a.C.K.A., *Principles and Practices of Heavy Construction*. Third ed. 1986, New Jersey: Prentice Hall.
55. 304, A.C., *Guide for Measuring, Mixing Transporting, and Placing Concrete*, ACI, Editor. 2009.
56. Becker, H.H., et al., *Determining the air void efficiency of fresh concrete mixtures with the Sequential air method*. Construction and Building Materials, 2021. **288**: p. 122865.
57. Yingling, J., G.M. Mullings, and R.D. Gaynor, *Loss of air content in pumped concrete*. Concrete International, 1992. **14**(10): p. 57-61.

58. Staffileno, C.J., *Field Investigation of Pumping Air Entrained Concrete and Validation of the Sam Test on Lightweight Aggregate Concrete Mixtures*. 2020, Oklahoma State University: Ann Arbor. p. 59.
59. Becker, J., *Investigation of Concrete Pumping Effects on Air-Entrained Concrete*. 2018, Oklahoma State University.
60. Hover, K.C. and R.J. Phares, *Impact of concrete placing method on air content, air-void system parameters, and freeze-thaw durability*. Transportation research record, 1996. **1532**(1): p. 1-8.
61. Elkey, W., D.J. Janssen, and K.C. Hover, *CONCRETE PUMPING EFFECTS ON ENTRAINED AIR-VOIDS. FINAL REPORT*. 1994.
62. Janssen, D., R. Dyer, and W. Elkey, *ENTRAINED AIR VOIDS: ROLE OF PRESSURE*. Concrete Under Severe Conditions: Environmental and Loading, 1995. **1**: p. 233.
63. Sutter, L., et al., *Petrographic evidence of calcium oxychloride formation in mortars exposed to magnesium chloride solution*. Cement and Concrete Research, 2006. **36**(8): p. 1533-1541.
64. Monosi, S. and L. Collepardi, *Chemical attack of calcium chloride on the Portland cement paste*. Cemento, 1989. **86**(2): p. 97-104.
65. Monosi, S. and M. Collepardi, *Research on $3\text{CaO}\cdot\text{CaCl}_2\cdot 15\text{H}_2\text{O}$ identified in concretes damaged by CaCl_2 attack*. Cemento, 1990. **87**(1): p. 3-8.
66. Collepardi, M., L. Coppola, and C. Pistolesi. *Durability of concrete structures exposed to CaCl_2 based deicing salts*. in *Proceedings of the 3rd CANMENT/ACI International Conference*. 1994. France: American Concrete Institute.
67. Sutter, L., et al., *The Deleterious Chemical Effects of Concentrated Deicing Solutions on Portland Cement Concrete* 2008, Michigan Tech Transportation Insitute South Dakota Department of Transportation p. 216.
68. Shi, X., et al., *Freeze–thaw damage and chemical change of a portland cement concrete in the presence of diluted deicers*. Materials and Structures, 2010. **43**(7): p. 933-946.
69. Janusz, A.E., *Investigation of deicing chemicals and their interactions with concrete materials*. 2010.
70. Lee, H., et al., *Effects of various deicing chemicals on pavement concrete deterioration*. 2000.
71. Wang, K., D.E. Nelsen, and W.A. Nixon, *Damaging effects of deicing chemicals on concrete materials*. Cement and Concrete Composites, 2006. **28**(2): p. 173-188.
72. Lawrence, M. and H.E. Vivian, *Action of calcium chloride on mortar and concrete*. 1960.

73. Van Niejenhuis, C.B. and C.M. Hansson, *Detrimental Effects of Anti-Icing Brines on Concrete Durability*. Concrete International, 2019. **41**(11): p. 30-34.
74. Ghazy, A. and M.T. Bassuoni, *Resistance of concrete to different exposures with chloride-based salts*. Cement and Concrete Research, 2017. **101**: p. 144-158.
75. Chatterji, S., *Mechanism of the CaCl₂ attack on Portland cement concrete*. Cement and Concrete Research, 1978. **8**(4): p. 461-467.
76. Li, W., et al., *Water absorption and critical degree of saturation relating to freeze-thaw damage in concrete pavement joints*. Journal of Materials in Civil Engineering, 2012. **24**(3): p. 299-307.
77. Litvan, G.G., *Frost action in cement in the presence of de-icers*. Cement and Concrete Research, 1976. **6**(3): p. 351-356 %@ 0008-8846.
78. Spragg, R.P., et al., *Wetting and drying of concrete using aqueous solutions containing deicing salts*. Cement and Concrete Composites, 2011. **33**(5): p. 535-542.
79. Taylor, P., L. Sutter, and J. Weiss, *Investigation of deterioration of joints in concrete pavements*. 2012.
80. Sutter, L., et al., *Long-term effects of magnesium chloride and other concentrated salt solutions on pavement and structural Portland cement concrete*. Transportation research record, 2006. **1979**(1): p. 0361-1981.
81. Pour-Ghaz, M., et al. *Numerical and experimental assessment of unsaturated fluid transport in saw-cut (notched) concrete elements*. 2009.
82. Golias, M., et al., *Can Soy Methyl Esters Improve Concrete Pavement Joint Durability?* Transportation research record, 2012. **2290**(1): p. 60-68 %@ 0361-1981.
83. Hall, K.T., et al., *Performance of Sealed and Unsealed Concrete Pavement Joints*. 2009, United States. Federal Highway Administration.
84. MacInnis, C. and Y.R. Nathawad, *The effects of a deicing agent on the absorption and permeability of various concretes*, in *Durability of Building Materials and Components*. 1980, ASTM International.
85. Castro, J., et al., *Portland cement concrete pavement performance relative to permeability*. JTRP Rep. SPR-3093, Indiana Department of Transportation, West Lafayette, IN, 2010.
86. Barde, V., et al., *Relating material properties to exposure conditions for predicting service life in concrete bridge decks in Indiana*. 2009.
87. Rangaraju, P.R., *Investigating premature deterioration of a concrete highway*. Transportation research record, 2002. **1798**(1): p. 1-7 %@ 0361-1981.

88. Peterson, K., et al., *Observations of chloride ingress and calcium oxychloride formation in laboratory concrete and mortar at 5° C.* Cement and Concrete Research, 2013. **45**: p. 79-90.
89. Demediuk, T., W.F. Cole, and H.V. Hueber, *Studies on magnesium and calcium oxychlorides.* Australian Journal of Chemistry, 1955. **8**(2): p. 215-233.
90. Mori, H., et al., *Deterioration of hardened cement pastes immersed in calcium chloride solution.* Cement Science and Concrete Technology, 2012. **66**(1): p. 79-86.
91. Qiao, C., et al., *The Influence of calcium chloride on flexural strength of cement-based materials*, in *High Tech Concrete: Where Technology and Engineering Meet: Proceedings of the 2017 fib Symposium, held in Maastricht, The Netherlands, June 12–14, 2017*, D.A. Hordijk and M. Luković, Editors. 2018, Springer International Publishing: Cham. p. 2041-2048.
92. Qiao, C., P. Suraneni, and J. Weiss, *Flexural strength reduction of cement pastes exposed to CaCl₂ solutions.* Cement and Concrete Composites, 2018. **86**: p. 297-305.
93. Julio-Betancourt, G.A. and R.D. Hooton. *Calcium and magnesium chloride attack on cement-based materials: formation, stability, and effects of oxychlorides.* 2009.
94. Farnam, Y., et al., *The influence of calcium chloride deicing salt on phase changes and damage development in cementitious materials.* Cement and Concrete Composites, 2015. **64**: p. 1-15.
95. Berntsson, L. and S. Chandra, *Damage of concrete sleepers by calcium chloride.* Cement and Concrete Research, 1982. **12**(1): p. 87-92.
96. Smolczyk, H.G. *Chemical Reactions of strong Chloride-Solution with Concrete.* 1968.
97. Chatterji, S. and J. Ad, *Studies of the mechanism of calcium chloride attack on Portland cement concrete.* 1975.
98. Rita M. Ghantous, K.Z., Hope Hall Becker, Amir Behravan, M. Tyler Ley, O. Burkan Isgor, and W. Jason Weiss, *The Influence of Air Voids and Fluid Absorption on Salt-Induced Calcium Oxychloride Damage.* Cement and Concrete Composites, Under Review 2022.
99. Winkler, E.M. and P.C. Singer, *Crystallization pressure of salts in stone and concrete.* Geological society of America bulletin, 1972. **83**(11): p. 3509-3514.
100. Scherer, G.W., *Crystallization in pores.* Cement and Concrete Research, 1999. **29**(8): p. 1347-1358.
101. Scherer, G.W., *Stress from crystallization of salt.* Cement and Concrete Research, 2004. **34**(9): p. 1613-1624.

102. Qiao, C., P. Suraneni, and J. Weiss, *Measuring volume change due to calcium oxychloride phase transformation in a $\text{Ca}(\text{OH})_2\text{-CaCl}_2\text{-H}_2\text{O}$ system*. *Advances in Civil Engineering Materials*, 2017. **6**(1): p. 157-169.
103. Christiansen, B.A., *Effect of micro-computed tomography voxel size and segmentation method on trabecular bone microstructure measures in mice*. *Bone reports*, 2016. **5**: p. 136-140.
104. Hu, Q., et al., *Direct three-dimensional observation of the microstructure and chemistry of C3S hydration*. *Cement and concrete research*, 2016. **88**: p. 157-169.
105. Romão, M., et al., *Micro-computed tomography and histomorphometric analysis of human alveolar bone repair induced by laser phototherapy: a pilot study*. *International journal of oral and maxillofacial surgery*, 2015. **44**(12): p. 1521-1528.
106. Nguyen, T.T., *Modeling of complex microcracking in cement based materials by combining numerical simulations based on a phase-field method and experimental 3D imaging*. 2015, Paris Est.
107. Kim, K.Y., T.S. Yun, and K.P. Park, *Evaluation of pore structures and cracking in cement paste exposed to elevated temperatures by X-ray computed tomography*. *Cement and Concrete Research*, 2013. **50**: p. 34-40.
108. Sinha, S.K. and P.W. Fieguth, *Automated detection of cracks in buried concrete pipe images*. *Automation in construction*, 2006. **15**(1): p. 58-72.
109. Moradian, M., et al., *Direct in-situ observation of early age void evolution in sustainable cement paste containing fly ash or limestone*. *Composites Part B: Engineering*, 2019. **175**: p. 107099.
110. Hu, Q., et al., *Combined three-dimensional structure and chemistry imaging with nanoscale resolution*. *Acta materialia*, 2014. **77**: p. 173-182.
111. Hu, Q., et al., *3D chemical segmentation of fly ash particles with X-ray computed tomography and electron probe microanalysis*. *Fuel*, 2014. **116**: p. 229-236.
112. Ley, M., et al. *Combining nano X-ray tomography and nano X-ray fluorescence to create time-dependent three dimensional constitutive maps*. in *2nd International Conference on Tomography of Materials and Structures Quebec City, Canada*. 2015.
113. Gallucci, E., et al., *3D experimental investigation of the microstructure of cement pastes using synchrotron X-ray microtomography (μCT)*. *Cement and Concrete Research*, 2007. **37**(3): p. 360-368.
114. Hu, Q., et al., *Direct measurements of 3d structure, chemistry and mass density during the induction period of C3s hydration*. *Cement and concrete research*, 2016. **89**: p. 14-26.

115. Sokhansefat, G., *Feature Investigation using Micro Computed Tomography within Materials*. 2018, Oklahoma State University.
116. Fukuda, D., et al., *Investigation of self-sealing in high-strength and ultra-low-permeability concrete in water using micro-focus X-ray CT*. *Cement and Concrete Research*, 2012. **42**(11): p. 1494-1500.
117. Zolghadr, A., et al., *Biomass microspheres—A new method for characterization of biomass pyrolysis and shrinkage*. *Bioresource technology*, 2019. **273**: p. 16-24.
118. Sokhansefat, G., et al., *Using X-ray computed tomography to investigate mortar subjected to freeze-thaw cycles*. *Cement and Concrete Composites*, 2020. **108**: p. 103520.
119. Promentilla, M.A.B. and T. Sugiyama, *X-ray microtomography of mortars exposed to freezing-thawing action*. *Journal of Advanced Concrete Technology*, 2010. **8**(2): p. 97-111.
120. Sugiyama, T., et al., *Application of synchrotron microtomography for pore structure characterization of deteriorated cementitious materials due to leaching*. *Cement and Concrete Research*, 2010. **40**(8): p. 1265-1270.
121. Tekin, I., R. Birgul, and H.Y. Aruntas, *Determination of the effect of volcanic pumice replacement on macro void development for blended cement mortars by computerized tomography*. *Construction and Building Materials*, 2012. **35**: p. 15-22.
122. Farnam, Y., et al., *Measuring freeze and thaw damage in mortars containing deicing salt using a low-temperature longitudinal guarded comparative calorimeter and acoustic emission*. *Advances in Civil Engineering Materials*, 2014. **3**(1): p. 316-337.
123. *ASTM C143/C143M-20 Standard Test Method for Slump of Hydraulic-Cement Concrete*, A. International, Editor. 2020.
124. *ASTM C172/C172M-17 Standard Practice for Sampling Freshly Mixed Concrete*, A. International, Editor. 2017: West Conshohocken, PA.
125. Ghantous, R.M., et al., *Examining the influence of the Degree of Saturation on Length Change and Freeze Thaw Damage*. Submitted to *Advances in Civil Engineering Materials*, 2018.
126. Otsu, N., *A threshold selection method from gray-level histograms*. *IEEE transactions on systems, man, and cybernetics*, 1979. **9**(1): p. 62-66.
127. Markoe, A., *Analytic tomography*. Vol. 13. 2006: Cambridge University Press.
128. Wong, R. and K.T. Chau, *Estimation of air void and aggregate spatial distributions in concrete under uniaxial compression using computer tomography scanning*. *Cement and Concrete Research*, 2005. **35**(8): p. 1566-1576.

129. De Borst, R., et al., *Fundamental issues in finite element analyses of localization of deformation*. Engineering computations, 1993.
130. Lenoir, N., et al., *Volumetric digital image correlation applied to X-ray microtomography images from triaxial compression tests on argillaceous rock*. Strain, 2007. **43**(3): p. 193-205.
131. Marsh, B.K. and R.L. Day, *Pozzolanic and cementitious reactions of fly ash in blended cement pastes*. Cement and concrete research, 1988. **18**(2): p. 301-310.
132. Saeki, T. and P.J. Monteiro, *A model to predict the amount of calcium hydroxide in concrete containing mineral admixtures*. Cement and Concrete Research, 2005. **35**(10): p. 1914-1921.

APPENDICES

APPENDIX A – Supplementary Information for Chapter II

The raw data from the mixtures are presented below.

Table A.1. Oklahoma State University Laboratory Concrete Testing Data

Mixture	Slump (mm)	SAM Number				Air from Super Air Meter (%)	ASTM C138	ASTM C457		
		Meter A	Meter B	Meter C	Average		Gravimetric Air (%)	Hard Air (%)	Spacing Factor (µm)	Specific Surface (mm ⁻¹)
WROS 0.45	76	0.11	0.33		0.22	3.9	3.7	4.0	206	27
	89	0.16	0.1		0.13	5.1	4.6	5.5	178	27
	114	0.19	0.15		0.17	8.5	8.6	5.6	147	32
	64	0.19	0.17		0.18	4.1	3.7	4.0	244	22
	89	0.19	0.26		0.23	3.7	2.9	3.7	211	27
	76	0.24	0.36		0.3	3.1	2.3	3.7	246	23
	64	0.53	0.58		0.56	2.2	2.2	2.3	368	19
	64	0.6	0.56		0.58	2.5	2.3	2.2	325	22
	44	0.54	0.65		0.59	2.5	2.6	3.4	333	18
	76	0.61	0.7		0.66	2.0	1.5	2.8	368	18
83	0.67	0.76		0.72	2.4	1.5	3.7	262	22	
SYNTH 0.45	76	0.33	0.1	0.13	0.19	4.5	4.2	4.3	203	26
	76	0.16	0.15		0.15	6.0	5.6	4.3	196	27
	108	0.09	0.23		0.16	5.2	5.2	4.5	150	35
	76	0.19	0.19		0.19	5.8	5.8	5.3	193	25
	89	0.42	0.29	0.22	0.31	3.7	3.1	3.5	229	26
	89	0.28	0.25	0.35	0.29	3.0	2.3	2.2	295	24
	79	0.28	0.26	0.35	0.3	2.7	3.1	2.1	340	21
	67	0.42	0.28		0.35	2.1	2.1	3.5	249	23
	70	0.31	0.35		0.33	2.8	3.0	2.8	335	19
	114	0.31			0.31	2.8	3.4	1.7	307	26
	83	0.34	0.38		0.36	3.6	3.5	2.3	302	23
	89	0.3	0.36		0.33	3.4	2.1	2.5	234	29
	83	0.4	0.37		0.38	2.9	3.1	2.5	353	19
	83	0.47			0.47	2.2	2.4	1.8	467	17
	76	0.07	0.33		0.20	3.9		4.4	198	27
89	0.31	0.45		0.38	4.2		4.2	191	28	
WROS 0.53	216	0.12			0.12	8.6	8.4	7.0	155	29
	229	0.17	0.12		0.15	7.9	7.8	8.1	142	28
	229	0.17	0.1		0.14	6.2	5.8	6.3	188	25
	229	0.2	0.22		0.21	6.0	5.8	6.7	185	25
	216	0.25	0.25		0.25	5.5	5.4	6.2	198	24
	229	0.46	0.63		0.54	4.4	3.9	5.5	241	21
	229	0.43	0.63		0.53	3.6	3.3	4.1	244	23
	216	0.76	0.7		0.73	2.7	2.7	3.5	320	19
WROS 0.41	38	0.32	0.16		0.24	3.5	3.2	3.5	244	23
	51	0.19			0.19	5.7	5.8	5.7	191	24
	44	0.2	0.29	0.22	0.24	4.5	4.2	3.5	188	30
	38	0.19	0.19		0.19	5.1	4.9	5.1	170	28

Table A.1. continued

Mixture	Slump (mm)	SAM Number				Air from Super Air Meter (%)	ASTM C138	ASTM C457		
		Meter A	Meter B	Meter C	Average		Gravimetric Air (%)	Hard Air (%)	Spacing Factor (μm)	Specific Surface (mm^{-1})
WROS 0.41	44	0.15	0.2		0.17	3.8	3.3	3.1	287	21
	51	0.36	0.21	0.13	0.23	3.6	3.3	4.5	229	22
	38	0.55	0.32		0.44	3.1	2.8	3.0	292	21
	44	0.6	0.5		0.55	2.7	2.7	2.1	297	24
	54	0.6	0.4		0.5	2.0	1.8	1.1	417	23
	44	0.29	0.55	0.54	0.46	2.2	2.3	1.5	361	23
	29	0.56	0.67		0.61	2.7	2.4	2.9	320	20
	29	0.63	0.6		0.61	2.5	2.2	2.5	338	20
WROS 0.39	13	0.17	0.13		0.15	4.3	3.4	4.7	226	22
	19	0.12	0.19		0.15	6.1	6.0	7.3	127	29
	19	0.19	0.26		0.23	3.7	3.2	4.0	269	20
	19	0.51	0.5		0.5	2.8	2.9	3.8	292	19
	25		0.6		0.6	2.7	2.2	4.4	259	20
	19	0.61	0.54		0.57	2.6	2.5	3.3	264	22
	19	0.48	0.61		0.55	2.5	2.3	2.9	483	13
	25	0.58	0.7		0.64	2.2	1.7	3.1	264	22
	19	0.19			0.19	3.3		2.2	381	18
25	0.28	0.25	0.29	0.27	4.9		3.8	213	26	
WROS + PC1 0.45	254	0.11	0.04		0.07	8.0	7.5	8.9	163	20
	229	0.09	0.14		0.12	10.5	10.1	7.3	155	26
	241	0.16	0.12		0.14	7.2	6.2	7.3	180	22
	241	0.14	0.24	0.22	0.2	6.3	7.0	5.4	277	17
	241	0.31	0.25		0.28	5.5	5.3	5.0	366	14
	229	0.49	0.31	0.17	0.32	3.1	2.9	3.9	406	14
	235	0.3	0.23		0.27	6.2	5.9	6.8	361	12
	235	0.55	0.38	0.4	0.44	5.3	5.2	8.0	257	14
	216	0.39	0.37		0.38	2.7	3.1	3.7	338	17
	241	0.41	0.25	0.42	0.36	5.2	5.0	6.2	302	15
	248	0.4	0.39		0.39	2.3	2.6	3.0	409	15
	229	0.44	0.27		0.35	3.8	3.7	4.3	340	16
241	0.44	0.39	0.4	0.41	3.8	3.5	4.0	361	15	
SYNTH + PC1 0.45	216	0.06	0.12	0.09	0.09	8.5	7.3	6.2	147	31
	235	0.15	0.05		0.1	5.6	5.3	4.4	191	28
	229	0.14	0.15		0.15	7.1	6.9	5.6	157	30
	229	0.43	0.39	0.18	0.33	3.5	3.0	2.5	274	25
	210	0.58	0.23	0.2	0.34	5.0	4.7	3.6	292	20
	229	0.36	0.21	0.11	0.23	4.6	4.2	4.6	277	19
	229	0.51	0.38	0.46	0.45	3.4	3.1	5.1	267	18
235	0.37	0.45	0.37	0.4	2.7	2.7	2.4	432	16	

Table A.1. continued

Mixture	Slump (mm)	SAM Number				Air from Super Air Meter (%)	ASTM C138	ASTM C457		
		Meter A	Meter B	Meter C	Average		Gravimetric Air (%)	Hard Air (%)	Spacing Factor (µm)	Specific Surface (mm ⁻¹)
SYNTH + PC1 0.45	216	0.46	0.54	0.5	0.5	2.9	2.4	3.0	353	18
	216	0.46	0.62	0.5	0.53	3.6	3.5	3.6	297	19
WROS 20% Fly Ash 0.45	178	0.1			0.1	8.0	7.5	7.5	178	22
	165	0.15	0.45		0.3	6.7	6.3	8.2	130	28
	191	0.16	0.25		0.21	5.6	5.2	4.2	198	27
	172	0.23	0.18		0.21	6.1	5.4	6.0	175	26
	165	0.27	0.2		0.23	3.4	3.0	3.4	262	23
	165	0.76	0.77		0.76	2.4	2.0	3.4	284	21
	140	0.82	0.71		0.77	2.3	1.9	2.7	282	23
TEMP MIXES	64	0.36	0.4	0.4	0.39	2.9		3.0	282	22
	51	0.16	0.18	0.2	0.18	3.7		3.2	257	24
	64	0.54	0.52		0.53	2.9		2.8	373	17
	70	0.14	0.16		0.15	4.6		4.4	183	29
	89	0.36	0.24	0.32	0.31	2.9		5.4	208	23
	95	0.07	0.12		0.10	5.2		4.3	152	35
	76	0.71	0.66	0.35	0.68	2.6		2.6	226	29
	70	0.13	0.14	0.16	0.14	4.0		4.7	173	30
	64	0.2	0.14	0.19	0.18	3.2		3.7	262	22
	44	0.19	0.17	0.14	0.17	3.7		5.1	180	27
	64	0.1	0.05	0.22	0.14	3.3		3.6	216	27
	83	0.15	0.09	0.14	0.15	5.2		6.1	155	29
	95	0.15	0.09	0.14	0.13	4.1		5.4	173	28
	89	0.04	0.25	0.26	0.19	2.7		4.0	221	25
	89	0.15	0.13	0.1	0.13	5.3		4.8	173	30
	140	0.96	0.54	0.53	0.68	2.0		2.6	284	24
	114	0.41			0.41	3.3		2.9	201	30
127	0.12	0.25	0.13	0.17	5.0		6.8	145	29	
WROS + 20% Fly Ash 0.45	203	0.12	0.12	0.19	0.14	5.5	5.0	5.2	191	26
	165	0.23	0.28	0.21	0.24	3.9	3.7	4.5	224	24
	140	0.28	0.34		0.31	3.0	2.6	3.1	236	26
	152	0.23	0.16	0.16	0.18	4.9	4.3	5.1	198	25
	152	0.06	0.12	0.17	0.12	6.6	5.9	6.9	150	29
	146	0.34	0.39	0.37	0.37	1.3	1.1	2.0	338	22
	152	0.1	0.11	0.16	0.12	5.8	5.3	5.0	183	28
WROS + 20% Fly Ash 0.40	70	0.56	0.43		0.50	2.0	1.7	3.6	356	16
	64	0.4			0.4	2.6	2.1	2.5	368	18
	70	0.2	0.19		0.2	3.0	2.4	4.5	208	25
	64	0.21	0.19	0.3	0.23	3.3	2.9	3.5	272	21
	76	0.2	0.08		0.14	3.7	3.1	3.4	216	27

Table A.1. continued

Mixture	Slump (mm)	SAM Number				Air from Super Air Meter (%)	ASTM C138	ASTM C457		
		Meter A	Meter B	Meter C	Average		Gravimetric Air (%)	Hard Air (%)	Spacing Factor (µm)	Specific Surface (mm ⁻¹)
WROS + 20% Fly Ash 0.40	64	0.1	0.15	0.18	0.14	4.4	4.2	6.0	185	24
	70	0.19	0.11		0.15	4.9	4.4	4.2	163	32
	76	0.12	0.12		0.12	5.5	5.0	3.4	201	29
WROS + PC1 0.40	165	0.35			0.35	2.4	2.1	1.6	820	10
	216	0.38	0.39		0.39	4.3	4.2	4.6	356	14
	229	0.34	0.39		0.36	4.7	4.8	4.6	315	16
	191	0.49	0.46		0.47	4.9	5.1	5.0	373	13
	216	0.24	0.35		0.3	5.7	5.6	5.2	246	19
	191	0.17	0.16		0.16	6.7	6.4	8.0	183	19
	216	0.16	0.18		0.17	7.2	6.8	5.8	251	18
	216	0.15	0.15		0.15	7.3	6.8	7.3	203	19
203	0.11	0.18		0.15	7.5	7.1	8.4	196	17	
WROS + PC1 0.35	184	0.29	0.25		0.27	2.5	2.4	2.5	488	13
	165	0.32	0.29		0.31	3.6	3.4	4.3	399	13
	64	0.42	0.43		0.43	2.9	2.0	3.4	295	19
	64	0.34	0.3	0.41	0.35	4.0	3.5	4.5	264	19
	133		0.23		0.23	6.0	5.4	4.5	396	13
	222	0.14	0.17		0.15	9.2	8.9	8.5	140	22
	83	0.2	0.2	0.33	0.24	5.1	4.5	4.9	239	20
	114	0.12			0.12	5.5	5.2	4.3	211	24
	76	0.13	0.08		0.11	5.3	5.1	6.1	226	19
51	0.39	0.53		0.46	2.4	2.0	3.6	396	14	
WROS + PC2 0.40	76	0.13	0.11		0.12	7.5	6.7	7.0	124	32
	64	0.13	0.13		0.13	5.8	5.1	4.4	165	31
	127	0.49	0.52		0.5	2.4	2.5	2.8	315	20
	114	0.32			0.32	3.0	2.7	2.6	348	19
	64	0.26	0.22		0.24	3.3	2.9	2.9	320	20
	70	0.07	0.11		0.09	4.7	4.1	5.8	163	28
WROS + PC3 0.40	76	0.54	0.43		0.48	2.5	1.8	1.9	640	12
	114	0.23	0.19		0.21	3.8	3.3	3.3	239	25
	102	0.11	0.07		0.09	5.0	5.1	3.6	193	29
	114	0.02	0.15		0.09	5.1	4.5	4.5	175	29
	121	0.07	0.12		0.1	6.8	6.3	5.8	147	31
WROS + PC4 0.40	203	0.23	0.36		0.29	3.8	3.5	2.1	460	16
	241	0.03	0.07		0.05	6.8	5.8	5.6	178	26
	229	0.04	0.08		0.06	5.6	4.4	5.5	170	27
WROS + WR 0.40	83	0.16	0.57		0.36	3.5	2.8	2.8	188	34
	102	0.12	0.23		0.18	5.3	4.8	4.7	137	36
	64	0.48	0.27		0.38	3.1	2.7	3.3	236	25

Table A.1. continued

Mixture	Slump (mm)	SAM Number				Air from Super Air Meter (%)	ASTM C138	ASTM C457		
		Meter A	Meter B	Meter C	Average		Gravimetric Air (%)	Hard Air (%)	Spacing Factor (μm)	Specific Surface (mm^{-1})
WROS + WR 0.40	76	0.19	0.25		0.22	3.7	3.3	3.9	211	26
	76	0.5	0.74		0.62	2.0	1.7	1.4	653	13
WROS + PC5 0.40	203	0.12	0.07		0.1	5.6	5.7	5.5	191	24
	197	0.09	0.08		0.08	8.7	9.3	8.2	155	22
	121	0.35	0.57		0.46	2.9	2.8	2.7	340	19
	165	0.15	0.41		0.28	4.0	4.1	4.0	224	24
WROS 0.40	19	0.11	0.11		0.11	5.0		5.6	201	23
	13		0.2		0.20	4.1		3.0	249	25
	19	0.09	0.11		0.10	5.8		9.5	122	24
	13	0.28	0.27		0.28	3.5		3.4	409	14
	13	0.13	0.15		0.13	4.5		4.9	201	24
	13	0.48	0.47		0.48	2.8		3.2	361	17
WROS+ PC1 0.40	216	0.11	0.13		0.12	6.5		8.3	193	17
	216	0.4	0.38		0.39	4.9		5.4	262	18
	216	0.24	0.4		0.32	5.2		6.4	239	18
	216	0.48	0.53		0.50	3.7		4.2	315	17
	229	0.13	0.12		0.13	6.9		9.3	150	20
WROS 0.45	32	0.57	0.54		0.56	2.5		4.0	302	18
	25	0.71	0.66		0.68	3.0		4.6	254	20
	13	0.35	0.31		0.33	3.5		3.5	394	14
	25	0.14	0.26		0.20	4.2		5.5	188	24
	38	0.11	0.14		0.13	5.7		5.1	165	29
	38	0.11	0.12		0.11	6.3		4.7	185	26
WROS+ PC1 0.45	191	0.41	0.47		0.44	4.0		3.5	343	17
	203	0.27	0.33		0.30	5.1		4.9	323	15
	203	0.2	0.22		0.21	6.2		4.5	244	21
	216	0.1	0.1		0.10	6.8		9.5	170	17
0.50 WROS	102	0.16	0.16		0.16	6.4		7.0	137	30
	76	0.4	0.47		0.44	2.6		3.3	284	21
	51	0.51	0.43		0.47	3.5		4.2	229	23
	146	0.09	0.1		0.09	7.7		8.9	109	29
	76	0.19	0.19		0.19	4.6		6.1	201	22
0.50 WROS+ PC1	203	0.05	0.06		0.06	9.0		7.0	99	21
	203	0.32	0.36		0.34	2.7		3.7	373	15
	203	0.34	0.32		0.33	5.3		6.1	269	17
	203	0.14	0.16		0.15	6.5		7.6	234	16

Table A.2. FHWA Turner Fairbanks Highway Research Center Laboratory Concrete Testing Data

Mixture	Slump (mm)	SAM Number	Air from Super Air Meter (%)	ASTM C138	ASTM C457		
				Gravimetric Air (%)	Hard Air (%)	Spacing Factor (μm)	Specific Surface (mm^{-1})
1	25	0.35	2.3	2.3	2.4	614	11
2	38	0.56	2.6	2.5	2.2	598	12
3	19	0.78	2.9	2.6	3.9	293	19
4	51	0.17	3.7	3.5	3.2	251	24
5	44	0.22	4.3	4.2	4.6	148	34
6	44	0.20	4.7	4.8	4.1	177	30
7	64	0.17	5.4	5.1	4.4	150	34
8	76	0.17	6.3	6.3	6.5	95	44
9	76	0.14	7.3	7.4	5.6	118	39
10	19	0.28	2.2	2.3	1.9	466	16
11	25	0.43	2.6	2.9	2.2	479	15
12	32	0.64	3.0	3.1	3.4	364	16
13	32	0.55	3.3	3.6	3.8	316	18
14	38	0.54	3.5	3.7	3.9	317	17
15	44	0.37	3.5	3.9	3.8	208	26
16	57	0.33	4.0	4.2	4.3	214	25
17	51	0.17	4.9	5.2	5.4	159	30
18	70	0.11	6.9	7.3	7.0	93	43
19	6	0.42	3.0	3.4	3.0	430	14
20	19	0.42	3.2	3.4	4.8	303	16
21	25	0.47	3.3	3.8	3.0	604	10
22	32	0.56	3.4	3.7	4.1	280	19
23	25	0.50	3.5	3.9	3.9	377	14
24	25	0.44	3.7	4.0	3.6	319	17
25	38	0.34	2.7	3.8	4.4	376	13
26	51	0.07	7.2	8.1	9.2	128	22
27	51	0.16	4.8	5.3	6.4	228	18
28	25	0.34	3.1	3.7	3.9	444	12
29	25	0.42	3.1	3.7	3.6	507	11
30	38	0.47	3.4	4.1	4.1	337	15
31	25	0.25	3.3	4.0	3.6	372	15
32	38	0.22	3.9	4.4	4.6	267	18
33	38	0.23	4.3	4.8	6.0	238	18
34	57	0.10	7.6	8.4	9.5	95	29
35	25	0.49	2.9	3.5	3.7	300	18
36	6	0.40	3.0	3.9	4.0	297	18
37	13	0.50	3.1	3.5	3.9	224	24

Table A.2. continued

Mixture	Slump (mm)	SAM Number	Air from Super Air Meter (%)	ASTM C138	ASTM C457		
				Gravimetric Air (%)	Hard Air (%)	Spacing Factor (μm)	Specific Surface (mm^{-1})
38	25	0.53	3.2	3.6	4.8	251	19
39	25	0.50	3.5	4.1	4.7	320	15
40	51	0.17	5.9	6.5	7.7	132	25
41	25	0.16	4.9	5.4	5.2	207	22
42	38	0.20	6.4	7.0	7.2	98	37
43	25	0.45	3.4	4.2	3.0	449	13
44	25	0.44	3.7	4.6	5.0	221	22
45	32	0.43	3.8	4.8	4.9	245	20
46	38	0.21	4.4	5.4	7.0	259	15
47	32	0.41	4.3	5.1	5.8	199	22
48	51	0.13	5.5	6.4	7.0	282	13
49	25	0.48	3.1	4.1	4.2	325	16
50	51	0.13	5.4	6.1	6.8	202	19
51	51	0.13	6.0	6.8	5.6	218	20
52	6	0.74	3.0	3.3	3.5	365	15
53	6	0.48	2.8	3.2	2.8	314	20
54	6	0.54	3.0	3.5	3.2	467	12
55	13	0.47	3.3	3.6	3.7	366	15
56	32	0.65	3.8	4.2	3.6	268	20
57	51	0.15	5.3	6.0	5.7	144	31
58	32	0.41	2.8	3.7	2.8	658	9
59	76	0.22	5.9	7.8	4.6	228	22
60	25	0.40	3.1	3.8	4.4	411	12
61	19	0.55	3.0	3.7	3.0	298	20
62	32	0.34	3.5	4.3	3.8	360	15
63	38	0.44	3.5	4.2	4.2	277	19
64	38	0.34	4.0	4.8	6.6	198	20
65	44	0.24	4.8	5.5	5.9	192	23

Table A.3. Field Concrete Testing Data

State	Slump (mm)	SAM Number	Air from Super Air Meter (%)	ASTM C457		
				Hard Air (%)	Spacing Factor (μm)	Specific Surface (mm^{-1})
Alaska	51	0.03	5.7	4.5	198	27
Arizona	30	0.28	2.7	2.4	295	23
Colorado	203	0.07	7.0	6.1	180	26
Colorado	159	0.11	6.0	4.5	191	28
Colorado	171	0.39	3.8	2.8	478	13
Colorado	171	0.19	4.9	6.0	216	22
Colorado	140	0.13	9.7	8.0	155	22
Colorado	203	0.31	6.2	8.1	152	23
Colorado	114	0.21	6.4	6.2	152	29
Colorado	114	0.22	7.2	7.1	147	24
Colorado	102	0.05	5.2	3.7	178	29
Colorado		0.38	4.4	3.8	312	18
Colorado		0.11	5.7	4.1	193	28
Colorado	133	0.29	8.0	7.8	170	23
Colorado	51	0.48	3.5	1.8	582	13
Colorado		0.58	3.0	1.5	462	18
Florida	38	0.12	5.7	4.8	201	24
Idaho	32	0.11	3.7	3.2	236	27
Idaho	51	0.40	3.9	2.5	196	36
Idaho	38	0.38	4.0	3.3	206	30
Idaho	38	0.56	3.8	3.2	196	32
Idaho	38	0.29	4.5	3.0	241	27
Idaho	13	0.38	3.5	2.7	267	25
Idaho	25	0.34	3.7	2.9	333	19
Illinois	25	0.13	5.5	5.9	191	25
Illinois	38	0.09	6.1	6.6	196	23
Illinois	32	0.20	5.7	4.4	234	23
Iowa		0.44	7.4	6.8	122	30
Iowa		0.37	6.0	6.0	175	26
Iowa		0.25	5.6	6.0	160	28
Iowa		0.18	7.3	6.7	91	40
Iowa		0.15	8.4	7.5	102	32
Iowa		0.20	7.1	7.0	97	37
Iowa		0.12	5.8	5.7	119	36
Iowa		0.08	5.5	5.5	119	37
Iowa		0.10	5.4	5.2	132	34
Kansas	44	0.27	6.0	6.5	155	25
Kansas	76	0.08	8.8	8.5	114	26

Table A.3. continued

State	Slump (mm)	SAM Number	Air from Super Air Meter (%)	ASTM C457		
				Hard Air (%)	Spacing Factor (μm)	Specific Surface (mm^{-1})
Kansas	76	0.14	7.6	8.0	107	30
Kansas		0.18	6.0	6.4	114	32
Kansas	38	0.13	5.9	7.4	123	25
Kansas	32	0.14	5.4	6.7	124	29
Kansas	127	0.18	8.1	7.5	108	30
Kansas	70	0.27	6.9	6.8	116	31
Kansas	127	0.15	6.2	7.8	140	23
Kansas		0.10	6.8	6.9	114	31
Kansas	13	0.24	4.5	6.4	216	17
Kansas	32	0.14	5.4	6.1	131	30
Kansas	38	0.25	6.4	7.3	123	29
Kansas	127	0.18	8.1	6.8	108	34
Kansas	127	0.15	6.2	7.7	118	27
Kansas	102	0.10	7.7	7.8	80	40
Kansas	102	0.28	6.9	6.7	118	33
Kansas	127	0.22	7.8	9.3	137	20
Kansas	38	0.13	5.9	7.4	123	25
Kansas	70	0.27	6.9	6.8	116	31
Kansas	32	0.17	6.0	6.6	123	29
Kansas	140	0.28	5.3	4.6	164	30
Kansas		0.19	8.4	9.2	89	33
Manitoba	45	0.15	5.4	5.0	147	30
Manitoba	25	0.28	4.6	3.6	180	29
Manitoba	30	0.09	6.8	6.9	97	34
Manitoba	35	0.23	6.3	8.1	84	34
Michigan	64	0.10	6.3	4.7	135	35
Michigan	76	0.05	7.7	7.4	107	30
Michigan	64	0.05	7.6	6.5	112	33
Michigan	25	0.12	6.6	5.3	137	32
Michigan	51	0.18	7.0	7.1	99	34
Michigan	76	0.13	7.5	7.5	97	33
Michigan	44	0.06	6.1	6.1	112	35
Michigan	32	0.33	6.2	6.0	145	30
Michigan	114	0.23	6.5	4.5	163	31
Michigan	146	0.07	6.6	6.0	135	33
Michigan	140	0.17	6.0	4.1	155	35
Michigan	32	0.24	5.6	4.0	147	36
Michigan	165	0.09	6.1	5.8	147	28

Table A.3. continued

State	Slump (mm)	SAM Number	Air from Super Air Meter (%)	ASTM C457		
				Hard Air (%)	Spacing Factor (μm)	Specific Surface (mm^{-1})
Michigan	89	0.06	5.6	4.3	145	36
Michigan	13	0.19	6.1	6.2	117	33
Michigan	13	0.11	6.5	5.3	135	34
Michigan	127	0.19	6.6	6.7	145	32
Michigan	114	0.19	6.5	4.7	150	36
Minnesota	102	0.11	7.4	6.3	132	33
Minnesota	70	0.16	5.8	4.1	203	25
Minnesota	152	0.24	7.7	7.3	183	21
Minnesota	25	0.10	6.3	5.5	264	18
Minnesota	51	0.05	6.9	5.3	267	18
Minnesota	64	0.27	5.6	4.5	239	21
Minnesota	140	0.04	9.3	8.7	168	17
Minnesota	44	0.09	6.2	5.4	206	23
Minnesota	38	0.29	6.8	5.3	333	14
Minnesota	203	0.15	13.0	11.6	122	18
Minnesota	152	0.07	10.4	10.4	170	15
Minnesota	102	0.23	4.7	5.9	208	21
Minnesota		0.23	7.3	6.8	132	29
Minnesota		0.10	8.0	6.2	135	31
Minnesota		0.26	7.2	7.1	168	22
Minnesota		0.25	6.6	4.7	203	24
Minnesota		0.24	7.1	6.2	185	23
Minnesota		0.24	6.9	7.2	168	22
Minnesota		0.07	7.7	8.2	122	25
Minnesota		0.05	7.0	8.6	104	28
Minnesota		0.01	6.8	7.2	127	27
Minnesota		0.21	6.8	6.4	170	23
Minnesota		0.06	6.8	5.9	203	21
Minnesota		0.23	6.9	5.6	147	30
Minnesota		0.06	4.2	5.2	178	26
North Dakota	51	0.11	8.1	9.9	104	25
North Dakota	51	0.23	7.5	9.3	119	23
North Dakota	51	0.12	7.9	7.7	109	31
North Dakota	76	0.06	8.6	8.9	99	29
North Dakota	57	0.34	8.0	6.9	140	27
North Dakota	51	0.19	7.2	6.6	117	33
North Dakota	13	0.08	5.3	4.4	150	32
North Dakota	13	0.17	5.6	4.8	142	32

Table A.3. continued

State	Slump (mm)	SAM Number	Air from Super Air Meter (%)	ASTM C457		
				Hard Air (%)	Spacing Factor (μm)	Specific Surface (mm^{-1})
North Dakota	19	0.21	5.3	4.0	178	29
North Dakota	6	0.07	7.2	6.1	203	21
North Dakota	44	0.24	5.7	5.4	173	27
North Dakota	57	0.21	6.5	7.5	180	20
North Dakota	25	0.28	6.1	5.7	168	26
North Dakota	51	0.09	7.9	8.9	104	28
North Dakota	38	0.41	7.1	5.3	145	32
Ohio	57	0.22	7.2	6.6	145	27
Ohio	76	0.10	9.2	7.8	112	30
Ohio	64	0.15	8.6	7.2	114	32
Ohio	76	0.32	7.2	6.5	122	33
Ohio	89	0.15	8.7	8.3	97	33
Oklahoma	31	0.05	5.5	5.1	157	26
Oklahoma	38	0.16	5.4	4.9	150	28
Oklahoma	216	0.66	3.4	5.2	335	14
Oklahoma	178	0.67	2.7	4.3	305	17
Oklahoma	203	0.75	3.0	4.3	417	12
Oklahoma	108	0.13	9.4	9.7	124	20
Oklahoma	178	0.75	2.9	4.4	302	17
Oklahoma	216	0.58	3.0	4.5	264	19
Oklahoma	216	0.62	3.0	4.6	277	18
Oklahoma	102	0.18	4.9	6.0	173	25
Oklahoma	152	0.17	5.7	5.7	160	28
Oklahoma	64	0.26	5.5	5.2	193	24
Oklahoma	64	0.25	4.9	4.2	234	22
Oklahoma	89	0.16	5.1	5.5	196	23
Oklahoma	102	0.17	7.3	8.4	140	22
Oklahoma	140	0.19	6.8	6.3	157	26
Oklahoma	203	0.24	5.6	5.4	193	24
Oklahoma	203	0.15	6.6	7.5	150	23
Oklahoma	38	0.32	4.5	3.6	274	20
Oklahoma		0.54	4.3	3.6	295	19
Oklahoma		0.55	4.3	4.1	221	23
Oklahoma		0.32	4.6	3.5	300	18
Oklahoma		0.15	4.4	5.4	178	25
Oklahoma	38	0.25	4.6	4.8	241	20
Oklahoma		0.36	4.1	4.1	257	20
Oklahoma	25	0.67	3.1	2.8	257	24

Table A.3. continued

State	Slump (mm)	SAM Number	Air from Super Air Meter (%)	ASTM C457		
				Hard Air (%)	Spacing Factor (μm)	Specific Surface (mm^{-1})
Oklahoma		0.64	3.0	2.7	320	20
Oklahoma		0.62	2.9	3.9	302	18
Oklahoma		0.44	3.1	3.5	274	17
Oklahoma	32	0.40	3.1	4.2	251	21
Oklahoma		0.34	3.0	4.0	384	14
Oklahoma		0.58	3.0	3.7	290	19
Oklahoma		0.41	3.0	4.0	264	20
Oklahoma	19	0.32	3.0	3.2	277	21
Oklahoma	32	0.37	4.0	4.8	226	21
Oklahoma		0.31	3.9	4.6	229	21
Oklahoma		0.35	4.0	4.0	226	23
Oklahoma		0.17	3.9	5.4	203	22
Oklahoma	241	0.15	5.2	5.6	193	22
Oklahoma	222	0.15	6.5	7.0	145	23
Oklahoma	76	0.29	3.6	3.4	213	25
Oklahoma	229	0.10	6.1	7.9	160	18
Oklahoma	216	0.15	5.6	4.9	168	27
Oklahoma	222	0.13	5.9	5.2	203	22
Oklahoma	51	0.35	7.2	5.8	160	24
Oklahoma		0.18	6.8	7.0	135	24
Oklahoma		0.12	6.7	5.3	175	25
Oklahoma		0.13	7.3	5.6	163	25
Oklahoma		0.12	7.3	6.7	163	21
Oklahoma		0.32	6.7	5.2	180	24
Oklahoma		0.18	7.6	7.3	119	26
Oklahoma		0.14	6.7	6.7	135	25
Pennsylvania	102	0.17	8.0	6.3	163	27
Pennsylvania	58	0.19	4.9	4.7	175	29
Pennsylvania*	597	0.34	7.4	5.5	183	
Pennsylvania*	540	0.28	7.4	6.6	224	
Pennsylvania*	521	0.39	5.8	7.7	224	
Pennsylvania*	533	0.52	5.4	4.3	221	
Pennsylvania	203	0.65	3.3	3.7	290	
Pennsylvania	108	0.30	5.4	3.7	241	
Pennsylvania	191	0.30	4.0	4.8	307	
Pennsylvania	197	0.54	3.9	4.0	315	
Pennsylvania	197	0.44	5.5	3.9	345	
Pennsylvania	191	0.42	4.8	4.1	254	

Table A.3. continued

State	Slump (mm)	SAM Number	Air from Super Air Meter (%)	ASTM C457		
				Hard Air (%)	Spacing Factor (μm)	Specific Surface (mm^{-1})
Pennsylvania*	635	0.12	7.6	9.2	81	
Pennsylvania	146	0.11	5.6	6.7	117	
Pennsylvania*	572	0.16	6.7	7.8	122	
Pennsylvania	197	0.34	4.0	5.0	191	
Pennsylvania	171	0.49	5.4	5.0	145	
Pennsylvania*	559	0.15	8.3	9.5	91	
Pennsylvania	152	0.22	4.6	4.5	135	
Pennsylvania	108	0.20	4.8	5.3	99	
Pennsylvania	51	0.19	5.1	4.2	89	
Pennsylvania	127	0.22	5.3	6.0	109	
Pennsylvania*	635	0.48	7.1	6.6	315	
Pennsylvania*	686	0.53	5.1	4.8	239	
Pennsylvania	178	0.45	2.7	1.2	709	
Pennsylvania	184	0.31	2.7	1.4	584	
Pennsylvania*	635	0.18	7.7	7.2	196	
Pennsylvania*	597	0.18	8.1	7.9	127	
Pennsylvania	102	0.19	7.3	5.4	142	
Pennsylvania	86	0.13	5.7	6.2	122	
Pennsylvania	89	0.20	8.0	8.1	94	
Pennsylvania		0.18	6.8	6.4	107	
Pennsylvania	102	0.46	6.0	7.6	117	
Pennsylvania	127	0.37	7.1	8.5	91	
Pennsylvania	89	0.19	6.8	8.1	102	
South Dakota	32	0.08	5.5	4.0	203	27
Tennessee	76	0.22	4.8	4.2	180	28
Tennessee	38	0.13	5.1	5.8	175	22
Tennessee	19	0.21	4.4	5.4	208	20
Tennessee	51	0.25	4.4	4.1	188	27
Utah	146	0.15	5.1	3.8	221	27
Utah		0.36	7.4	6.8	386	12
Utah	229	0.36	5.6	4.8	277	20
Washington	32	0.38	5.1	5.2	150	32
Washington	25	0.32	5.0	5.2	152	31
West Virginia	64	0.09	9.1	7.5	102	35
West Virginia	51	0.25	7.7	6.0	107	41
West Virginia	44	0.15	7.6	7.0	91	42
Wisconsin	76	0.18	7.5	7.1	119	29
Wisconsin	44	0.23	7.9	5.9	130	33

Table A.3. continued

State	Slump (mm)	SAM Number	Air from Super Air Meter (%)	ASTM C457		
				Hard Air (%)	Spacing Factor (μm)	Specific Surface (mm^{-1})
Wisconsin	44	0.14	5.3	5.2	203	23
Wisconsin	64	0.08	6.7	6.3	13	26
Wisconsin	64	0.18	6.3	5.8	13	28

*Slump (mm) was recorded as slump flow plus spread.

APPENDIX B – Supplementary Information for Chapter III

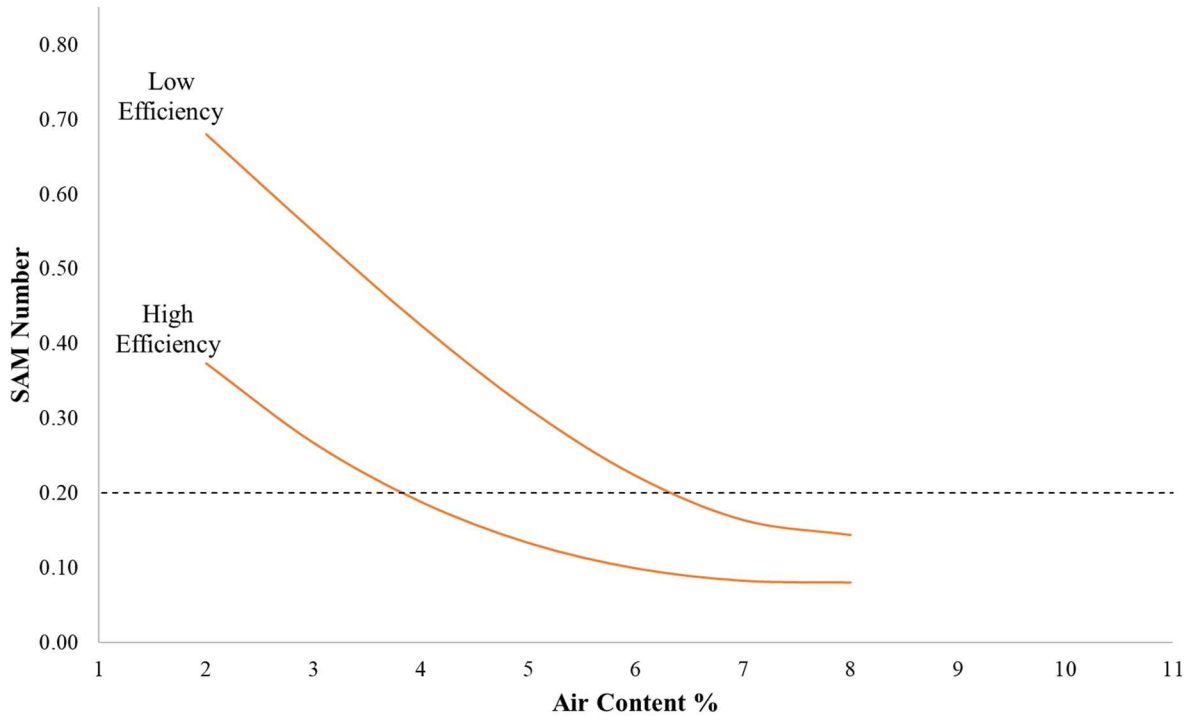


Figure B.1. Efficiency Chart

Tables B.1 and B.2 are the summary of results from the XLSTAT quantile analysis [45]. Each variable from Equations (3.1) and (3.2) is shown along with the standard error. The values listed correspond to the coefficients in the cubic efficiency lines plotted in Figure B.1. The standard error is the square root of the standard deviation divided by the number of data points. The lower the standard error the more certain the results. Since the standard errors are low on the squared and cubic terms it means that these terms are more precise than the other terms. Since these terms are important for defining the shape of the line it suggests that the overall shape and fit to the data is acceptable.

Table B.1. 15th Quantile Line of SAM Number (Equation (3.1)).

Variable	Value	Standard Error
Intercept	0.6804	0.0177
Air Content	-0.1888	0.0112
Air Content ²	0.0186	0.0022
Air Content ³	-0.0006	0.0001

Table B.2. 85th Quantile Line of SAM Number (Equation (3.2)).

Variable	Value	Standard Error
Intercept	0.9213	0.0149
Air Content	-0.1061	0.0095
Air Content ²	-0.0102	0.0018
Air Content ³	0.0014	0.0001

The raw data from the mixtures are presented below.

Table B.3. Concrete Testing Data

Mixture	Slump (mm)	SAM Number				Air from Super Air Meter (%)	ASTM C138	ASTM C457		
		Meter A	Meter B	Meter C	Average		Gravimetric Air (%)	Hard Air (%)	Spacing Factor (μm)	Specific Surface (mm^{-1})
WROS 0.45	76	0.11	0.33		0.22	3.9	3.7	4.0	206	27
	89	0.16	0.1		0.13	5.1	4.6	5.5	178	27
	114	0.19	0.15		0.17	8.5	8.6	5.6	147	32
	64	0.19	0.17		0.18	4.1	3.7	4.0	244	22
	89	0.19	0.26		0.23	3.7	2.9	3.7	211	27
	76	0.24	0.36		0.3	3.1	2.3	3.7	246	23
	64	0.53	0.58		0.56	2.2	2.2	2.3	368	19
	64	0.6	0.56		0.58	2.5	2.3	2.2	325	22
	44	0.54	0.65		0.59	2.5	2.6	3.4	333	18
	76	0.61	0.7		0.66	2.0	1.5	2.8	368	18
83	0.67	0.76		0.72	2.4	1.5	3.7	262	22	
SYNTH 0.45	76	0.33	0.1	0.13	0.19	4.5	4.2	4.3	203	26
	76	0.16	0.15		0.15	6.0	5.6	4.3	196	27
	108	0.09	0.23		0.16	5.2	5.2	4.5	150	35
	76	0.19	0.19		0.19	5.8	5.8	5.3	193	25
	89	0.42	0.29	0.22	0.31	3.7	3.1	3.5	229	26
	89	0.28	0.25	0.35	0.29	3.0	2.3	2.2	295	24
	79	0.28	0.26	0.35	0.3	2.7	3.1	2.1	340	21
	67	0.42	0.28		0.35	2.1	2.1	3.5	249	23
	70	0.31	0.35		0.33	2.8	3.0	2.8	335	19
	114	0.31			0.31	2.8	3.4	1.7	307	26
	83	0.34	0.38		0.36	3.6	3.5	2.3	302	23
	89	0.3	0.36		0.33	3.4	2.1	2.5	234	29
	83	0.4	0.37		0.38	2.9	3.1	2.5	353	19
	83	0.47			0.47	2.2	2.4	1.8	467	17
	76	0.07	0.33		0.20	3.9		4.4	198	27
89	0.31	0.45		0.38	4.2		4.2	191	28	
WROS 0.53	216	0.12			0.12	8.6	8.4	7.0	155	29
	229	0.17	0.12		0.15	7.9	7.8	8.1	142	28
	229	0.17	0.1		0.14	6.2	5.8	6.3	188	25
	229	0.2	0.22		0.21	6.0	5.8	6.7	185	25
	216	0.25	0.25		0.25	5.5	5.4	6.2	198	24
	229	0.46	0.63		0.54	4.4	3.9	5.5	241	21
	229	0.43	0.63		0.53	3.6	3.3	4.1	244	23
	216	0.76	0.7		0.73	2.7	2.7	3.5	320	19
WROS 0.41	38	0.32	0.16		0.24	3.5	3.2	3.5	244	23
	51	0.19			0.19	5.7	5.8	5.7	191	24
	44	0.2	0.29	0.22	0.24	4.5	4.2	3.5	188	30
	38	0.19	0.19		0.19	5.1	4.9	5.1	170	28

Table B.3. continued

Mixture	Slump (mm)	SAM Number				Air from Super Air Meter (%)	ASTM C138	ASTM C457		
		Meter A	Meter B	Meter C	Average		Gravimetric Air (%)	Hard Air (%)	Spacing Factor (μm)	Specific Surface (mm^{-1})
WROS 0.41	44	0.15	0.2		0.17	3.8	3.3	3.1	287	21
	51	0.36	0.21	0.13	0.23	3.6	3.3	4.5	229	22
	38	0.55	0.32		0.44	3.1	2.8	3.0	292	21
	44	0.6	0.5		0.55	2.7	2.7	2.1	297	24
	54	0.6	0.4		0.5	2.0	1.8	1.1	417	23
	44	0.29	0.55	0.54	0.46	2.2	2.3	1.5	361	23
	29	0.56	0.67		0.61	2.7	2.4	2.9	320	20
	29	0.63	0.6		0.61	2.5	2.2	2.5	338	20
WROS 0.39	13	0.17	0.13		0.15	4.3	3.4	4.7	226	22
	19	0.12	0.19		0.15	6.1	6.0	7.3	127	29
	19	0.19	0.26		0.23	3.7	3.2	4.0	269	20
	19	0.51	0.5		0.5	2.8	2.9	3.8	292	19
	25		0.6		0.6	2.7	2.2	4.4	259	20
	19	0.61	0.54		0.57	2.6	2.5	3.3	264	22
	19	0.48	0.61		0.55	2.5	2.3	2.9	483	13
	25	0.58	0.7		0.64	2.2	1.7	3.1	264	22
	19	0.19			0.19	3.3		2.2	381	18
25	0.28	0.25	0.29	0.27	4.9		3.8	213	26	
WROS + PC1 0.45	254	0.11	0.04		0.07	8.0	7.5	8.9	163	20
	229	0.09	0.14		0.12	10.5	10.1	7.3	155	26
	241	0.16	0.12		0.14	7.2	6.2	7.3	180	22
	241	0.14	0.24	0.22	0.2	6.3	7.0	5.4	277	17
	241	0.31	0.25		0.28	5.5	5.3	5.0	366	14
	229	0.49	0.31	0.17	0.32	3.1	2.9	3.9	406	14
	235	0.3	0.23		0.27	6.2	5.9	6.8	361	12
	235	0.55	0.38	0.4	0.44	5.3	5.2	8.0	257	14
	216	0.39	0.37		0.38	2.7	3.1	3.7	338	17
	241	0.41	0.25	0.42	0.36	5.2	5.0	6.2	302	15
	248	0.4	0.39		0.39	2.3	2.6	3.0	409	15
	229	0.44	0.27		0.35	3.8	3.7	4.3	340	16
241	0.44	0.39	0.4	0.41	3.8	3.5	4.0	361	15	
SYNTH + PC1 0.45	216	0.06	0.12	0.09	0.09	8.5	7.3	6.2	147	31
	235	0.15	0.05		0.1	5.6	5.3	4.4	191	28
	229	0.14	0.15		0.15	7.1	6.9	5.6	157	30
	229	0.43	0.39	0.18	0.33	3.5	3.0	2.5	274	25
	210	0.58	0.23	0.2	0.34	5.0	4.7	3.6	292	20
	229	0.36	0.21	0.11	0.23	4.6	4.2	4.6	277	19
	229	0.51	0.38	0.46	0.45	3.4	3.1	5.1	267	18
	235	0.37	0.45	0.37	0.4	2.7	2.7	2.4	432	16

Table B.3. continued

Mixture	Slump (mm)	SAM Number				Air from Super Air Meter (%)	ASTM C138	ASTM C457		
		Meter A	Meter B	Meter C	Average		Gravimetric Air (%)	Hard Air (%)	Spacing Factor (μm)	Specific Surface (mm^{-1})
SYNTH + PC1 0.45	216	0.46	0.54	0.5	0.5	2.9	2.4	3.0	353	18
	216	0.46	0.62	0.5	0.53	3.6	3.5	3.6	297	19
WROS 20% Fly Ash 0.45	178	0.1			0.1	8.0	7.5	7.5	178	22
	165	0.15	0.45		0.3	6.7	6.3	8.2	130	28
	191	0.16	0.25		0.21	5.6	5.2	4.2	198	27
	172	0.23	0.18		0.21	6.1	5.4	6.0	175	26
	165	0.27	0.2		0.23	3.4	3.0	3.4	262	23
	165	0.76	0.77		0.76	2.4	2.0	3.4	284	21
TEMP MIXES	140	0.82	0.71		0.77	2.3	1.9	2.7	282	23
	64	0.36	0.4	0.4	0.39	2.9		3.0	282	22
	51	0.16	0.18	0.2	0.18	3.7		3.2	257	24
	64	0.54	0.52		0.53	2.9		2.8	373	17
	70	0.14	0.16		0.15	4.6		4.4	183	29
	89	0.36	0.24	0.32	0.31	2.9		5.4	208	23
	95	0.07	0.12		0.10	5.2		4.3	152	35
	76	0.71	0.66	0.35	0.68	2.6		2.6	226	29
	70	0.13	0.14	0.16	0.14	4.0		4.7	173	30
	64	0.2	0.14	0.19	0.18	3.2		3.7	262	22
	44	0.19	0.17	0.14	0.17	3.7		5.1	180	27
	64	0.1	0.05	0.22	0.14	3.3		3.6	216	27
	83	0.15	0.09	0.14	0.15	5.2		6.1	155	29
	95	0.15	0.09	0.14	0.13	4.1		5.4	173	28
	89	0.04	0.25	0.26	0.19	2.7		4.0	221	25
	89	0.15	0.13	0.1	0.13	5.3		4.8	173	30
140	0.96	0.54	0.53	0.68	2.0		2.6	284	24	
114	0.41			0.41	3.3		2.9	201	30	
127	0.12	0.25	0.13	0.17	5.0		6.8	145	29	
WROS + 20% Fly Ash 0.45	203	0.12	0.12	0.19	0.14	5.5	5.0	5.2	191	26
	165	0.23	0.28	0.21	0.24	3.9	3.7	4.5	224	24
	140	0.28	0.34		0.31	3.0	2.6	3.1	236	26
	152	0.23	0.16	0.16	0.18	4.9	4.3	5.1	198	25
	152	0.06	0.12	0.17	0.12	6.6	5.9	6.9	150	29
	146	0.34	0.39	0.37	0.37	1.3	1.1	2.0	338	22
152	0.1	0.11	0.16	0.12	5.8	5.3	5.0	183	28	
WROS + 20% Fly Ash 0.40	70	0.56	0.43		0.50	2.0	1.7	3.6	356	16
	64	0.4			0.4	2.6	2.1	2.5	368	18
	70	0.2	0.19		0.2	3.0	2.4	4.5	208	25
	64	0.21	0.19	0.3	0.23	3.3	2.9	3.5	272	21
	76	0.2	0.08		0.14	3.7	3.1	3.4	216	27

Table B.3. continued

Mixture	Slump (mm)	SAM Number				Air from Super Air Meter (%)	ASTM C138	ASTM C457		
		Meter A	Meter B	Meter C	Average		Gravimetric Air (%)	Hard Air (%)	Spacing Factor (μm)	Specific Surface (mm^{-1})
WROS + 20% Fly Ash 0.40	64	0.1	0.15	0.18	0.14	4.4	4.2	6.0	185	24
	70	0.19	0.11		0.15	4.9	4.4	4.2	163	32
	76	0.12	0.12		0.12	5.5	5.0	3.4	201	29
WROS + PC1 0.40	165	0.35			0.35	2.4	2.1	1.6	820	10
	216	0.38	0.39		0.39	4.3	4.2	4.6	356	14
	229	0.34	0.39		0.36	4.7	4.8	4.6	315	16
	191	0.49	0.46		0.47	4.9	5.1	5.0	373	13
	216	0.24	0.35		0.3	5.7	5.6	5.2	246	19
	191	0.17	0.16		0.16	6.7	6.4	8.0	183	19
	216	0.16	0.18		0.17	7.2	6.8	5.8	251	18
	216	0.15	0.15		0.15	7.3	6.8	7.3	203	19
203	0.11	0.18		0.15	7.5	7.1	8.4	196	17	
WROS + PC1 0.35	184	0.29	0.25		0.27	2.5	2.4	2.5	488	13
	165	0.32	0.29		0.31	3.6	3.4	4.3	399	13
	64	0.42	0.43		0.43	2.9	2.0	3.4	295	19
	64	0.34	0.3	0.41	0.35	4.0	3.5	4.5	264	19
	133		0.23		0.23	6.0	5.4	4.5	396	13
	222	0.14	0.17		0.15	9.2	8.9	8.5	140	22
	83	0.2	0.2	0.33	0.24	5.1	4.5	4.9	239	20
	114	0.12			0.12	5.5	5.2	4.3	211	24
	76	0.13	0.08		0.11	5.3	5.1	6.1	226	19
	51	0.39	0.53		0.46	2.4	2.0	3.6	396	14
WROS + PC2 0.40	76	0.13	0.11		0.12	7.5	6.7	7.0	124	32
	64	0.13	0.13		0.13	5.8	5.1	4.4	165	31
	127	0.49	0.52		0.5	2.4	2.5	2.8	315	20
	114	0.32			0.32	3.0	2.7	2.6	348	19
	64	0.26	0.22		0.24	3.3	2.9	2.9	320	20
	70	0.07	0.11		0.09	4.7	4.1	5.8	163	28
WROS + PC3 0.40	76	0.54	0.43		0.48	2.5	1.8	1.9	640	12
	114	0.23	0.19		0.21	3.8	3.3	3.3	239	25
	102	0.11	0.07		0.09	5.0	5.1	3.6	193	29
	114	0.02	0.15		0.09	5.1	4.5	4.5	175	29
	121	0.07	0.12		0.1	6.8	6.3	5.8	147	31
WROS + PC4 0.40	203	0.23	0.36		0.29	3.8	3.5	2.1	460	16
	241	0.03	0.07		0.05	6.8	5.8	5.6	178	26
	229	0.04	0.08		0.06	5.6	4.4	5.5	170	27
WROS + WR 0.40	83	0.16	0.57		0.36	3.5	2.8	2.8	188	34
	102	0.12	0.23		0.18	5.3	4.8	4.7	137	36
	64	0.48	0.27		0.38	3.1	2.7	3.3	236	25

Table B.3. continued

Mixture	Slump (mm)	SAM Number				Air from Super Air Meter (%)	ASTM C138	ASTM C457		
		Meter A	Meter B	Meter C	Average		Gravimetric Air (%)	Hard Air (%)	Spacing Factor (µm)	Specific Surface (mm ⁻¹)
WROS + WR 0.40	76	0.19	0.25		0.22	3.7	3.3	3.9	211	26
	76	0.5	0.74		0.62	2.0	1.7	1.4	653	13
WROS + PC5 0.40	203	0.12	0.07		0.1	5.6	5.7	5.5	191	24
	197	0.09	0.08		0.08	8.7	9.3	8.2	155	22
	121	0.35	0.57		0.46	2.9	2.8	2.7	340	19
	165	0.15	0.41		0.28	4.0	4.1	4.0	224	24
WROS 0.40	19	0.11	0.11		0.11	5.0		5.6	201	23
	13		0.2		0.20	4.1		3.0	249	25
	19	0.09	0.11		0.10	5.8		9.5	122	24
	13	0.28	0.27		0.28	3.5		3.4	409	14
	13	0.13	0.15		0.13	4.5		4.9	201	24
	13	0.48	0.47		0.48	2.8		3.2	361	17
WROS+ PC1 0.40	216	0.11	0.13		0.12	6.5		8.3	193	17
	216	0.4	0.38		0.39	4.9		5.4	262	18
	216	0.24	0.4		0.32	5.2		6.4	239	18
	216	0.48	0.53		0.50	3.7		4.2	315	17
	229	0.13	0.12		0.13	6.9		9.3	150	20
WROS 0.45	32	0.57	0.54		0.56	2.5		4.0	302	18
	25	0.71	0.66		0.68	3.0		4.6	254	20
	13	0.35	0.31		0.33	3.5		3.5	394	14
	25	0.14	0.26		0.20	4.2		5.5	188	24
	38	0.11	0.14		0.13	5.7		5.1	165	29
	38	0.11	0.12		0.11	6.3		4.7	185	26
WROS+ PC1 0.45	191	0.41	0.47		0.44	4.0		3.5	343	17
	203	0.27	0.33		0.30	5.1		4.9	323	15
	203	0.2	0.22		0.21	6.2		4.5	244	21
	216	0.1	0.1		0.10	6.8		9.5	170	17
0.50 WROS	102	0.16	0.16		0.16	6.4		7.0	137	30
	76	0.4	0.47		0.44	2.6		3.3	284	21
	51	0.51	0.43		0.47	3.5		4.2	229	23
	146	0.09	0.1		0.09	7.7		8.9	109	29
	76	0.19	0.19		0.19	4.6		6.1	201	22
0.50 WROS+ PC1	203	0.05	0.06		0.06	9.0		7.0	99	21
	203	0.32	0.36		0.34	2.7		3.7	373	15
	203	0.34	0.32		0.33	5.3		6.1	269	17
	203	0.14	0.16		0.15	6.5		7.6	234	16

Table B.3. continued

Mixture	Slump (mm)	SAM Number				Air from Super Air Meter (%)	ASTM C138	ASTM C457		
		Meter A	Meter B	Meter C	Average		Gravimetric Air (%)	Hard Air (%)	Spacing Factor (μm)	Specific Surface (mm^{-1})
0.45 WROS (C1)	76	0.33	0.28	0.32	0.31	3.3		1.8	310	26
	83	0.23	0.21	0.26	0.23	5.1		5.8	130	36
	76	0.20	0.20	0.17	0.19	6.7		4.5	188	28
	83	0.17	0.12	0.20	0.16	8.0		8.3	119	29
0.45 WROS (C2)	89	0.16	0.12	0.16	0.15	4.8		5.4	165	29
	114	0.06	0.10	0.07	0.08	6.4		8.9	109	30
	108	0.12	0.09	0.08	0.10	3.6		4.8	193	27
	51	0.20	0.31	0.34	0.28	2.6		3.0	264	24
	51	0.28	0.31	0.37	0.32	3.1		4.6	175	30

Table B.4. FHWA Turner Fairbanks Highway Research Center Laboratory Concrete Testing Data

Mixture	Slump (mm)	SAM Number	Air from Super Air Meter (%)	ASTM C138	ASTM C457		
				Gravimetric Air (%)	Hard Air (%)	Spacing Factor (μm)	Specific Surface (mm^{-1})
1	25	0.35	2.3	2.3	2.4	614	11
2	38	0.56	2.6	2.5	2.2	598	12
3	19	0.78	2.9	2.6	3.9	293	19
4	51	0.17	3.7	3.5	3.2	251	24
5	44	0.22	4.3	4.2	4.6	148	34
6	44	0.20	4.7	4.8	4.1	177	30
7	64	0.17	5.4	5.1	4.4	150	34
8	76	0.17	6.3	6.3	6.5	95	44
9	76	0.14	7.3	7.4	5.6	118	39
10	19	0.28	2.2	2.3	1.9	466	16
11	25	0.43	2.6	2.9	2.2	479	15
12	32	0.64	3.0	3.1	3.4	364	16
13	32	0.55	3.3	3.6	3.8	316	18
14	38	0.54	3.5	3.7	3.9	317	17
15	44	0.37	3.5	3.9	3.8	208	26
16	57	0.33	4.0	4.2	4.3	214	25
17	51	0.17	4.9	5.2	5.4	159	30
18	70	0.11	6.9	7.3	7.0	93	43
19	6	0.42	3.0	3.4	3.0	430	14
20	19	0.42	3.2	3.4	4.8	303	16
21	25	0.47	3.3	3.8	3.0	604	10
22	32	0.56	3.4	3.7	4.1	280	19
23	25	0.50	3.5	3.9	3.9	377	14
24	25	0.44	3.7	4.0	3.6	319	17
25	38	0.34	2.7	3.8	4.4	376	13
26	51	0.07	7.2	8.1	9.2	128	22
27	51	0.16	4.8	5.3	6.4	228	18
28	25	0.34	3.1	3.7	3.9	444	12
29	25	0.42	3.1	3.7	3.6	507	11
30	38	0.47	3.4	4.1	4.1	337	15
31	25	0.25	3.3	4.0	3.6	372	15
32	38	0.22	3.9	4.4	4.6	267	18
33	38	0.23	4.3	4.8	6.0	238	18
34	57	0.10	7.6	8.4	9.5	95	29
35	25	0.49	2.9	3.5	3.7	300	18
36	6	0.40	3.0	3.9	4.0	297	18
37	13	0.50	3.1	3.5	3.9	224	24

Table B.4. continued

Mixture	Slump (mm)	SAM Number	Air from Super Air Meter (%)	ASTM C138	ASTM C457		
				Gravimetric Air (%)	Hard Air (%)	Spacing Factor (μm)	Specific Surface (mm^{-1})
38	25	0.53	3.2	3.6	4.8	251	19
39	25	0.50	3.5	4.1	4.7	320	15
40	51	0.17	5.9	6.5	7.7	132	25
41	25	0.16	4.9	5.4	5.2	207	22
42	38	0.20	6.4	7.0	7.2	98	37
43	25	0.45	3.4	4.2	3.0	449	13
44	25	0.44	3.7	4.6	5.0	221	22
45	32	0.43	3.8	4.8	4.9	245	20
46	38	0.21	4.4	5.4	7.0	259	15
47	32	0.41	4.3	5.1	5.8	199	22
48	51	0.13	5.5	6.4	7.0	282	13
49	25	0.48	3.1	4.1	4.2	325	16
50	51	0.13	5.4	6.1	6.8	202	19
51	51	0.13	6.0	6.8	5.6	218	20
52	6	0.74	3.0	3.3	3.5	365	15
53	6	0.48	2.8	3.2	2.8	314	20
54	6	0.54	3.0	3.5	3.2	467	12
55	13	0.47	3.3	3.6	3.7	366	15
56	32	0.65	3.8	4.2	3.6	268	20
57	51	0.15	5.3	6.0	5.7	144	31
58	32	0.41	2.8	3.7	2.8	658	9
59	76	0.22	5.9	7.8	4.6	228	22
60	25	0.40	3.1	3.8	4.4	411	12
61	19	0.55	3.0	3.7	3.0	298	20
62	32	0.34	3.5	4.3	3.8	360	15
63	38	0.44	3.5	4.2	4.2	277	19
64	38	0.34	4.0	4.8	6.6	198	20
65	44	0.24	4.8	5.5	5.9	192	23

VITA

Hope Elizabeth Hall Becker

Candidate for the Degree of

Doctor of Philosophy

Dissertation: QUANTIFYING THE EFFICIENCY AND QUALITY OF AIR VOID
DISTRIBUTION IN CONCRETE

Major Field: Civil Engineering

Biographical:

Education:

Completed the requirements for the Doctor of Philosophy in Civil Engineering at Oklahoma State University, Stillwater, Oklahoma in May, 2022.

Completed the requirements for the Master of Science in Civil Engineering at Oklahoma State University, Stillwater, Oklahoma in 2018.

Completed the requirements for the Bachelor of Science in Architectural Engineering at Oklahoma State University, Stillwater, Oklahoma in 2015.